

SPATIAL HOMOGENIZATION METHODS FOR  
LIGHT WATER REACTOR ANALYSIS

by

Kord Sterling Smith

B.S., Kansas State University (1976)

S.M., Massachusetts Institute of Technology (1979)

Nucl. E., Massachusetts Institute of Technology (1979)

SUBMITTED IN PARTIAL FULFILLMENT

OF THE REQUIREMENTS FOR THE

DEGREE OF

DOCTOR OF PHILOSOPHY

AT THE

MASSACHUSETTS INSTITUTE OF TECHNOLOGY

JUNE 1980

© MASSACHUSETTS INSTITUTE OF TECHNOLOGY 1980

Signature of Author . . . . .  
Department of Nuclear Engineering, June 1980

Certified by . . . . . Allan F. Henry  
Thesis Supervisor

Accepted by . . . . . Allan F. Henry  
Chairman, Departmental Graduate Committee  
ARCHIVES  
MASSACHUSETTS INSTITUTE  
OF TECHNOLOGY

NOV 3 1980

LIBRARIES

SPATIAL HOMOGENIZATION METHODS FOR  
LIGHT WATER REACTOR ANALYSIS

by

Kord Sterling Smith

Submitted to the Department of Nuclear Engineering on June 13, 1980,  
in partial fulfillment of the requirements for the degree of Doctor of  
Philosophy in the field of Nuclear Engineering.

ABSTRACT

The objective of this research is to develop accurate and efficient spatial homogenization methods for coarse mesh analysis of light water reactors. Koebke's "equivalence theory" homogenization scheme is generalized to obtain a homogenization method which is also capable of reproducing rigorously all node-integrated properties of any known heterogeneous reference solution. Methods for computing approximate equivalence parameters are also developed for the practical case in which reference solutions are not known.

Two methods for computing approximate equivalence parameters from heterogeneous cell calculations are presented. Analysis of several BWR benchmark problems demonstrates that use of these parameters leads to homogenized power distributions with maximum errors in assembly powers of approximately 3%. Such equivalence parameters are found to predict assembly powers with three to five times greater accuracy than is obtained with flux-weighting methods.

More sophisticated methods for computing approximate equivalence parameters are also introduced. These methods make use of nonlinear iterations between homogenized reactor calculations and local fixed-source calculations to compute equivalence parameters. Through use of such equivalence parameters, it is shown that homogenized BWR power distributions are predicted with maximum errors in assembly powers of approximately 1 %.

Thesis Supervisor: Allan F. Henry

Title: Professor of Nuclear Engineering

## TABLE OF CONTENTS

	<u>Page</u>
<b>Abstract</b>	ii
<b>Acknowledgments</b>	vi
<b>Biographical Note</b>	vii
<b>List of Figures</b>	viii
<b>List of Tables</b>	x
<b>Chapter 1. INTRODUCTION</b>	1-1
1.1 Overview and Motivations for Spatial Homogenization	1-1
1.2 Spatially Homogenized Diffusion Parameters	1-3
1.3 Traditional Approaches to Spatial Homogenization	1-7
1.4 More Sophisticated Homogenization Methods	1-9
1.5 Objectives and Summary	1-11
<b>Chapter 2. THEORETICALLY EXACT HOMOGENIZATION METHODS</b>	2-1
2.1 Introduction	2-1
2.1.1 Notation	2-2
2.2 Koebke's Homogenization Method	2-3
2.3 Generalization of Koebke's Homogenization Method	2-10
2.3.1 Generalized Equivalence Theory	2-12
2.3.2 Summary of the Generalized Equivalence Theory Homogenization Method	2-14
2.4 Implementation of Equivalence Theory Parameters into the QUANDRY Nodal Code	2-15
2.5 QUANDRY Spatial Approximations	2-20

	<u>Page</u>
<b>2.6 Benchmark Problems</b>	<b>2-23</b>
2.6.1 The Henry-Worley BWR Problem	2-23
2.6.2 The CISE BWR Benchmark Problem	2-28
<b>2.7 Summary</b>	<b>2-33</b>
 <b>Chapter 3. EVALUATION OF APPROXIMATE EQUIVALENCE PARAMETERS FROM CELL CALCULATIONS</b>	 <b>3-1</b>
3.1 Introduction	3-1
3.2 Spatial Invariance of the Generalized Equivalence Parameters	3-2
3.3 Simple Cell Calculations	3-4
3.4 Benchmark BWR Results Using CDF	3-10
3.4.1 The Henry-Worley BWR Problem	3-10
3.4.2 The CISE BWR Problem	3-12
3.4.3 An Extremely Heterogeneous BWR Problem	3-14
3.5 More Sophisticated Cell Calculations	3-16
3.6 Summary	3-19
 <b>Chapter 4. EVALUATION OF APPROXIMATE EQUIVALENCE PARAMETERS FROM LOCAL HETEROGENEOUS PROBLEMS</b>	 <b>4-1</b>
4.1 Introduction	4-1
4.2 Evaluation of Exact Equivalence Parameters from Local Heterogeneous Problems	4-2
4.3 Techniques for Solving the Local Fixed-Source Problems	4-7
4.4 Results Obtained by Using Approximate Discontinuity Factors Obtained from Local Heterogeneous Fixed- Source Calculations	4-10
4.4.1 Results Obtained Using Single-Assembly Fixed-Source Calculations	4-11

	<u>Page</u>
4.4.2 Results Obtained Using Five-Assembly Fixed-Source Calculations	4-15
4.5 Possible Modifications of the Solution Method for the Global Homogenized Problem	4-18
4.5.1 Simplified Flux-Current Coupling Relation- ships in Global Solution Methods	4-18
4.5.2 Simplified Neutron Energy Group Representations	4-19
4.5.3 The Use of Multi-Assembly Nodes in the Global Solution	4-20
4.6 Summary	4-23
 Chapter 5. SUMMARY AND CONCLUSIONS	5-1
5.1 Overview of the Investigation	5-1
5.2 Possibilities of Using Response Matrix Methods for Solving the Local Fixed-Source Problems	5-5
5.3 Recommendations for Future Research	5-7
5.3.1 Refinements in Cell Calculations Used to Obtain Approximate Equivalence Parameters	5-7
5.3.2 PWR Applications	5-8
5.3.3 3-D Effects	5-8
5.3.4 Response Matrix Considerations	5-9
 References	6-1
 Appendix 1. DESCRIPTION OF BWR TEST PROBLEMS	A1-1
 Appendix 2. NORMALIZED ASSEMBLY POWER DENSITIES	A2-0

## ACKNOWLEDGMENTS

The author extends his sincerest appreciation to his thesis supervisor, Professor Allan F. Henry, for his invaluable assistance and support during the course of this investigation. His willingness to teach, argue, listen and learn has made the author's association with him an extremely rewarding experience.

Thanks are also due to Professor David D. Lanning who served as reader for this thesis.

The author is also indebted to his office mates, Greg Greenman, Jean Koclas, Chris Hoxie and Rich Loretz for the opportunity to work, study and learn with them.

The author also wishes to thank Mrs. Mary Bosco for her assistance in the preparation of this document. Her patience and skill have made the author's association with her a distinct pleasure. The author is eternally grateful for all of her efforts.

The financial support of this research by the Electric Power Research Institute is gratefully acknowledged.

## BIOGRAPHICAL NOTE

Kord S. Smith was born August 7, 1954 in Slayton, Minnesota. He spent most of his youth in rural South Dakota and graduated with honors from Rapid City Stevens High School in May 1972.

The author enrolled at Kansas State University in September 1972 and was an active member of the Delta Sigma Phi social fraternity. He received the Durland Award for Outstanding Students in Engineering and participated in the Honors Engineering Program. He graduated Magna cum Laude and received the degree of Bachelor of Science in Nuclear Engineering in May 1976.

The author entered graduate school at the Massachusetts Institute of Technology in September 1976. In March 1979, he was awarded the degrees of Nuclear Engineer and Master of Science. During his graduate career, the author spent four summers as a research associate in the Applied Physics Division of Argonne National Laboratory at Idaho Falls, Idaho. The author received the Ph.D. degree in Nuclear Engineering in September 1980 and subsequently returned to Argonne National Laboratory.

## LIST OF FIGURES

<u>Figure</u>	<u>Page</u>
A2-1      Normalized assembly power densities and errors for the Henry-Worley BWR problem; flux- weighted solutions	A2-1
A2-2      Normalized assembly power densities and errors for the Henry-Worley BWR problem; two-group generalized equivalence parameters	A2-2
A2-3      Normalized assembly power densities and errors for the Henry-Worley BWR problem; one-group generalized equivalence parameters	A2-3
A2-4      Normalized assembly power densities and errors for the CISE BWR problem; comparison of flux- weighted (cell) and exact flux-weighted solutions	A2-4
A2-5      Normalized assembly power densities and errors for the Henry-Worley problem; comparison of flux-weighted and cell equivalence solutions (entire assemblies)	A2-5
A2-6      Normalized assembly power densities and errors for the Henry-Worley problem; comparison of flux-weighted and cell equivalence solutions (quarter assemblies)	A2-6
A2-7      Normalized assembly power densities and errors for the CISE BWR problem; comparison of flux- weighted and cell equivalence solutions	A2-7
A2-8      Normalized assembly power densities and errors for the HAFAS BWR problem; comparison of flux- weighted and cell equivalence solutions	A2-8
A2-9      Normalized assembly power densities and errors for the Henry-Worley BWR problem; comparison of flux-weighted, cell, and modified-cell equiva- lence solutions	A2-9
A2-10     Normalized assembly power densities and errors for the CISE BWR problem; comparison of flux- weighted, cell, and modified-cell equivalence solutions	A2-10

<u>Figure</u>	<u>Page</u>
A2-11 Normalized assembly power densities and errors for the HAFAS BWR problem; comparison of flux-weighted, cell, and modified-cell equivalence solutions	A2-11
A2-12 Normalized assembly power densities and errors for the Henry-Worley BWR problem; comparison of solutions obtained with single-assembly, fixed-source calculations	A2-12
A2-13 Normalized assembly power densities and errors for the CISE BWR problem; comparison of solutions obtained with single-assembly, fixed-source calculations	A2-13
A2-14 Normalized assembly power densities and errors for the HAFAS BWR problem; comparison of solutions obtained with single-assembly, fixed-source calculations	A2-14
A2-15 Normalized assembly power densities and errors for the CISE BWR problem; comparison of solutions obtained by various equivalence schemes	A2-15
A2-16 Normalized assembly power densities and errors for the HAFAS BWR problem; comparison of solutions obtained by various equivalence schemes	A2-16

## LIST OF TABLES

<u>Table</u>		<u>Page</u>
2-1	Summary of Results for the Henry-Worley BWR Problem Using Flux-Weighted Constants	2-24
2-2	Homogenized Parameters for the Henry-Worley BWR Problem	2-26
2-3	Summary of Results for the CISE BWR Problem Using Flux-Weighted Constants	2-29
2-4	Generalized Equivalence Theory Discontinuity Factors for the CISE BWR Problem	2-32
3-1	Mean Values and Standard Deviations of the Reference Equivalence Parameters for the CISE BWR Problem	3-3
3-2	Mean Values and Standard Deviations of the Reference Discontinuity Factors for the CISE BWR Problem as a Function of Assembly Type	3-5
3-3	Cell Discontinuity Factors and Their Deviations from the Mean Values of the Reference Equivalence Parameters for the CISE BWR Problem as a Function of Assembly Type	3-9
3-4	Comparison of Results for the Henry-Worley BWR Benchmark Problem Using FWC and CDF	3-11
3-5	Comparison of Results for the CISE BWR Problem Using FWC and CDF	3-13
3-6	Comparison of Results for the CISE BWR Problem Using CDF and Several Spatial Approximations	3-13
3-7	Comparison of Results for the HAFAS BWR Problem Using FWC and CDF	3-16
3-8	MCDF and Their Deviations from the Mean Values of the Reference Equivalence Parameters for the CISE BWR Problem as a Function of Assembly Type	3-18
3-9	Summary of Results for the Three BWR Benchmark Problems Using CDF and MCDF	3-20

<u>Table</u>		<u>Page</u>
4-1	Summary of Results for the Henry-Worley BWR Homogenization Problem Using Single-Assembly Fixed-Source Calculations	4-12
4-2	Summary of Results for the CISE BWR Homogenization Problem Using Single-Assembly Fixed-Source Calculations	4-14
4-3	Summary of Results for the HAFAS BWR Homogenization Problem Using Single-Assembly Fixed-Source Calculations	4-14
4-4	Comparison of Results for the CISE BWR Problem	4-17
4-5	Comparison of Results for the HAFAS BWR Problem	4-17
5-1	Comparison of Solutions to the HAFAS BWR Homogenization Problem Obtained by Various Homogenization Schemes	5-4

## Chapter 1

### INTRODUCTION

#### 1.1 OVERVIEW AND MOTIVATIONS FOR SPATIAL HOMOGENIZATION

The design and analysis of modern light water reactors require an extensive knowledge of spatial power distributions, control rod worths and neutron absorption rates. Determination of these quantities requires a knowledge of the free neutron density in space, direction, and energy. Transport theory tools such as continuous-energy Monte Carlo or multigroup discrete ordinates methods are capable of performing the required analyses.<sup>1</sup> Unfortunately, the complexity which is inherent in explicit transport theory modeling of heterogeneous reactor details (such as control rods, burnable poisons, and water rods) results in mathematical problems of such a magnitude as to be intractable for even the most advanced digital computers.

The most commonly-employed alternative to solving the global transport equation is to approximate the solution of the transport equation by solving the multigroup diffusion equation.<sup>2</sup> However, the diffusion theory approximation implicitly assumes that the angular distribution of neutrons be at most linearly anisotropic,<sup>2</sup> and this restricted representation does not approximate accurately the actual angular distributions which occur near regions of high neutron absorption (such as control rods or burnable poison pins) or near highly scattering regions with little absorption (such as water rods, water gaps, or reflectors).

Nevertheless, the actual quantities of interest (power distributions, control rod worths, etc.) can be predicted accurately by diffusion theory models provided "equivalent" homogenized cross sections and diffusion coefficients can be determined.<sup>3</sup>

The processes by which these "equivalent" diffusion theory parameters are evaluated for each localized heterogeneous region (fuel pins, control rods, etc.) can constitute a distinct level of homogenization. However, even if this single level of homogenization is carried out, the resulting diffusion theory problem may remain quite intractable. The reason for this is simply that there exist a very large number of spatial regions in a reactor core. Typically, a reactor may contain several hundred fuel assemblies, and each fuel assembly may contain several hundred fuel pins. Hence, explicit representation of heterogeneous assemblies requires tens of thousands of distinct regions for each axial plane in the reactor core that is to be analyzed. Since many core calculations are required in the design and analysis of a nuclear reactor, there is considerable economic incentive to develop methods of analysis which avoid the explicit modeling of full heterogeneous details. The usual approach to this problem is to treat large "nodes" (usually entire assemblies in a radial plane) as homogenized regions. If "equivalent" diffusion theory parameters (usually spatially constant within each node) can be determined, the reactor core calculation can be reduced to a problem involving only several hundred homogeneous regions in each axial plane of the reactor core.

Once this latter stage of homogenization has been reached, the resulting diffusion theory calculations can be performed by nodal or

finite element methods.<sup>4,5,6</sup> These methods for solving the neutron diffusion equation are capable of employing very large mesh spacings within each of the homogenized regions; hence, they are computationally very efficient. Techniques by which these desired "equivalent" diffusion theory parameters can be obtained are the subject of this thesis.

## 1.2 SPATIALLY HOMOGENIZED DIFFUSION PARAMETERS

The use of homogenized parameters to predict reactor properties results in an inevitable loss of certain information which is otherwise available if the reactor is analyzed by methods which do not involve homogenization. Nevertheless, it is possible to determine homogenized parameters which preserve certain important characteristics of the reactor. It is important to ascertain which reactor properties are the most significant and to devise homogenization methods which preserve these properties.

The most fundamental system parameter that should be preserved in the homogenization process is the reactor eigenvalue ( $k_{eff}$ ). There are also many local reactor properties that should be preserved. Naturally, it is very difficult (if not impossible) to preserve quantities which characterize any particular subregion that is contained within a homogenized region. Consequently, one is forced to settle for the preservation of the spatial integrals (over the local homogenized regions) of the quantities of interest. Such quantities of prime importance are the node-averaged neutron reaction rates in each neutron energy group and the node-averaged power densities. It is also desirable that the

homogenization methods preserve the integrals of the group currents on all of the surfaces of each homogenized region.

Perhaps the simplest means of demonstrating the difficulties associated with spatial homogenization is to assume that one knows the exact values (as functions of space, direction, and energy) of all reactor quantities that may be of interest and to attempt to define homogenized parameters which preserve all of the aforementioned reactor properties. Since the exact solution to the heterogeneous reactor problem is assumed to be known, the following quantities are also known:

$\phi_g(\underline{r})$      = scalar neutron flux in group g ( $\text{cm}^{-2} \text{ sec}^{-1}$ )

$J_g^u(\underline{r})$      = net neutron current in direction u and group g  
( $\text{cm}^{-2} \text{ sec}^{-1}$ )

$\Sigma_{tg}(\underline{r})$      = macroscopic total cross section for group g ( $\text{cm}^{-1}$ )

$\Sigma_{gg'}(\underline{r})$      = macroscopic transfer cross section from group g' to group g ( $\text{cm}^{-1}$ )

$x_g(\underline{r})$      = fission neutron spectrum to group g

$\nu \Sigma_{fg}(\underline{r})$      = macroscopic fission cross section for group g times the mean number of neutrons emitted per fission ( $\text{cm}^{-1}$ )

$\lambda$      = reactor eigenvalue ( $k_{\text{eff}}$ ).

If the corresponding quantities for the homogenized diffusion theory problem are denoted by addition of a circumflex, the homogenized parameters should be determined such that

i) all group reaction rates are preserved,

$$\int_{V_i} \hat{\Sigma}_{\alpha g}(\underline{r}) \hat{\phi}_g(\underline{r}) d\underline{r} = \int_{V_i} \Sigma_{\alpha g}(\underline{r}) \phi_g(\underline{r}) d\underline{r}; \quad g = 1, 2, \dots, G \\ \alpha = t, f, g', \text{ etc.}, \\ (1-1a)$$

ii) all group surface currents are preserved,

$$- \int_{S_i^k} \hat{D}_g(\underline{r}) \frac{\partial}{\partial \underline{n}} \hat{\phi}_g(\underline{r}) \cdot d\underline{S} = \int_{S_i^k} J_g^u(\underline{r}) \cdot d\underline{S}; \quad g = 1, 2, \dots, G \\ k = 1, 2, \dots, K, \\ (1-1b)$$

iii) the reactor eigenvalue is preserved,

$$- \sum_{k=1}^K \int_{S_i^k} \hat{D}_g(\underline{r}) \nabla \hat{\phi}_g(\underline{r}) \cdot d\underline{S} + \int_{V_i} \hat{\Sigma}_t g(\underline{r}) \hat{\phi}_g(\underline{r}) d\underline{r} \\ = \sum_{g'=1}^G \left( \int_{V_i} \hat{\Sigma}_{gg'}(\underline{r}) \hat{\phi}_{g'}(\underline{r}) d\underline{r} + \frac{1}{\lambda} \int_{V_i} \hat{x}_g(\underline{r}) \nu \hat{\Sigma}_f g'(\underline{r}) \hat{\phi}_{g'}(\underline{r}) d\underline{r} \right); \\ g = 1, 2, \dots, G, \\ (1-1c)$$

where  $G$  is the total number of neutron energy groups,  $K$  is the number of surfaces for each homogenized region,  $V_i$  is the volume of the  $i$ th homogenized region, and  $S_i^k$  is the  $k$ th surface of the  $i$ th homogenized region.

If all homogenized parameters are assumed to be spatially constant within each node, the "ideal" homogenized parameters can be rigorously defined by

$$\hat{\Sigma}_{\alpha g}^{(i)} = \frac{\int_{V_i} \Sigma_{\alpha g}(\underline{r}) \phi_g(\underline{r}) d\underline{r}}{\int_{V_i} \hat{\phi}_g(\underline{r}) d\underline{r}}; \quad g = 1, 2, \dots, G$$

$\alpha = t, f, g', \text{etc.}$

(1-2a)

and

$$\hat{D}_g^{(i)} = - \frac{\int_{S_i^k} J_g^u(\underline{r}) \cdot d\underline{S}}{\int_{S_i^k} \frac{\partial}{\partial u} \hat{\phi}_g(\underline{r}) \cdot d\underline{S}}; \quad g = 1, 2, \dots, G$$

$k = 1, 2, \dots, K.$

(1-2b)

The difficulties in evaluating homogenized parameters become clear when Eqs. 1-2 are examined closely. First, an a priori knowledge of integrated reaction rates and net currents for each node is required. Second, even if these quantities are assumed known, the flux shape which results from the use of the homogenized constants must also be known. Since the homogenized flux shape is strongly coupled to the values of the homogenized parameters, a nonlinearity is introduced into the process of evaluating homogenized parameters. An additional dilemma also exists in that the relationship expressed by Eq. 1-2b must be valid for all of the K surfaces of the ith node. If conventional continuity conditions (of scalar flux and net current) are imposed on all nodal surfaces, Eq. 1-2b will define values of  $\hat{D}_g^{(i)}$  which are different for each surface of node i. This contradicts the assumption that all of the homogenized parameters are spatially constant within each node. Thus, it appears to be impossible to define spatially constant values of  $\hat{D}_g^{(i)}$  which preserve all of the conditions of Eqs. 1-1 (except for very special cases). Consequently, this

situation dictates that either additional degrees of freedom be added to the homogenized parameters such that the conditions of Eqs. 1-1 can be met or that some of the conditions be relaxed.

### 1.3 TRADITIONAL APPROACHES TO SPATIAL HOMOGENIZATION

The most commonly-employed procedures for determining homogenized parameters avoid the theoretical pitfalls mentioned in the preceding section by relaxing the conditions for which the quantities of interest are preserved. Since in practice the exact solution to the reactor problem is never known, the numerators of Eqs. 1-2 are approximated by performing a cell calculation for each distinct type of fuel assembly.<sup>2</sup> That is, a high-order calculation (which either directly or indirectly represents all heterogeneous details) is performed for each assembly type, with a zero net neutron current condition imposed across each assembly surface. The assumption that homogenized parameters can be computed from a cell calculation with zero current boundary conditions is usually rationalized by noting that most assemblies in a reactor are surrounded by other assemblies of a similar composition. Also, global flux shapes are such that only a slight amount of curvature exists across each assembly and consequently, net surface currents should be small in magnitude. The higher-order methods used to solve the cell problem can be Monte Carlo, multigroup discrete ordinates, integral transport, multigroup diffusion theory, or multilevel schemes which combine several of these methods.<sup>1</sup> Regardless of the particular choice of methods used to solve the cell problem, once the problem has been solved, the

numerators of Eqs. 1-2 are assumed known.

The next approximation which is generally made is that

$$\int_{V_i} \hat{\phi}(\underline{r}) d\underline{r} = \int_{V_i} \phi(\underline{r}) d\underline{r} .$$

This approximation, although plausible, is never strictly valid since none of the homogenized regions in realistic reactors satisfies the conditions (zero net current on each surface) for which the heterogeneous flux shape is computed.

The last and perhaps most inaccurate approximation that is frequently made is that the homogenized diffusion coefficients can be defined such that

$$\frac{1}{\hat{D}_g^{(i)}} \equiv \frac{\int_{V_i} \frac{1}{D_g(\underline{r})} \phi_g(\underline{r}) d\underline{r}}{\int_{V_i} \phi_g(\underline{r}) d\underline{r}} . \quad (1-3)$$

The justification for this approximation is that  $1/D_g(\underline{r})$  is proportional to the macroscopic neutron transport cross section,<sup>2</sup> and it is desired to preserve the neutron transport rate. Close scrutiny, however, reveals that the transport cross section is a function of the net neutron current and hence, weighting the transport cross section by the flux does not preserve the transport rate.

Homogenized parameters determined by making the previous three approximations are generally referred to as flux-weighted constants (FWC). Use of the flux-weighting method to obtain homogenized parameters is very common in modern LWR analysis. On theoretical grounds, there exist many deficiencies in this method, and in a

rigorous sense the solution to the global homogenized reactor problem preserves none of the quantities of Eqs. 1-1. Although the aforementioned assumptions are plausible, there exist many assemblies in a reactor for which they are quite invalid. For instance, assemblies which contain control rods, assemblies adjacent to rodded assemblies, and assemblies near the reflector have net surface currents which are quite large. Consequently, the zero net current assumption may be grossly in error.

Flux-weighted parameters have many practical limitations, as well as theoretical deficiencies, in light water reactor applications. In BWR analysis, flux-weighted two-group constants tend to overpredict significantly the thermal neutron currents between assemblies. As a result, the predicted assembly power densities may be in error by as much as 10%.<sup>7</sup> Many prescriptions for eliminating the inaccuracies which result from the use of flux-weighted parameters have been developed.<sup>8</sup> However, many of these prescriptions have questionable theoretical foundations and consequently, their adoption is justified primarily by empirical demonstrations of their accuracy.

#### 1.4 MORE SOPHISTICATED HOMOGENIZATION METHODS

Although flux-weighting methods are the most commonly-employed homogenization techniques, there are several homogenization schemes which have stronger theoretical foundations. For example, in one-dimensional homogenization problems, exact homogenized parameters can be determined if the constraint of Eq. 1-1b is relaxed such that only the group-summed reaction rates are preserved (i.e., individual group reaction rates are not preserved).<sup>3</sup> However, Henry et al. have

found that such formulations may produce homogenized parameters which appear to be unphysical (e.g., negative cross sections, negative diffusion coefficients), even though they do preserve the overall reaction rates and reactor eigenvalue.<sup>3</sup> Unfortunately, such techniques can not be extended to the multidimensional case.

Since most LWR assemblies display significant heterogeneity in at least two dimensions, the one-dimensional homogenization methods are not directly useable in LWR analysis. However, some of the ideas developed in one dimension can be adapted to multidimensional homogenization problems. One such homogenization method is that of Worley and Henry.<sup>9</sup> In this method, the heterogeneous reaction rates (numerator of Eq. 1-2a) are computed by response matrix techniques. The difficulties in determining the integral of the homogenized flux (denominator of Eq. 1-2b) are avoided by assuming that the homogenized fluxes can be expanded in cubic Hermite polynomials whose coefficients are chosen by matching the values of the homogenized fluxes and their derivatives on each surface of the assembly. This approximation is much superior to the assumption of the flux-weighting methods (equivalence of heterogeneous and homogenized flux integrals) because homogenized flux shapes tend to be relatively smooth, as are the cubic Hermite polynomials. Lastly, the homogenized diffusion coefficients are chosen in such a way that the G largest homogenized response matrix elements match the corresponding heterogeneous response matrix elements. This approximation permits the homogenized parameters to match many leakage characteristics of the heterogeneous assembly.

Although Worley's homogenization method is not exact, in the sense that none of the quantities of Eq. 1-1 is preserved exactly, the method has been demonstrated to be more accurate than flux-weighting methods for several test problems. The primary drawbacks to Worley's method are its somewhat complicated nature and its computational efficiency. There also exists some evidence which demonstrates that the use of Worley's method may lead to larger errors than flux-weighting methods in certain reactor problems.<sup>10</sup>

Many additional homogenization methods exist in the literature,<sup>11, 12, 13</sup> some of which lack the firm theoretical basis that is desirable. They will not be described here. There is, however, one unique homogenization method which is capable of reproducing rigorously all of the desired quantities of Eqs. 1-1. This method, due to Koebke,<sup>14</sup> is described in detail in Chapter 2.

## 1.5 OBJECTIVES AND SUMMARY

The objective of this thesis is to develop accurate efficient diffusion theory homogenization methods for coarse mesh analysis of light water reactors (LWRs). In Chapter 2, a theoretically exact homogenization method is derived by generalizing some of Koebke's previous work.<sup>14</sup> In Chapter 3, an approximation to the theoretically exact method is introduced, and results of several test problems are presented. Additional and more accurate approximations are developed in Chapter 4, and the results of several complicated BWR problems are detailed. Finally, a summary of this investigation, conclusions about the homogenization methods, and recommendations for future research are given in Chapter 5.

## Chapter 2

### THEORETICALLY EXACT HOMOGENIZATION METHODS

#### 2.1 INTRODUCTION

In Chapter 1, the theoretical deficiencies of conventional homogenization methods were discussed. In particular, it was shown that flux-weighted constants do not preserve any of the integral quantities of interest ( $k_{eff}$ , nodal reaction rates, and nodal surface currents) from a heterogeneous reference solution. Other more sophisticated homogenization schemes were also shown to possess this same shortcoming.

In this chapter, Koebke's "equivalence theory" homogenization method will be presented and demonstrated to be capable of reproducing exactly node-averaged reaction rates for any heterogeneous reactor. Koebke's method will then be extended to obtain a "generalized equivalence theory" homogenization method which is also capable of reproducing the node-averaged properties of any reference solution. The mathematical details of the implementation of generalized equivalence theory into the coarse mesh nodal code QUANDRY will be presented, and two BWR benchmark problems will be solved to demonstrate that the homogenization method does reproduce exactly all of the desired quantities from the heterogeneous reference solution.

### 2.1.1 Notation

Throughout the course of this investigation, the global heterogeneous reactor problem and the corresponding homogenized problem are treated in three-dimensional Cartesian geometry. The methods to be developed are applicable to other geometries, but such applications are not pursued in this thesis. In addition to using  $x$ ,  $y$ , and  $z$  to represent the three coordinate directions, a more general notation for coordinate directions proves quite useful. Accordingly,  $u$ ,  $v$ , and  $w$  are used as generalized coordinate subscripts. The spatial domain of the homogenized problem is subdivided into a regular array of right rectangular parallelepipeds (nodes) with grid indices defined by  $u_\ell$ ,  $v_m$ ,  $w_n$  where

$$\ell, m, n \equiv \begin{cases} i = 1, 2, \dots, I; u, v, w = x \\ j = 1, 2, \dots, J; u, v, w = y \\ k = 1, 2, \dots, K; u, v, w = z. \end{cases}$$

As an example of the future use of this generalized coordinate notation, the net currents on the faces of node  $(i, j, k)$  as a function of the two transverse directions are expressed as

$$\hat{J}_{g_{i,j,k}}^u(v, w) = -\hat{D}_{g_{i,j,k}} \frac{\partial}{\partial u} \hat{\phi}_g(u_\ell, v, w); \quad u = x, y, z \\ v \neq u \\ w \neq u \neq v.$$

This single equation actually expresses three equations:

- 1) The  $x$ -directed net current on the  $x=x_i$  face, as a function of  $y$  and  $z$  ( $u = x$ ,  $v = y$ ,  $w = z$ )

- 2) The  $y$ -directed net current on the  $y = y_j$  face, as a function of  $x$  and  $z$  ( $u = y$ ,  $v = x$ ,  $w = z$ )
- 3) The  $z$ -directed net current on the  $z = z_k$  face, as a function of  $x$  and  $y$  ( $u = z$ ,  $v = x$ ,  $w = y$ ).

The node  $(i, j, k)$  is defined by

$$x \in [x_i, x_{i+1}]$$

$$y \in [y_j, y_{j+1}]$$

$$z \in [z_k, z_{k+1}].$$

The node widths are then defined as

$$h_\ell^u \equiv u_{\ell+1} - u_\ell; \quad u = x, y, z,$$

and the node volume is

$$V_{i,j,k} \equiv h_i^x h_j^y h_k^z.$$

## 2.2 KOEBKE'S HOMOGENIZATION METHOD

In order to derive Koebke's homogenization method, one must assume that the exact global reactor solution is known. With this lone assumption, it is possible to derive, in a formal fashion, a set of homogenized differential equations whose solution will preserve simultaneously all of the quantities ( $k_{eff}$ , group reaction rates, and group surface currents) of Eqs. 1-1 in all homogenized regions.

Neutron balance in node  $(i, j, k)$  of the heterogeneous reactor can be expressed using the notation of the previous section as

$$\begin{aligned}
& h_j^y h_k^z \left( J_{g_{i+1,j,k}}^x - J_{g_{i,j,k}}^x \right) + h_i^x h_k^z \left( J_{g_{i,j+1,k}}^y - J_{g_{i,j,k}}^y \right) \\
& + h_i^x h_j^y \left( J_{g_{i,j,k+1}}^z - J_{g_{i,j,k}}^z \right) + V_{i,j,k} \bar{\Sigma}_{t_{g_{i,j,k}}} \bar{\phi}_{g_{i,j,k}} \\
& = \sum_{g'=1}^G V_{i,j,k} \left( \bar{\Sigma}_{gg'_{i,j,k}} + \frac{1}{\lambda} \overline{x_g \nu \Sigma_{fg'_{i,j,k}}} \right) \bar{\phi}_{g'_{i,j,k}} ; \\
& g = 1, 2, \dots, G , \quad (2-1)
\end{aligned}$$

where

$$\begin{aligned}
\bar{\phi}_{g_{i,j,k}} &= \frac{\int_{x_i}^{x_{i+1}} dx \int_{y_j}^{y_{j+1}} dy \int_{z_k}^{z_{k+1}} dz \phi_g(x,y,z)}{V_{i,j,k}} \\
\bar{\Sigma}_{\alpha g_{i,j,k}} &= \frac{\int_{x_i}^{x_{i+1}} dx \int_{y_j}^{y_{j+1}} dy \int_{z_k}^{z_{k+1}} dz \Sigma_{\alpha g}(x,y,z) \phi_g(x,y,z)}{\bar{\phi}_{g_{i,j,k}} V_{i,j,k}} ; \\
& \alpha = t, f, g' , \text{etc.}
\end{aligned}$$

$$\begin{aligned}
J_{g_{i,j,k}}^u &= \frac{\int_{v_m}^{v_{m+1}} dv \int_{w_n}^{w_{n+1}} dw J_g^u(u_\ell, v, w)}{h_m^v h_n^w} ; \quad u = x, y, z \\
& \quad v \neq u \\
& \quad w \neq u \neq v .
\end{aligned}$$

Similarly, if the homogenized cross sections are defined to be equal to the flux-weighted heterogeneous cross sections for each node (i.e.,  $\hat{\Sigma}_{\alpha g_{i,j,k}} = \bar{\Sigma}_{\alpha g_{i,j,k}}$ ), the homogenized neutron balance relationship, Eq. 1-1c, can be expressed as

$$\begin{aligned}
& h_j^y h_k^z \left( \hat{j}_{g_{i+1,j,k}}^x - \hat{j}_{g_{i,j,k}}^x \right) + h_i^x h_k^z \left( \hat{j}_{g_{i,j+1,k}}^y - \hat{j}_{g_{i,j,k}}^y \right) \\
& + h_i^x h_j^y \left( \hat{j}_{g_{i,j,k+1}}^z - \hat{j}_{g_{i,j,k}}^z \right) + v_{i,j,k} \hat{\Sigma}_t_{g_{i,j,k}} \hat{\phi}_{g_{i,j,k}} \\
& = \sum_{g'=1}^G v_{i,j,k} \left( \hat{\Sigma}_{gg'}_{i,j,k} + \frac{1}{\lambda} \chi_g \nu \hat{\Sigma}_f_{g'}_{i,j,k} \right) \hat{\phi}_{g'}_{i,j,k}; \\
& g = 1, 2, \dots, G. \quad (2-2)
\end{aligned}$$

Since each of the surface terms of Eqs. 2-1 and 2-2 are by assumption identical and the terms involving cross sections are by definition equal, the homogeneous average flux must be equal to the heterogeneous average flux (i.e.,  $\hat{\phi}_{g_{i,j,k}} = \bar{\phi}_{g_{i,j,k}}$ ) in each homogenized node. Consequently, these homogenized parameters preserve the reactor eigenvalue and group reaction rates, provided that additional homogenized parameters can be constructed such that all group surface currents are preserved.

In order to determine surface currents, it is necessary to postulate a relationship between the homogenized currents and homogenized fluxes, and to maintain continuity with conventional homogenization methods, Koebke assumes that

$$\begin{aligned}
\hat{j}_g^u(\underline{r}) &= -\hat{D}_g^u \frac{\partial}{\partial u} \hat{\phi}_g(\underline{r}); \quad g = 1, 2, \dots, G \\
u &= x, y, z, \quad (2-3)
\end{aligned}$$

where the diffusion coefficient is assumed to be directionally dependent. The diffusion coefficients are not, however, related to those of the flux-weighting methods, but rather, they are treated as totally artificial quantities which can be chosen in such a manner as to match the nodal

leakage terms. With this definition for homogenized current, the differential equations which describe the homogenized flux distribution in node  $(i, j, k)$  can be written as

$$\begin{aligned}
 & -\nabla \cdot \hat{\underline{D}}_{g_{i,j,k}} \cdot \nabla \hat{\phi}_g(x, y, z) + \hat{\Sigma}_{t_{g_{i,j,k}}} \hat{\phi}_{g_{i,j,k}}(x, y, z) \\
 & = \sum_{g'=1}^G \left( \hat{\Sigma}_{gg'}{}_{i,j,k} + \frac{1}{\lambda} \chi_g \nu \hat{\Sigma}_{f_{g'}}{}_{i,j,k} \right) \hat{\phi}_{g'}{}_{i,j,k}(x, y, z); \\
 & g = 1, 2, \dots, G, \quad (2-4)
 \end{aligned}$$

where the tensor notation of Ref. 2 has been used to account for the directional dependence of the homogenized diffusion coefficient.

The conditions of Eq. 1-1b do not require that the homogenized group surface currents match the heterogeneous surface currents, but only that the averages are preserved. Therefore, the differential equations which the homogenized fluxes must obey can be determined by treating the directions one at a time and spatially integrating Eq. 2-4 over the two directions transverse to the direction of interest, to obtain for direction  $u$  and node  $(\ell, m, n)$

$$\begin{aligned}
 & -h_m^v h_n^w \hat{D}_{g_{\ell,m,n}}^u \frac{\partial^2}{\partial u^2} \hat{\phi}_{g_{\ell,m,n}}^{(u)} - \hat{D}_{g_{\ell,m,n}}^v \int_{v_m}^{v_{m+1}} dv \int_{w_n}^{w_{n+1}} dw \frac{\partial^2}{\partial v^2} \hat{\phi}_g^{(u,v,w)} \\
 & - \hat{D}_{g_{\ell,m,n}}^w \int_{v_m}^{v_{m+1}} dv \int_{w_n}^{w_{n+1}} dw \frac{\partial^2}{\partial w^2} \hat{\phi}_g^{(u,v,w)} + h_m^v h_n^w \hat{\Sigma}_{t_{g_{\ell,m,n}}} \hat{\phi}_{g_{\ell,m,n}}^{(u)} \\
 & = \sum_{g'=1}^G h_m^v h_n^w \left( \hat{\Sigma}_{gg'}{}_{\ell,m,n} + \frac{1}{\lambda} \chi_g \nu \hat{\Sigma}_{f_{g'}}{}_{\ell,m,n} \right) \hat{\phi}_{g'}{}_{\ell,m,n}^{(u)}; \\
 & g = 1, 2, \dots, G, \quad u = x, y, z, \\
 & v \neq u, \quad w \neq u \neq v, \quad (2-5)
 \end{aligned}$$

where

$$\hat{\phi}_{g_{\ell,m,n}}^u(u) \equiv \frac{\int_{v_m}^{v_{m+1}} dv \int_{w_n}^{w_{n+1}} dw \hat{\phi}_g(u, v, w)}{h_m^v h_n^w}.$$

Equation 2-5, when multiplied by  $du$ , is simply a statement of neutron balance within a slab contained in node  $(\ell, m, n)$  which has the height and depth of the node, but which is of thickness  $du$  (in the  $u$  direction) about the point  $u$ . Hence, the two integrals represent the net rate at which neutrons leak out of the four surfaces of the slab which are transverse to direction  $u$ . The following notation for the net leakages is convenient:

$$h_n^w \hat{L}_g^v(\mathbf{u}) = -\hat{D}_g^v \int_{v_m}^{v_{m+1}} dv \int_{w_n}^{w_{n+1}} dw \frac{\partial^2}{\partial v^2} \hat{\phi}_g(u, v, w);$$

$$g = 1, 2, \dots, G \quad u = x, y, z$$

$$v = x, y, z \quad v \neq u$$

$$w = y, z \quad w \neq u \neq v. \quad (2-6)$$

Also, by defining the sum of the two net leakages transverse to direction  $u$ , per unit  $u$ , divided by  $h_m^v h_n^w$  as

$$\hat{S}_{g_{\ell,m,n}}^u(u) \equiv \frac{1}{h_m^v} \hat{L}_g^v(\mathbf{u}) + \frac{1}{h_n^w} \hat{L}_g^w(\mathbf{u});$$

$$g = 1, 2, \dots, G \quad u = x, y, z$$

$$v \neq u \quad w \neq u \neq v, \quad (2-7)$$

Equation 2-5 can be cast in the form

$$\begin{aligned}
& -\hat{D}_{g_{\ell,m,n}}^u \frac{\partial^2}{\partial u^2} \hat{\phi}_{g_{\ell,m,n}}^u(u) + \hat{\Sigma}_{t_{g_{\ell,m,n}}} \hat{\phi}_{g_{\ell,m,n}}^u(u) \\
& - \sum_{g'=1}^G \left( \hat{\Sigma}_{gg'}{}_{\ell,m,n} + \frac{1}{\lambda} x_g \nu \hat{\Sigma}_{f_{g'}{}_{\ell,m,n}} \right) \hat{\phi}_{g'{}_{\ell,m,n}}^u(u) = -\hat{S}_{g_{\ell,m,n}}^u(u); \\
& g = 1, 2, \dots, G \\
& u = x, y, z. \quad (2-8)
\end{aligned}$$

By virtue of the fact that the exact global reactor solution is assumed known, the net leakage distribution (Eq. 2-7) is also known. Thus, Eq. 2-7, Eq. 2-8, and two appropriate boundary conditions per group constitute a well-posed, one-dimensional boundary value problem for the one-dimensional homogenized flux distributions in node  $(\ell, m, n)$ .

By choosing the two boundary conditions for the boundary value problem to be the values of the heterogeneous group surface currents, one is assured that the homogenized nodal flux solution will preserve the surface currents. However, one must consider that ultimately it is the global homogenized reactor equations which must be solved. In doing so, it is necessary to relate group surface currents and surface fluxes between adjacent homogenized regions. Since the heterogeneous group surface currents are continuous and since preservation of the group surface currents is postulated, it is necessary that the homogenized group surface currents be continuous at all nodal interfaces.

The situation with respect to group surface fluxes is much less clear. Any arbitrary choice for  $\hat{D}_{g_{\ell,m,n}}^u$  will result in a unique solution to the boundary value problem of Eq. 2-8, but unfortunately, the homogenized flux shapes will be such that the homogenized surface

fluxes do not match the heterogeneous surface fluxes. Consequently, it is difficult to determine the appropriate interface relationship between nodal surface fluxes. It is possible, however, to adjust the group diffusion coefficients of Eq. 2-8 such that the homogenized surface fluxes match the heterogeneous surface fluxes on one boundary of node  $(\ell, m, n)$ . Unfortunately, in the general case, the homogenized surface fluxes on the opposite surface will not match the heterogeneous surface fluxes, and the difficulty of relating homogenized surface fluxes at nodal interfaces remains. Hence, it can be concluded that Eq. 2-8 does not have enough degrees of freedom to permit the homogenized solution to match both surface currents and fluxes at all nodal interfaces.

Koebke overcame this difficulty by postulating the existence of an additional homogenization parameter. He defined the ratios of the known heterogeneous surface fluxes to the homogenized surface fluxes to be "heterogeneity factors":

$$f_{g_{\ell,m,n}}^u(u_\ell) = \frac{\phi_{g_{\ell,m,n}}^u(u_\ell)}{\hat{\phi}_{g_{\ell,m,n}}^u(u_\ell)} ; \quad g = 1, 2, \dots, G \\ u = x, y, z . \quad (2-9)$$

Since the values of the diffusion coefficients remained to be specified, Koebke chose to restrict the values of  $\hat{D}_{g_{\ell,m,n}}^u$  such that

$$f_{g_{\ell,m,n}}^u(u_\ell) = f_{g_{\ell,m,n}}^u(u_{\ell+1}) , \quad (2-10)$$

that is, such that for a given direction the heterogeneity factors are the same on both opposite surfaces of a given node. By virtue of the

fact that the heterogeneous surface fluxes must be continuous, the homogenized flux continuity condition must be

$$\hat{\phi}_{g_{\ell-1,m,n}}^u (u_\ell) f_{g_{\ell-1,m,n}}^u = \hat{\phi}_{g_{\ell,m,n}}^u (u_\ell) f_{g_{\ell,m,n}}^u ; \quad g = 1, 2, \dots, G \\ u = x, y, z , \quad (2-11)$$

where the arguments of the heterogeneity factors have been dropped to reflect the fact that they are identical on both surfaces of a given node.

Koebke's homogenization method is very different from conventional schemes in that continuity of homogenized fluxes at nodal interfaces is not assumed, and the magnitude of the discontinuity is treated as a homogenization parameter. The homogenized parameters in Koebke's method are evaluated by finding the values of the diffusion coefficients such that the solution to Eq. 2-8 (with heterogeneous surface currents as boundary conditions) satisfies Eq. 2-10. The homogenized parameters consist of cross sections (Eq. 2-1), diffusion coefficients (for each direction), and heterogeneity factors. Once these parameters are evaluated for each node, the global homogenized differential equation (Eq. 2-4) can be solved (with Eq. 2-11 and current continuity as interface conditions), and the homogenized solution will preserve  $k_{eff}$ , all group reaction rates, and group surface currents. Koebke calls this homogenization method "equivalence theory."

## 2.3 GENERALIZATION OF KOEBKE'S HOMOGENIZATION METHOD

Koebke's equivalence theory is a significant development in homogenization theory, since it provides a systematic means of defining the

system of homogenized equations which when solved will reproduce all of the desired heterogeneous quantities ( $k_{\text{eff}}$ , group reaction rates, and group surface currents). No mention has been made of the number of neutron energy groups employed in the equivalence theory problem, and in fact, the preservation of reaction rates, currents and  $k_{\text{eff}}$  is independent of the number of groups that are used. In a formal fashion (the true heterogeneous reactor solution must be known), it is possible to define "exact" homogenized parameters via equivalence theory with only one neutron energy group.

Koebke's method of constraining the diffusion coefficients such that the heterogeneity factors are (for a given direction) identical on both surfaces of a given node requires that an iterative method be used to determine the diffusion coefficients. At each step in the iteration, Eq. 2-8 must be solved (for all groups) to ascertain if the constraining conditions (Eq. 2-10) have been met. If the conditions have not been met, new values of the diffusion coefficients must be computed, and the process repeated until convergence is achieved. This iteration must be performed for each node and each direction. Thus the process is somewhat awkward (especially as the number of neutron energy groups increase), and methods for avoiding completely the iteration are introduced in the following section.

If for a given direction, there exists a homogenized region which is situated such that the reactor is symmetric with respect to that region, there exist an infinite number of combinations of diffusion coefficients and heterogeneity factors for which the solution to Eq. 2-8 will satisfy the boundary conditions and the constraint of Eq. 2-10. In such

cases, Koebke fixes arbitrarily the diffusion coefficients and computes the corresponding heterogeneity factors.

### 2.3.1 Generalized Equivalence Theory

Equivalence theory, as introduced by Koebke, contains no theoretical stumbling blocks. However, in practice it would be very convenient if one could avoid the necessity of iterating to evaluate the homogenized parameters and if the special cases (where an infinite number of combinations of homogenized parameters are possible) could be eliminated. Fortunately, there exists a simple method for avoiding these two problem areas.

As was mentioned previously, an arbitrary choice of diffusion coefficients results in a unique solution to the boundary value problem (Eq. 2-8) which is used to determine Koebke's heterogeneity factors. Koebke's iterative problem arises from the demand that the diffusion coefficients be determined such that the heterogeneity factors are the same on opposite surfaces of a given node. If one uses any arbitrary choice of diffusion coefficients and defines two discontinuity factors for each node (and each direction) by

$$f_{g_{\ell,m,n}}^u - = \frac{\phi_{g_{\ell,m,n}}^u (u_{\ell})}{\hat{\phi}_{g_{\ell,m,n}}^u (u_{\ell})} \quad (2-12)$$

$$f_{g_{\ell,m,n}}^u + = \frac{\phi_{g_{\ell,m,n}}^u (u_{\ell+1})}{\hat{\phi}_{g_{\ell,m,n}}^u (u_{\ell+1})},$$

it is also possible to define "exact" homogenized parameters which preserve all of the quantities of interest. This method also avoids the problems associated with symmetrically-positioned nodes, since Koebke's assumption of arbitrary diffusion coefficients is a special case of this method. The new flux continuity condition which corresponds to Eq. 2-11 is given by

$$\hat{\phi}_{g_{\ell-1,m,n}}^u (u_\ell) f_{g_{\ell-1,m,n}}^{u^+} = \hat{\phi}_{g_{\ell,m,n}}^u (u_\ell) f_{g_{\ell,m,n}}^u ; \quad u = x, y, z. \quad (2-13)$$

The  $f_{g_{\ell,m,n}}^u$ 's will be referred to as "discontinuity factors" to distinguish them from Koebke's heterogeneity factors. As a consequence of this generalization of equivalence theory, two discontinuity factors are defined for each node (for each direction) in the homogenized problem, instead of Koebke's single heterogeneity factor for each node (for each direction).

There also exists a much more subtle but very important implication of equivalence theory. This implication is that "exact" homogenized parameters can be defined even if the one-dimensional boundary value problem (which defines the homogenized parameters) is solved by an approximate method. The only constraints on the approximate methods used to solve Eq. 2-8 are that they preserve the average surface currents for all surfaces. For example, the transverse leakage source term of Eq. 2-8 can be approximated as spatially flat or the second derivative term can be approximated as spatially constant. Any approximations that are made to solve Eq. 2-8 will change the values of the discontinuity factors, but the "equivalence" parameters

will preserve all of the quantities of interest when the global homogenized problem is solved. In this sense, the discontinuity factors reflect all of the approximations (including classic spatial truncation) which are made in solving the boundary value problem. The important point to note, however, is that it is crucial that identical approximations be made in both the determination of discontinuity factors and in solving the homogenized reactor equations (Eq. 2-4). This aspect of equivalence theory is unique in that one is not attempting to find homogenized parameters which reproduce the exact reactor solution when the homogenized reactor equations are solved exactly, but rather, one defines homogenized parameters which reproduce the exact reactor solution even though the homogenized reactor equations are solved approximately.

### 2.3.2 Summary of the Generalized Equivalence Theory Homogenization Method

The steps involved in the implementation of generalized equivalence theory can be summarized as follows:

- i) The exact solution to the heterogeneous global reactor problem is assumed to be known.
- ii) Flux-weighted cross sections (Eq. 2-1) are evaluated for each node by weighting with the local heterogeneous fluxes.
- iii) The diffusion coefficients are arbitrarily chosen for each node (usually computed by weighting the heterogeneous diffusion coefficients with the local heterogeneous flux).
- iv) One-dimensional boundary value problems (Eq. 2-8) are solved (with heterogeneous surface currents as boundary conditions) to

obtain the one-dimensional homogenized surface fluxes for each node and each direction.

- v) Discontinuity factors are computed (Eq. 2-12) for each surface of each homogenized region.
- vi) The global homogenized reactor equations (Eq. 2-4) are solved (allowing flux discontinuities at all surfaces), perhaps approximately, but using approximations identical to those employed in Step iv.

This homogenization method is "exact" in the sense that the solution to the homogenized reactor equations will reproduce the reactor eigenvalue ( $k_{eff}$ ), all group reaction rates, and all group surface currents of the heterogeneous solution.

## 2.4 IMPLEMENTATION OF EQUIVALENCE THEORY PARAMETERS INTO THE QUANDRY NODAL CODE

Koebke modified successfully the nodal expansion method<sup>5</sup> (NEM) to solve the equivalence equations (Eq. 2-8) to obtain the current coupling between adjacent homogenized regions. In solving these equations, NEM approximates the transverse leakage shapes and group flux shapes by low-order polynomials, and weighted residual techniques are applied to obtain the flux expansion coefficients. Despite the approximations that are made, Koebke demonstrated that his homogenization method is capable of reproducing "exactly" (i.e., exact to five significant figures) the known heterogeneous solution for a simple benchmark problem.<sup>14</sup>

Equivalence theory can be incorporated into the framework of any consistently-formulated method that solves the conventional diffusion

equations. There exist many nodal methods<sup>4, 5, 6</sup> which solve directly the one-dimensional flux equations (Eq. 2-8) to obtain the current coupling between nodes. Consequently, it is much easier to incorporate equivalence theory into such nodal methods than it is to make the adaptations for non-nodal methods (e.g., fine mesh finite difference methods). In this thesis, in order to test generalized equivalence theory and many approximate equivalence methods (to be presented in forthcoming chapters), the 2-group coarse mesh nodal code, QUANDRY,<sup>4</sup> is extended to solve the generalized equivalence equations.

The QUANDRY code employs the Analytic Nodal Method to solve the one-dimensional flux equations (Eq. 2-8). In solving these equations, the only assumption which is required is that the transverse leakage shape (Eq. 2-7) within a node can be approximated by low-order polynomials (flat or quadratic). For present purposes, knowledge of several mathematical relationships which are embodied in QUANDRY will suffice to illustrate the modifications that are required to incorporate generalized equivalence theory into QUANDRY.

Application of the Analytic Nodal Method results in two approximate equations for the surface fluxes (at  $u = u_\ell$ ) of the following form:

$$\begin{aligned}
 [\hat{\phi}_{\ell-1,m,n}^u(u_\ell)] &= [B_{\ell-1,m,n}^u][\hat{\phi}_{\ell-1,m,n}] - [A_{\ell-1,m,n}^u][\hat{j}_{\ell-1,m,n}^u(u_\ell)] \\
 &\quad - \{[C_{\ell-1,m,n}^{u+}]a_{\ell-1}^{u-} + [D_{\ell-1,m,n}^{u+}]b_{\ell-1}^{u-} + [E_{\ell-1,m,n}^{u+}]c_{\ell-1}^{u-}\}[\hat{s}_{\ell-2,m,n}^u] \\
 &\quad - \{[C_{\ell-1,m,n}^{u+}](1 - a_{\ell-1}^{u-} - a_{\ell-1}^{u+}) + [D_{\ell-1,m,n}^{u+}](-b_{\ell-1}^{u-} - b_{\ell-1}^{u+}) \\
 &\quad \quad + [E_{\ell-1,m,n}^{u+}](-c_{\ell-1}^{u-} - c_{\ell-1}^{u+})\}[\hat{s}_{\ell-1,m,n}^u] \\
 &\quad - \{[C_{\ell-1,m,n}^{u+}]a_{\ell-1}^{u+} + [D_{\ell-1,m,n}^{u+}]b_{\ell-1}^{u+} + [E_{\ell-1,m,n}^{u+}]c_{\ell-1}^{u+}\}[\hat{s}_{\ell,m,n}^u]
 \end{aligned} \tag{2-14a}$$

$$\begin{aligned}
[\hat{\phi}_{\ell,m,n}^u(u_\ell)] &= [B_{\ell,m,n}^u][\hat{\phi}_{\ell,m,n}] + [A_{\ell,m,n}^u][\hat{J}_{\ell,m,n}(u_\ell)] \\
&\quad - \{[C_{\ell,m,n}^u]a_\ell^{u^-} + [D_{\ell,m,n}^u]b_\ell^{u^-} + [E_{\ell,m,n}^u]c_\ell^{u^-}\} [\hat{S}_{\ell-1,m,n}^u] \\
&\quad - \{[C_{\ell,m,n}^u](1 - a_\ell^{u^-} - a_\ell^{u^+}) + [D_{\ell,m,n}^u](-b_\ell^{u^-} - b_\ell^{u^+}) \\
&\quad \quad + [E_{\ell,m,n}^u](-c_\ell^{u^-} - c_\ell^{u^+})\} [\hat{S}_{\ell,m,n}^u] \\
&\quad - \{[C_{\ell,m,n}^u]a_\ell^{u^+} + [D_{\ell,m,n}^u]b_\ell^{u^+} + [E_{\ell,m,n}^u]c_\ell^{u^+}\} [\hat{S}_{\ell+1,m,n}^u]; \\
&\qquad u = x, y, z, \tag{2-14b}
\end{aligned}$$

where

$[\hat{\phi}_{\ell,m,n}]$  is a column vector of node-averaged homogenized group fluxes for node  $(\ell, m, n)$ ,

$[\hat{\phi}_{\ell,m,n}^u(u_\ell)]$  is a column vector of homogenized surface fluxes for node  $(\ell, m, n)$  at  $u = u_\ell$ ,

$[\hat{J}_{\ell,m,n}^u(u_\ell)]$  is a column vector of homogenized surface currents for node  $(\ell, m, n)$  and direction  $u$  at  $u = u_\ell$ ,

$[\hat{S}_{\ell,m,n}^u]$  is a column vector of node-averaged transverse leakages for node  $(\ell, m, n)$  and direction  $u$ , defined by Eq. 2-7.

The  $G \times G$  matrices in Eqs. 2-14 are defined in Appendix 3 of Reference 4; they depend only on the nodal cross sections, diffusion coefficients, mesh spacings and  $k_{eff}$ . The  $a_\ell^{u^\pm}$ ,  $b_\ell^{u^\pm}$ , and  $c_\ell^{u^\pm}$  are transverse leakage expansion coefficients which depend only on the nodal mesh spacings; they are defined in Appendix 1 of Reference 4.

In conventional diffusion theory, Eq. 2-14a and 2-14b are used to eliminate the surface fluxes at  $u = u_\ell$  by assuming continuity of homogenized fluxes, and the resulting equation yields an approximate expression for the surface currents at  $u = u_\ell$ . In generalized equivalence theory, Eq. 2-13 must be used to eliminate the surface fluxes since the homogenized fluxes may be discontinuous at nodal interfaces. Application of the equivalence theory interface conditions yields the following expression for the surface currents at  $u = u_\ell$ ,

$$\begin{aligned}
 [\hat{J}_{\ell,m,n}^u(u_\ell)] &= \left( [f_{\ell-1,m,n}^{u^+}] [A_{\ell-1,m,n}^u] + [f_{\ell,m,n}^{u^-}] [A_{\ell,m,n}^u] \right)^{-1} \cdot \\
 &\quad \left( [f_{\ell-1,m,n}^{u^+}] [B_{\ell-1,m,n}^u] [\hat{\phi}_{\ell-1,m,n}] - [f_{\ell,m,n}^{u^-}] [B_{\ell,m,n}^u] [\hat{\phi}_{\ell,m,n}] \right. \\
 &\quad + [f_{\ell-1,m,n}^{u^+}] \langle -[C_{\ell-1,m,n}^{u^+}] a_{\ell-1}^{u^-} - [D_{\ell-1,m,n}^{u^+}] b_{\ell-1}^{u^-} \\
 &\quad - [E_{\ell-1,m,n}^{u^-}] c_{\ell-1}^{u^-} \rangle [\hat{S}_{\ell-2,m,n}^u] \\
 &\quad + \left\{ [f_{\ell-1,m,n}^{u^+}] \langle -[C_{\ell-1,m,n}^{u^+}] (1 - a_{\ell-1}^{u^-} - a_{\ell-1}^{u^+}) \right. \\
 &\quad \left. - [D_{\ell-1,m,n}^{u^+}] (-b_{\ell-1}^{u^-} - b_{\ell-1}^{u^+}) - [E_{\ell-1,m,n}^{u^+}] (-c_{\ell-1}^{u^-} - c_{\ell-1}^{u^+}) \right\rangle \\
 &\quad + [f_{\ell,m,n}^{u^-}] \langle [C_{\ell,m,n}^{u^-}] a_\ell^{u^+} + [D_{\ell,m,n}^{u^-}] b_\ell^{u^+} + [E_{\ell,m,n}^{u^-}] c_\ell^{u^+} \rangle \} [\hat{S}_{\ell-1,m,n}^u] \\
 &\quad + \left\{ [f_{\ell-1,m,n}^{u^+}] \langle -[C_{\ell-1,m,n}^{u^+}] a_{\ell-1}^{u^+} - [D_{\ell-1,m,n}^{u^+}] b_{\ell-1}^{u^+} - [E_{\ell-1,m,n}^{u^+}] c_{\ell-1}^{u^+} \rangle \right. \\
 &\quad \left. + [f_{\ell,m,n}^{u^-}] \langle [C_{\ell,m,n}^{u^-}] (1 - a_\ell^{u^-} - a_\ell^{u^+}) + [D_{\ell,m,n}^{u^-}] (-b_\ell^{u^-} - b_\ell^{u^+}) \right. \\
 &\quad \left. + [E_{\ell,m,n}^{u^-}] (-c_\ell^{u^-} - c_\ell^{u^+}) \rangle \} [\hat{S}_{\ell,m,n}^u] \\
 &\quad + [f_{\ell,m,n}^{u^-}] \langle [C_{\ell,m,n}^{u^-}] a_\ell^{u^+} + [D_{\ell,m,n}^{u^-}] b_\ell^{u^+} + [E_{\ell,m,n}^{u^-}] c_\ell^{u^+} \rangle [\hat{S}_{\ell+1,m,n}^u] \right);
 \end{aligned}$$

$$u = x, y, z, \quad (2-15)$$

where

$[f_{\ell,m,n}^{u \pm}]$  is a diagonal matrix of group discontinuity factors for node  $(\ell, m, n)$  and direction  $u$ .

The functional form of Eq. 2-15 is much easier to see if the equation is simplified to obtain

$$\begin{aligned} [\hat{J}_{\ell,m,n}^u(u_\ell)] &= [F_{u_{\ell,m,n}}^{\ell-1}] [\hat{\phi}_{\ell-1,m,n}] + [F_{u_{\ell,m,n}}^\ell] [\hat{\phi}_{\ell,m,n}] \\ &\quad + [G_{u_{\ell,m,n}}^{\ell-2}] [\hat{S}_{\ell-2,m,n}^u] + [G_{u_{\ell,m,n}}^{\ell-1}] [\hat{S}_{\ell-1,m,n}^u] \\ &\quad + [G_{u_{\ell,m,n}}^\ell] [\hat{S}_{\ell,m,n}^u] + [G_{u_{\ell,m,n}}^{\ell+1}] [\hat{S}_{\ell+1,m,n}^u]; \\ u = x, y, z, \quad (2-16) \end{aligned}$$

where the definitions of spatial coupling matrices follow from Eq. 2-15. This expression relates the interface currents to node-averaged fluxes in two nodes and node-averaged transverse leakages in four nodes. Consequently, the equivalence theory spatial coupling is unaltered in form from the conventional diffusion theory coupling. However, the magnitudes of the coupling terms are altered by the discontinuity factors.

The two expressions for interface fluxes (Eqs. 2-14a and 2-14b) are also very useful in defining the discontinuity factors from the true heterogeneous reactor solution. By definition, all average surface currents are preserved by the homogenized parameters. Hence, all of the vectors on the right-hand sides of Eqs. 2-14 are identical in the homogeneous and heterogeneous cases. That is,

$$[\hat{\phi}_{\ell,m,n}] = [\bar{\phi}_{\ell,m,n}]$$

$$[\hat{J}_{\ell,m,n}^u] = [J_{\ell,m,n}^u]$$

$$[\hat{S}_{\ell,m,n}^u] = [\bar{S}_{\ell,m,n}^u].$$

All of the matrices in Eqs. 2-14 are computed from the homogenized cross sections, diffusion coefficients, mesh spacings, and  $k_{eff}$ , which are computed directly from the heterogeneous solution (Eq. 2-1). Hence, the homogenized interface fluxes are computed directly from Eqs. 2-14 (Eq. 2-14a for the upper (+) interface of a node and Eq. 2-14b for the lower (-) interface of a node). Subsequently, the discontinuity factors are evaluated by using Eq. 2-12 and the known heterogeneous surface fluxes. The modified spatial coupling equation (Eq. 2-15) and the equations for the discontinuity factors (Eqs. 2-14 and 2-12) describe fully the modifications that are required to incorporate generalized equivalence theory into the QUANDRY nodal code.

## 2.5 QUANDRY SPATIAL APPROXIMATIONS

The previously-mentioned fact that "exact" homogenized parameters can be defined even if the equivalence equations are solved approximately suggests some interesting possibilities. For example, are there advantages to using the simplest of approximations to solve the equivalence equations, since even the simplest of approximations can be made exact by an appropriate definition of equivalence parameters? Insofar as the goal is to match a heterogeneous solution, it would seem that one might just as well choose the simplest approximation. However, if one does not have a priori knowledge of the true

solution (so that, as a consequence, homogenized parameters must be approximated), the accuracy of the homogenized solution will depend on the approximations employed to solve the equivalence equations. For this reason, it is desirable to have a method for solving the equivalence equations which permits several degrees of approximation in the solution techniques.

In this thesis, three approximations are used. The first is the conventional QUANDRY method in which the only approximation is that the transverse leakage shapes in each node can be fit by quadratic polynomials. The second approximation is that the transverse leakages are represented as spatially flat within each node. This is accomplished by setting all of the leakage expansion coefficients ( $a_{\ell,m,n}^u, b_{\ell,m,n}^u, c_{\ell,m,n}^u$ ) in Eq. 2-15 equal to zero. The third approximation is that the interfacial currents can be computed directly by finite differences with one mesh point per node. The conventional mesh-centered finite-difference equations for the homogenized surface fluxes at  $u = u_\ell$  are given by

$$\begin{aligned} [\hat{j}_{\ell-1,m,n}(u_\ell)] &= -[D_{\ell-1,m,n}] \frac{2}{h_{\ell-1}} \{[\hat{\phi}_{\ell-1,m,n}^u(u_\ell)] - [\hat{\phi}_{\ell-1,m,n}] \} \\ [\hat{j}_{\ell,m,n}(u_\ell)] &= -[D_{\ell,m,n}] \frac{2}{h_\ell} \{[\hat{\phi}_{\ell,m,n}] - [\hat{\phi}_{\ell,m,n}^u(u_\ell)]\} ; \\ u &= x, y, z . \end{aligned} \quad (2-17)$$

These equations can be recast in a form similar to the QUANDRY equations (Eqs. 2-14a and 2-14b) as follows:

$$\begin{aligned}
 [\hat{\phi}_{\ell-1,m,n}^u(u_\ell)] &= [\hat{\phi}_{\ell-1,m,n}] - [D_{\ell-1,m,n}]^{-1} \frac{h_{\ell-1}}{2} [\hat{J}_{\ell-1,m,n}(u_\ell)] \\
 [\hat{\phi}_{\ell,m,n}^u(u_\ell)] &= [\hat{\phi}_{\ell,m,n}] + [D_{\ell,m,n}]^{-1} \frac{h_\ell}{2} [\hat{J}_{\ell,m,n}(u_\ell)]; \\
 u &= x, y, z. \quad (2-18)
 \end{aligned}$$

Clearly, this coarse mesh finite-difference approximation can be incorporated into QUANDRY by defining the matrices of Eqs. 2-14 as

$$[A_{\ell,m,n}^u] \equiv [D_{\ell,m,n}]^{-1} \frac{h_\ell}{2}$$

$$[B_{\ell,m,n}^u] \equiv [I], \text{ the identity matrix}$$

$$[C_{\ell,m,n}^{u^\pm}] \equiv [D_{\ell,m,n}^{u^\pm}] \equiv [E_{\ell,m,n}^{u^\pm}] \equiv [0], \text{ the null matrix.}$$

These three approximations will be referred to as the "quadratic," "flat," and "CMFD" (coarse mesh finite difference) methods.

In addition to these three spatial approximations, QUANDRY permits the use of either one or two neutron energy groups. Consequently, any one of six possible combinations of approximations can be used to define homogenized parameters and to solve the equivalence equations.

## 2.6 BENCHMARK PROBLEMS

Generalized equivalence theory can provide homogenized parameters which will preserve rigorously any known heterogeneous reactor solution. Unfortunately, the theory gives no indications as to the magnitudes of the homogenized parameters (particularly the discontinuity factors). Therefore, numerical benchmark problems are required to provide additional insight into the homogenization process.

No restrictions need be imposed with respect to the methods (Monte Carlo, transport theory, multigroup diffusion theory, etc.) employed to generate the global heterogeneous reactor solution. Although each solution method will produce a somewhat different global solution, homogenized parameters can be defined such that they reproduce exactly that particular solution. Consequently, the standard reference solutions may be generated by any method that one chooses, and the homogenization process can be explored with respect to that particular solution method. All reference solutions that are utilized in this thesis will be generated from heterogeneous, two-group diffusion theory calculations. This implies that homogenized parameters (i.e., pin cell cross sections) must be known for each of the heterogeneous regions (fuel pins, control rods, burnable poison rods, etc.). The reference solutions will be found by solving the fine mesh heterogeneous diffusion equations with QUANDRY (employing the flat transverse leakage approximation).

### 2.6.1 The Henry-Worley BWR Problem

In order to make contact with previous homogenization studies, it is interesting to examine the Henry-Worley benchmark problem.<sup>9</sup> This highly idealized two-dimensional BWR core consists of 25 fuel assemblies (with widths of 8 cm), and the core is surrounded radially by 8 cm of water. Within each fuel assembly, the fuel is modeled as homogeneous, but the control blades (or corresponding water blades) are modeled explicitly. The existence of the control blades gives rise to substantial spatial homogenization problems. Although this

benchmark problem is quite different from an actual BWR, it still serves as a meaningful test for homogenization methods. A complete description of this test problem is contained in Section A1.1 of Appendix 1.

The reference solution to the Henry-Worley problem is a QUANDRY solution involving 36 mesh points per assembly (maximum mesh spacing of 2.0 cm). This reference solution is slightly different from the solutions of Koebke<sup>14</sup> and Worley,<sup>9</sup> but the differences are quite small. It is interesting to examine the solutions which are obtained if conventional flux-weighted parameters are used. Table 2-1 summarizes the results of two calculations which used flux-weighted parameters and two mesh layouts. Comparisons of the reference and flux-weighting power densities are displayed in Fig. A2-1 of Appendix 2. It is clear from the results in Fig. A2-1 that the spatial truncation errors in the flux-weighted solutions are quite small. Hence, the remaining large errors are caused by the flux-weighting method of computing homogenized parameters.

TABLE 2-1  
Summary of Results for the Henry-Worley BWR Problem  
Using Flux-Weighted Constants (FWC)

	Mesh Layout	
	<u>8 × 8 cm</u>	<u>4 × 4 cm</u>
Error in eigenvalue <sup>a</sup>	-0.93%	-0.94%
Maximum error in assembly power density ( $\epsilon_{\max}$ )	6.6%	6.2%
Average error in assembly power density ( $\bar{\epsilon}$ )	4.1%	4.31%

<sup>a</sup> Reference: 0.80399

In order to demonstrate that the generalized equivalence theory parameters do preserve exactly all of the reaction rates and the reactor eigenvalue, equivalence theory homogenized parameters were computed from the reference solution. When the coarse mesh (one node per assembly) generalized equivalence equations were then solved by each of the six approximate methods (quadratic, flat, and CMFD using both one and two groups), all of the coarse mesh solutions reproduced the reference solution. That is, the eigenvalue and reaction rates of the coarse mesh calculations are equal (accurate to at least four significant figures) to those of the reference solution. Comparisons of assembly power densities for the reference solution and the six generalized equivalence solutions are displayed in Figures A2-2 and A2-3 of Appendix 2. The equivalence solutions are considered to be exact, in the sense that the small remaining discrepancies can be attributed to computer round-off errors.

Since the Henry-Worley problem is one test problem for which Koebke has published values for his equivalence parameters, it is interesting to examine the differences between the equivalence parameters and the generalized equivalence parameters. The nodes in which the differences tend to be most significant are those which have large flux gradients across them. Table 2-2 contains a summary of the equivalence parameters for two nodes of the Henry-Worley BWR problem. If the reference solutions to this problem were exact, the values of the cross sections for any given node should be the same for both equivalence theory and generalized equivalence theory. Very small differences in cross sections are evident in Table 2-2, but for all

TABLE 2-2

## Homogenized Parameters for the Henry-Worley BWR Problem

	<u>Node</u>			
	<u>x = 2, y = 2</u>		<u>x = 3, y = 3</u>	
	<u>Equivalence Theory</u>	<u>Generalized Equivalence Theory</u>	<u>Equivalence Theory</u>	<u>Generalized Equivalence Theory</u>
$\hat{\Sigma}_{a_1} \times 10^{-2}$	0.9707	0.9707	0.9700	0.9700
$\hat{\Sigma}_{21} \times 10^{-2}$	0.1421	0.1421	0.1419	0.1419
$\nu \hat{\Sigma}_{f_1} \times 10^{-2}$	0.6493	0.6494	0.6486	0.6486
$\hat{\Sigma}_{a_2}$	0.1216	0.1213	0.1192	0.1190
$\nu \hat{\Sigma}_{f_2}$	0.1430	0.1432	0.1442	0.1443
$\hat{D}_1^x, \hat{D}_1^y$	1.3978	1.3880	1.4259	1.3880
$\hat{D}_2^x, \hat{D}_2^y$	0.3660	0.3842	0.5008	0.3845
$f_1^{x^-}, f_1^{y^-}$	1.004	1.006	1.008	1.002
$f_1^{x^+}, f_1^{y^+}$	1.004	1.002	1.008	1.017
$f_2^{x^-}, f_2^{y^-}$	1.125	1.140	1.133	1.096
$f_2^{x^+}, f_2^{y^+}$	1.125	1.106	1.133	1.077

intents and purposes they can be considered the same. The differences in diffusion coefficients arise from the fact that Koebke's diffusion coefficients are chosen such that the discontinuity factors are the same on opposite surfaces of a given node (i.e.,  $f_g^u^+ = f_g^u^-$ ). In generalized equivalence theory, the diffusion coefficients are chosen to be the inverse flux-weighting values and the discontinuity factors are allowed to be different on each surface (i.e.,  $f_g^u^+ \neq f_g^u^-$ ). For the (2, 2) node, it can be seen from Table 2-2 that the diffusion coefficients and discontinuity factors are much the same for the two formulations. This is primarily due to the fact that the (2, 2) node does not have a large flux gradient across it. For the (3, 3) node, the situation is significantly different. The equivalence theory thermal diffusion coefficient must be 30% larger than the inverse flux-weighted diffusion coefficient in order to obtain equal discontinuity factors on opposite surfaces. The resulting equivalence theory discontinuity factors are also larger in magnitude than the corresponding generalized equivalence theory parameters. Nevertheless, both formulations reproduce exactly the reference solution, and there exist no theoretical reasons to prefer one formulation over the other.

It is important to note that the similarity of the equivalence parameters in the two formulations is highly dependent on the assembly geometry. In the Henry-Worley problem, all assemblies have 90 degree rotational symmetry. However, if one chooses coarse mesh nodes such that each node corresponds to an assembly of an actual BWR, this symmetry will not exist. For instance, an assembly might have a control rod on one surface and a water gap on the opposite

surface. In such cases, the equivalence parameters for the two formulations will be quite different from each other.

### 2.6.2 The CISE BWR Benchmark Problem

The CISE BWR benchmark problem<sup>7</sup> is an idealized model of a two-dimensional BWR which represents more accurately the actual BWR heterogeneities than does the Henry-Worley problem. The CISE BWR core consists of 208 fuel assemblies with widths of 15 cm, and the reactor core is surrounded radially by a 15 cm water reflector. The fuel in each assembly is modeled as homogeneous, but all control blades and water gaps are explicitly modeled. The major simplifications in this problem are that the actual fuel heterogeneities (enrichment zones, burnable poison rods, and water rods) are represented homogeneously. Nevertheless, the CISE problem provides a significant test for any homogenization scheme. A detailed description of this problem is contained in Section A1.2 of Appendix 1.

The reference solution to the CISE benchmark problem is a QUANDRY solution involving 64 mesh points per assembly (11 in each quarter of a control rod, 25 in the fuel region, and 28 in the gap regions). This reference solution is slightly less accurate than the solution of Bottoni et al.<sup>7</sup> For reasons of consistency, however, the QUANDRY reference solution is preferred for the analyses presented in this thesis.

The CISE problem provides an excellent example of the inaccuracy of conventional flux-weighted parameters. Table 2-3 summarizes the results of two QUANDRY calculations for the CISE problem with flux-

TABLE 2-3

Summary of Results for the CISE BWR Problem  
Using Flux-Weighted Constants

	Mesh Layout	
	<u>15 X 15 cm</u>	<u>7.5 X 7.5 cm</u>
Error in eigenvalue <sup>a</sup>	-. 15%	-. 16%
$\epsilon_{\max}$	10. 2%	9. 9%
$\bar{\epsilon}$	4. 2%	4. 2%

<sup>a</sup> Reference: 0.95240

weighted constants (FWC). The fact that the assembly power densities, as predicted with FWC, are in error by as much as 10% indicates that the flux-weighted constants have both theoretical and practical deficiencies.

When the generalized equivalence equations for the CISE problem are solved, the resulting solutions reproduce exactly the reference solution. That is, all of the quantities of interest from the heterogeneous reference solution ( $k_{eff}$ , node-averaged reaction rates and surface currents) are reproduced by the equivalence solution to within 0.01% of the reference solution (computer round-off limit). This is true for all six of the approximate methods of solving the equivalence equations.

The argument can be made that it is unfair to compare the accuracies of equivalence parameters and flux-weighted parameters, since knowledge of the reference solution is required for determination of equivalence parameters but not for flux-weighted parameters. The comparison can be made fair, however, by computing flux-weighting

constants directly from the reference solution, instead of from a cell calculation. That is, cross sections are computed from Eqs. 1-2a and 1-3, and the heterogeneous reference fluxes are used as the weighting functions. Homogenized parameters which are computed in this fashion are referred to as "exact flux-weighted constants" (EFWC). Since the reference flux distributions are different in each node, the EFWC are, in general, different for every node. If the EFWC are used, the diffusion theory solution to the CISE problem has a maximum error in nodal power density ( $\varepsilon_{\max}$ ) of 7.6% and an average error ( $\bar{\varepsilon}$ ) of 3.3%. The EFWC yield a more accurate solution than do the FWC, but the errors remain quite large. The normalized power densities obtained for the CISE problem using both the FWC and the EFWC are displayed in Fig. A2-4 of Appendix 2.

The primary reason that two-group flux-weighted constants fail to predict accurately the power distributions of BWRs is that the inter-assembly thermal diffusion terms are significantly overpredicted. This inaccuracy arises primarily from the use of flux-weighted (or inverse flux-weighted) diffusion coefficients. The heterogeneous thermal diffusion coefficients at the assembly interfaces have values characteristic of either the control rods or the water gaps. Since the thermal diffusion coefficients of the control rods and water gaps are smaller than the diffusion coefficients of the fuel, the flux-weighting procedure produces homogenized thermal diffusion coefficients which are larger than those of the control rod or water gap. Consequently, for a given flux gradient at an assembly interface, the homogenized diffusion coefficients will overpredict the interassembly thermal

currents. In addition, it has already been shown (Section 1.2) that even if the diffusion coefficients are allowed to be chosen in some other fashion, there do not exist enough degrees of freedom in conventional diffusion theory to permit the homogenized solution to reproduce exactly a reference solution. The additional degrees of freedom (discontinuity factors) which are postulated in generalized equivalence theory do permit the exact reproduction of any reference solution.

It is interesting to examine the discontinuity factors for the generalized equivalence theory solution to the CISE BWR problem. Table 2-4 summarizes the values of the discontinuity factors for a rodded assembly and an unrodded assembly in the CISE problem. The values of the discontinuity factors displayed in Table 2-4 vary significantly from unity, and they show a much larger variation than do the discontinuity factors of the Henry-Worley problem. The absolute magnitudes of the discontinuity factors are not important, since the expression for the interassembly currents (Eq. 2-15) depends only on differences in the discontinuity factors across an interface and not on the magnitudes of the discontinuity factors. From Table 2-4, it can be seen that the discontinuity in homogenized fast flux at the interface between the rodded and the unrodded assembly is about 3.5%. However, the discontinuity in the homogenized thermal flux is approximately 30% (i.e.,  $f_2^x(x=1, y=1) = 1.827$ ,  $f_2^x(x=2, y=1) = 1.471$ ). The fact that the homogenized fast flux is almost continuous and the homogenized thermal flux is quite discontinuous is consistent with the fact that the heterogeneous fast diffusion coefficients are much more homogeneous

TABLE 2-4

Generalized Equivalence Theory Discontinuity Factors<sup>\*</sup>  
for the CISE BWR Problem

<u>Equivalence Parameter</u>	<u>Node</u>	
	Rodded <u>x = 1, y = 1</u>	Unrodded <u>x = 2, y = 1</u>
$f_1^x^+$	1.004	0.955
$f_1^x^-$	.908	0.969
$f_1^y^+$	1.004	0.968
$f_1^y^-$	.908	0.956
$f_2^x^+$	1.827	1.440
$f_2^x^-$	0.675	1.471
$f_2^y^+$	1.827	1.470
$f_2^y^-$	0.675	1.440

---

\* Equivalence equations solved with quadratic transverse leakage approximation.

than are the thermal diffusion coefficients.

A much more thorough and systematic examination of the discontinuity factors for the CISE problem is presented in the following chapter.

## 2.7 SUMMARY

In this chapter, Koebke's equivalence theory homogenization method was examined and demonstrated to be capable of reproducing rigorously all of the integral quantities of interest from a known heterogeneous reference solution. This homogenization method was then extended to obtain a generalized equivalence theory homogenization method which also was capable of reproducing a known heterogeneous solution.

The mathematical details regarding the implementation of generalized equivalence theory into the Analytic Nodal Method (and more specifically, into the QUANDRY code) were presented. Two benchmark BWR problems were examined, and the actual reproduction of known heterogeneous solutions was demonstrated numerically. All of the developments in Chapter 2 were strictly formal, in the sense that a priori knowledge of the heterogeneous reference solution was required in order to determine the equivalence theory parameters.

In Chapters 3 and 4, approximate methods for obtaining generalized equivalence theory parameters (not based on knowledge of the full heterogeneous solution) will be presented. The accuracy of these approximate methods will be established by examination of several BWR benchmark problems.

## Chapter 3

### EVALUATION OF APPROXIMATE EQUIVALENCE PARAMETERS FROM CELL CALCULATIONS

#### 3.1 INTRODUCTION

In Chapter 2, the generalized equivalence theory homogenization method was derived, and the details of implementing the method into the nodal code, QUANDRY, were presented. This unique homogenization method was demonstrated, both theoretically and numerically, to be capable of reproducing exactly all of the node-averaged properties of any known heterogeneous reactor solution. However, an assumption was required in order to evaluate the equivalence theory homogenization parameters: the heterogeneous reactor solution had to be known.

The idea of spatial homogenization, however, is to be able to predict accurately the solution to the heterogeneous reactor without actually solving the heterogeneous problem. Hence, a homogenization method is of little practical value if it requires that the heterogeneous reactor solution be known in order to define the homogenized parameters.

In the following two chapters, approximate methods for obtaining generalized equivalence parameters not based on prior knowledge of the full heterogeneous solution are presented. In this present chapter, a method for approximating the generalized equivalence parameters based on heterogeneous cell calculations is detailed. Several BWR benchmark problems are examined to establish the accuracy of the

homogenized solutions which are obtained through use of this method.

### 3.2 SPATIAL INVARIANCE OF THE GENERALIZED EQUIVALENCE PARAMETERS

A detailed examination of the reference generalized equivalence parameters (i.e., those defined from a known heterogeneous reactor solution) provides valuable insight into the homogenization process. For this purpose, the equivalence parameters which were computed in Chapter 2 for the CISE BWR problem were examined. These equivalence parameters are unique to each homogenized node because of their dependence on the local heterogeneous solution. Nevertheless, certain patterns can be seen clearly if the equivalence parameters are examined as a function of the type of heterogeneous assembly that they represent. A summary of mean values and standard deviations of the equivalence theory cross sections and diffusion coefficients (for each assembly type in the CISE problem) is presented in Table 3-1. The fact that the standard deviations of the generalized equivalence parameters are so small suggests that equivalence parameters (at least cross sections and diffusion coefficients) have first-order dependence on assembly type and only second-order dependence on the local heterogeneous solution. It is also clear that the fast group parameters show less spatial variation than do the thermal group parameters. This behavior is reasonable since the fast fluxes tend to have much smoother shapes than the thermal fluxes.

In addition to cross sections and diffusion coefficients, discontinuity factors are necessary to form a complete set of equivalence

TABLE 3-1

Mean Values and Standard Deviations of the Reference Equivalence Parameters  
for the CISE BWR Problem as a Function of Assembly Type

Parameter	Assembly Type <sup>a</sup>			
	A	B	A <sup>+</sup>	B <sup>+</sup>
$\hat{\Sigma}_{r_1} \times 10^{-2}$	2.470 ± 0.005	2.479 ± 0.001	2.579 ± 0.004	2.583 ± 0.003
$\hat{\Sigma}_{21} \times 10^{-2}$	1.857 ± 0.007	1.871 ± 0.001	1.778 ± 0.004	1.786 ± 0.002
$\nu \hat{\Sigma}_{f_1} \times 10^{-2}$	0.4591 ± 0.001	0.3801 ± 0.001	0.4554 ± 0.001	0.3782 ± 0.001
$\hat{\Sigma}_{r_2} \times 10^{-2}$	5.908 ± 0.070	5.958 ± 0.003	7.354 ± 0.067	7.323 ± 0.034
$\nu \hat{\Sigma}_{f_2} \times 10^{-2}$	7.198 ± 0.103	6.612 ± 0.005	7.504 ± 0.016	6.804 ± 0.007
$\hat{D}_1$	1.844 ± 0.001	1.844 ± 0.001	1.858 ± 0.001	1.859 ± 0.001
$\hat{D}_2$	0.4270 ± 0.003	0.4289 ± 0.001	0.4271 ± 0.001	0.4267 ± 0.001

<sup>a</sup> Notation is that of the CISE problem description, Section A1.2 of Appendix 1.

parameters. Table 3-2 summarizes the mean values and standard deviations of the reference discontinuity factors (computed with the quadratic transverse leakage approximation) for the CISE BWR problem. The discontinuity factors also appear to be primarily a function of assembly type, as evidenced by the small magnitude of the standard deviations. The discontinuity factors for the reflector nodes (W) are very close to unity. The reason for the slight variations from unity is that the equivalence equations are solved using the QUANDRY nodal approximation. If the equivalence equations were solved in an exact manner, the values of the discontinuity factors for the reflector nodes (or any homogeneous node) would be unity.

The observation that all of the equivalence parameters appear to be primarily a function of assembly type leads one to suspect that there may exist methods for determining accurate (although approximate) equivalence parameters which do not require knowledge of the full heterogeneous solution. The remainder of this thesis is devoted to examining several approximate methods for determining equivalence parameters.

### 3.3 SIMPLE CELL CALCULATIONS

The fact that the reference equivalence parameters (for a given type of assembly in the CISE BWR problem) are quite insensitive to the locations of the assemblies indicates that the equivalence parameters are also quite insensitive to the actual distributions of the heterogeneous fluxes and currents. If the equivalence parameters were truly independent of the actual surface currents, it would be possible to fix

TABLE 3-2

Mean Values and Standard Deviations of the Reference Discontinuity Factors  
for the CISE BWR Problem as a Function of Assembly Type

Parameter	<u>Assembly Type<sup>a</sup></u>			
	A	B	A <sup>+</sup>	B <sup>+</sup>
$f_1^-$	$0.9560 \pm .009$	$0.9614 \pm .004$	$0.9090 \pm .001$	$0.9128 \pm .001$
$f_1^+$	$0.9560 \pm .009$	$0.9614 \pm .004$	$1.003 \pm .002$	$1.001 \pm .001$
$f_2^-$	$1.423 \pm .059$	$1.453 \pm .013$	$0.6785 \pm .004$	$0.6762 \pm .004$
$f_2^+$	$1.423 \pm .059$	$1.453 \pm .013$	$1.823 \pm .016$	$1.812 \pm .009$

<sup>a</sup> Notation is that of the CISE problem description, Section A1.2 of Appendix 1.

arbitrarily the magnitudes and shapes of the currents on the surfaces of a single assembly and to solve the corresponding heterogeneous fixed-source problem to obtain equivalence parameters. Since the actual surface currents for a given type of assembly vary depending on the locations of the assemblies in the reactor, the simplest arbitrary choice for the net surface currents is that they are identically zero. If this approximation is made, the corresponding heterogeneous fixed-source problem becomes the conventional "cell calculation" that is traditionally used to compute flux-weighted constants (FWC). Homogenized parameters defined from the cell calculation are used to represent all assemblies of that particular type regardless of the actual locations of the assemblies in the reactor.

If a "cell calculation" is performed for an assembly, the resulting equivalence theory cross sections and diffusion coefficients are identical to the FWC. However, equivalence theory also requires that values of the discontinuity factors be determined. One might think that a cell calculation does not provide the information that is needed to determine the discontinuity factors. However, there exists a homogeneous analog to the heterogeneous cell calculation which is simply a single-node problem with zero net current boundary conditions. Naturally, the homogenized fluxes in this problem are spatially flat. Since the cell-averaged fluxes in the homogeneous and heterogeneous cell calculations are by definition equal, the discontinuity factors are simply the ratios of the surface-averaged fluxes to the cell-averaged fluxes from the heterogeneous cell calculation. In this manner, it is possible to approximate all of the equivalence parameters by performing cell

calculations for each type of assembly. Such equivalence parameters are referred to collectively as "cell discontinuity factors" (CDF).

The heterogeneous cell calculation with homogeneous Neumann boundary conditions cannot be solved as a fixed-source problem. The cell calculation is generally treated as an eigenvalue problem, and typically,  $k_{\text{eff}}$  or the buckling<sup>2</sup> of the cell is treated as the eigenvalue. For reasons of simplicity in this thesis,  $k_{\text{eff}}$  is used as the eigenvalue. No assumptions are required with respect to the methods (Monte Carlo, multigroup discrete ordinates, integral transport theory, multigroup diffusion theory, etc.) that are used to perform the cell calculations. Presumably, the homogenized parameters found from a higher-order calculation produce global homogenized solutions which are more accurate than those which result from the use of lower-order cell calculations. However, in order to maintain consistency within the heterogeneous reference solutions that are used in this thesis, all cell calculations are heterogeneous two-group diffusion theory (QUANDRY) calculations. It is important to recognize that unlike the reference equivalence parameters, the CDF are independent of the approximations that are made in solving the global equivalence equations. Consequently, the CDF are the same for the quadratic, flat, and CMFD methods which were discussed in Section 2.5 of Chapter 2.

Since the use of cell calculations for approximating equivalence parameters was motivated by an examination of the spatial invariance of the equivalence parameters in the CISE BWR problem, a comparison of the reference equivalence parameters and those obtained from cell calculations provides a measure of the accuracy of the approximate

quantities. A summary of the CDF and their differences with respect to the mean values of the reference equivalence parameters is displayed in Table 3-3. The maximum difference in cross sections between the CDF and the mean values of the reference equivalence parameters can be seen from Table 3-3 to be approximately 1.0%. This implies that for given nodal fluxes, the CDF will predict node-averaged reaction rates with reasonable accuracy. However, to predict accurately the nodal fluxes, the global equivalence equations must predict accurately the nodal interface currents. Since the discontinuity factors appear explicitly in the equivalence expression for interfacial currents (Eq. 2-15), it is important that they be accurately predicted. From Table 3-3, it can be seen that the maximum difference in discontinuity factors between the CDF and the mean values of the reference equivalence parameters is approximately 4.0%. This discrepancy is not unreasonably large when one considers that the associated discontinuity factor is 90% larger than the unity value which conventional flux-weighting methods assume implicitly.

The type of agreement between the CDF and the mean values of the reference equivalence parameters that is displayed in Table 3-3 is encouraging. However, the true test of any homogenization method is how accurately it can predict the solutions to heterogeneous reactor problems.

TABLE 3-3

Cell Discontinuity Factors and Their Deviations from the Mean Values of the Reference Equivalence Parameters for the CISE BWR Problem as a Function of Assembly Type

Parameter	<u>Assembly Type</u>		
	A	B	A <sup>+</sup>
$\hat{\Sigma}_{r_1} \times 10^{-2}$	2.481 ( 0.5%)	2.482 (+0.1%)	2.576 (-0.1%)
$\hat{\Sigma}_{21} \times 10^{-2}$	1.874 (-0.9%)	1.874 (+0.2%)	1.772 (-0.3%)
$\nu \hat{\Sigma}_{f_1} \times 10^{-2}$	0.4566 (-0.6%)	0.3796 (-0.1%)	0.4565 (+0.2%)
$\hat{\Sigma}_{r_2} \times 10^{-2}$	5.946 (+0.6%)	5.946 (-0.2%)	7.416 (+0.8%)
$\nu \hat{\Sigma}_{f_2} \times 10^{-2}$	7.254 (+0.8%)	6.595 (-0.3%)	7.558 (+0.7%)
$\hat{D}_1$	1.844 ( 0.0%)	1.844 ( 0.0%)	1.858 ( 0.0%)
$\hat{D}_2$	0.4284 (+0.3%)	0.4284 (-0.1%)	0.4283 (+0.3%)
$f_1^-$	0.9623 (+0.7%)	0.9625 (+0.1%)	0.8955 (-1.5%)
$f_1^+$	0.9623 (+0.7%)	0.9625 (+0.1%)	1.015 (+1.2%)
$f_2^-$	1.451 (+2.0%)	1.451 (-0.1%)	0.6492 (-4.3%)
$f_2^+$	1.451 (+2.0%)	1.451 (-0.1%)	1.888 (+3.6%)
			0.4283 (+0.4%)

### 3.4 BENCHMARK BWR RESULTS USING CDF

The accuracy with which CDF (generalized equivalence parameters computed from cell calculations) predict the solutions to heterogeneous reactors can be investigated in an unambiguous manner by examining benchmark problems for which reference solutions are known. The benchmark problems that were chosen for analysis in this thesis are BWRs, since they display homogenization difficulties which are more severe than those of PWRs.

#### 3.4.1 The Henry-Worley BWR Problem

The Henry-Worley BWR problem<sup>3</sup> has a very simple, but heterogeneous geometry. The basic assembly consists of a homogeneous fuel composition which surrounds a cross-shaped region of control rod material or water. A complete problem description and the values of the equivalence parameters, as computed by cell calculations, are contained in Section A1.1 of Appendix 1. Since the basic cell in this problem has 90° rotational symmetry, the CDF are computed by modelling only one quadrant of the cell. This allows two possible geometrical representations of the homogenized problem. That is, either an entire assembly or a quarter assembly can be treated at a single node in the homogenized problem. The latter representation corresponds more closely to the geometry of a realistic BWR, in which four separate fuel assemblies surround a single control blade and for which it is desirable to know the power of each assembly.

The Henry-Worley BWR problem was solved using QUANDRY (with the quadratic transverse leakage approximation) for both 8 and 4 cm

spatial meshes. Since the reference solution to the heterogeneous problem is known, the accuracy of the homogenized solution (which used CDF) can be measured by comparing to the reference solution. In addition, it is interesting to examine the accuracy of the homogenized solution that is obtained when conventional flux-weighted constants (FWC) are used. By comparing the relative accuracy of the two homogenized solutions, one can measure the enhanced accuracy that is obtained by using CDF in place of conventional FWC. A summary of results for the Henry-Worley problem is presented in Table 3-4. The normalized nodal power densities are displayed in Fig. A2-5 and Fig. A2-6 of Appendix 2 for the 8 and 4 cm mesh cases, respectively.

TABLE 3-4

Comparison of Results for the Henry-Worley BWR  
Benchmark Problem Using FWC and CDF

	<u>Mesh Layout</u>			
	<u>8 X 8 cm</u>		<u>4 X 4 cm</u>	
	<u>FWC</u>	<u>CDF</u>	<u>FWC</u>	<u>CDF</u>
Error in eigenvalue <sup>a</sup>	-0.93%	-0.45%	-0.94%	-0.49%
Maximum error in nodal power	+6.64%	-3.44%	+8.13%	+4.10%
Average error in nodal powers	4.10%	1.41%	4.31%	1.34%

<sup>a</sup> Reference: 0.80399

These results indicate that use of CDF results in solutions which have an approximate factor of two reduction (when compared to solutions which use FWC) in the error in eigenvalue and maximum error in nodal powers.

The enhanced accuracy with which CDF predict the solution to the Henry-Worley problem is encouraging. However, the Henry-Worley problem does not model actual BWR heterogeneities. Results for a more realistic BWR benchmark problem are presented in the following section.

### 3.4.2 The CISE BWR Problem

The CISE BWR problem models explicitly the water gaps which surround each fuel assembly, as well as the control blades that are associated with rodded assemblies. The fuel assemblies in this problem are treated homogeneously, and two types of fuel assemblies (fresh and depleted) are also modeled. The complete problem description and values of the CDF are contained in Section A1.2 of Appendix 2.

The CISE BWR problem was solved with QUANDRY (quadratic transverse leakage approximation and 15 cm spatial mesh) using both the FWC and CDF. A summary of results is displayed in Table 3-5, and the normalized nodal power densities are presented in Fig. A2-7 of Appendix 2. These results show that the use of CDF leads to solutions which have an approximate factor of three reduction in the maximum and average errors in assembly powers, when compared to solutions generated with FWC. The accuracy with which the reactor eigenvalue is predicted is also significantly enhanced through use of CDF.

TABLE 3-5  
Comparison of Results for the CISE BWR Problem  
Using FWC and CDF

	<u>FWC</u>	<u>CDF</u>
Error in eigenvalue <sup>a</sup>	-0.16%	-0.03%
Maximum error in assembly power	+9.86%	-3.06%
Average error in assembly powers	4.19%	0.90%

<sup>a</sup> Reference: 0.95240

Since the CDF are independent of the approximations that are made in solving the global equivalence equations, the accuracy of the homogenized solutions using CDF depends upon the approximations that are made. Table 3-6 contains a summary of results for three calculations (using CDF) for the quadratic, flat, and CMFD spatial approximations.

TABLE 3-6  
Comparison of Results for the CISE BWR Problem  
Using CDF with Several Spatial Approximations

	<u>Spatial Approximation</u>		
	<u>Quadratic</u>	<u>Flat</u>	<u>CMFD</u>
Error in eigenvalue <sup>a</sup>	-0.03%	-0.04%	-2.29%
Maximum error in assembly power	3.06%	3.48%	37.6%
Average error in assembly powers	0.90%	1.32%	15.4%

<sup>a</sup> Reference: 0.095240

These results support the contention that the least approximate solution method (quadratic) should be employed, since the CDF (unlike the true equivalence parameters) have no means of compensating for the errors caused by the spatial approximations.

The CISE BWR problem provides a significant test for any homogenization method. However, many of the actual BWR heterogeneities are not present in this problem. Thus, before any general conclusions are drawn with respect to the accuracy of BWR solutions using CDF, it is important to examine still more realistic BWR problems.

### 3.4.3 An Extremely Heterogeneous BWR Problem

The heterogeneity which exists in actual BWR assemblies is much more pronounced than the heterogeneity which is modelled in the benchmark problems presented heretofore. In order to represent explicitly this heterogeneity, it is necessary to model individual fuel pins (because of radial enrichment zoning within assemblies) as well as water gaps and control rods. Such BWR problems require more computer storage than is available for use with the existing version of QUANDRY. In order to reduce the computer storage problems, a benchmark BWR problem which has a somewhat simplified assembly geometry was devised. In this problem, the radial enrichment zones in each assembly are modelled such that the fuel enrichment is constant within four fuel pin clusters. In this manner, the fuel zone is represented with only sixteen distinct regions. The radial enrichment is modelled by fuel pins with three different fuel enrichments. Water gaps between fuel assemblies are modelled more accurately than those

in the CISE BWR problem, in that both the "wide" and "narrow" gaps are represented explicitly.

The reactor core in this problem consists of 308 fuel assemblies with widths of 15.31 cm, and the core is surrounded by a 15.31 cm water reflector. An additional complexity is introduced by modelling several central assemblies as partially voided (both 40% and 70% voided). Sixteen control blades are also defined to be in their inserted positions. This problem displays most of the heterogeneity that exists in an actual BWR, and consequently, it serves as a rigorous test for any homogenization method. This problem is referred to as the HAFAS (Heterogeneously-Arranged Fuel Assembly) BWR problem. A complete description of the problem is contained in Section A1.3 of Appendix 1.

The reference solution to the HAFAS problem is a QUANDRY solution involving 49 mesh points per assembly (16 in the fuel region, 9 in each quarter of a control blade, and 24 in the gap regions). The HAFAS BWR problem was also solved with QUANDRY (quadratic transverse leakage approximation and 15.31 cm spatial mesh) using both FWC and CDF. A summary of results for this problem is presented in Table 3-7, and the normalized power densities are displayed in Fig. A2-8 of Appendix 2. The magnitude of the errors that exist in the flux-weighted solution indicates that the homogenization difficulties are quite severe in this problem. The flux-weighted solution displays large errors throughout the core, as evidenced by the 6.14% average error in assembly power. The homogenized solution obtained through use of CDF is more accurate in every respect than the solution which uses FWC.

TABLE 3-7  
Comparison of Results for the HAFAS BWR Problem  
Using FWC and CDF

	<u>FWC</u>	<u>CDF</u>
Error in eigenvalue <sup>a</sup>	-0.44%	-0.06%
Maximum error in assembly power	16.95%	5.29%
Average error in assembly power	6.14%	1.33%

<sup>a</sup> Reference: 1.04420

In fact, the increase in accuracy (with respect to FWC) which is obtained from CDF is proportionally larger in the HAFAS problem than in either the Henry-Worley or the CISE BWR problems. This implies that the CDF are equally well-suited for analysis of truly heterogeneous BWR assemblies as well as more homogeneous assemblies.

### 3.5 MORE SOPHISTICATED CELL CALCULATIONS

An examination of the detailed power distributions for the benchmark problems that have been presented reveals that the assemblies which have the largest errors are those which surround the control blades. This implies that the cross sections and/or the discontinuity factors for rodded assemblies are somewhat in error. This observation is also consistent with the results that were introduced in Table 3-3. From this table, it is clear that the largest deviations between the CDF and the mean values of the reference equivalence parameters

occur in the rodded assemblies, particularly in the thermal group cross sections and discontinuity factors. This fact is not surprising, in that the implicit assumptions of the cell calculations (zero net currents on the surfaces of each assembly) are least likely to be valid for the rodded assemblies.

Fortunately, there exist at least one simple method of obtaining more accurate equivalence parameters for the rodded assemblies. Instead of solving a single assembly cell calculation, one can perform a four assembly cell calculation with zero net current boundary conditions. Subsequently, the equivalence parameters can be computed for the rodded assembly. In this manner, the rodded assembly does not have zero net current conditions imposed on the unrodded surfaces (although zero net currents are imposed for the rodded surfaces) and the characteristic flux depressions in the rodded assemblies are modelled more accurately. Such cell calculations produce equivalence parameters which are relatively independent of the type of assemblies which are chosen to be adjacent to the rodded assembly. The equivalence parameters which are generated in this fashion are then used throughout the core to represent the rodded assemblies. Table 3-8 contains a summary of the values of equivalence parameters that were computed in this manner for the CISE BWR problem. These equivalence parameters are referred to as modified cell discontinuity factors (MCDF). These MCDF have significantly better agreement with the mean values of the reference equivalence parameters in the rodded assemblies than do the CDF. Particularly noteworthy is the agreement in thermal discontinuity factors (~1.0% for the MCDF versus ~4.0% for the CDF).

TABLE 3-8

MCDF and Their Deviations from the Mean Values of the Reference  
 Equivalence Parameters for the CISE BWR Problem  
 as a Function of Assembly Type

Parameter	<u>Assembly Type</u>	
	A <sup>+</sup>	B <sup>+</sup>
$\hat{\Sigma}_{r_1} \times 10^{-2}$	2.580 (+0.1%)	2.584 (-0.0%)
$\hat{\Sigma}_{21} \times 10^{-2}$	1.782 (+0.2%)	1.791 (+0.3%)
$\nu \hat{\Sigma}_{f_1} \times 10^{-2}$	0.4547 (-0.2%)	.3776 (-0.2%)
$\hat{\Sigma}_{r_2} \times 10^{-2}$	7.322 (-0.4%)	7.277 (-0.6%)
$\nu \hat{\Sigma}_{f_2} \times 10^{-2}$	7.490 (-0.2%)	6.784 (-0.3%)
$\hat{D}_1$	1.858 (0.0%)	1.859 (0.0%)
$\hat{D}_2$	0.4269 (-0.1%)	0.4264 (0.0%)
$f_1^-$	0.9106 (+0.2%)	0.9170 (+0.5%)
$f_1^+$	1.002 (-0.0%)	0.9979 (-0.3%)
$f_2^-$	0.6737 (-0.7%)	0.6818 (+0.8%)
$f_2^+$	1.813 (-0.6%)	1.790 (-1.2%)

Cell calculations have been performed and the MCDF computed for the three BWR benchmark problems. All three problems were then solved using the MCDF. A summary of results from these calculations is displayed in Table 3-9. The normalized power densities are presented in Figs. A2-9, A2-10, and A2-11, for the Henry-Worley, CISE and HAFAS BWR problems, respectively. The use of the MCDF leads to homogenized solutions which have even greater accuracy than that obtained with the CDF. With the MCDF, assembly power distributions are predicted with a maximum error of approximately 3.% and an average error of approximately 1.%.

Despite the fact that the MCDF are in good agreement with the mean values of the reference equivalence parameters, small errors in the homogenized solutions still exist. These errors are due to the fact that the reference equivalence parameters deviate from their mean values because of the influences of neighboring assemblies, and the cell calculations have no means of predicting these deviations.

### 3.6 SUMMARY

In this chapter, a method for computing approximate equivalence parameters from heterogeneous cell calculations was introduced. Through use of these approximate parameters (MCDF), homogenized power distributions were predicted with maximum and average errors in assembly powers of approximately 3.0% and 1.0%, respectively. When compared to the accuracy of conventional flux-weighting homogenization methods, equivalence theory with MCDF was found to predict assembly powers with errors that are factors of three to five times

**TABLE 3-9**  
**Summary of Results for Three BWR Benchmark Problems Using CDF and MCDF**

	<u>Henry-Worley</u>		<u>CISE</u>		<u>HAFAS</u>	
	<u>CDF</u>	<u>MCDF</u>	<u>CDF</u>	<u>MCDF</u>	<u>CDF</u>	<u>MCDF</u>
Error in eigenvalue	-0. 49%	-0. 22%	-0. 03%	-0. 05%	-0. 06%	-0. 02%
Maximum error in assembly power	+4. 10%	+2. 90%	-3. 06%	+2. 61%	5. 29%	4. 00%
Average error in assembly powers	1. 34%	1. 02%	0. 90%	1. 30%	1. 33%	1. 05%

smaller than the flux-weighted methods. Since the CDF and FWC are both derived from the same cell calculations, there is strong motivation to use CDF. Significant enhancement in accuracy is obtained without additional expense.

Additional refinements of the cell calculations can lead to enhanced accuracy of the approximate equivalence solutions. For example, two assembly cell calculations can be used to obtain more accurate equivalence parameters for assemblies which are adjacent to the reflector. However, the introduction of many special cases detracts from the simplicity of approximating equivalence parameters from simple cell calculations.

In Chapter 4, additional methods for computing equivalence parameters will be presented. These methods will account for many of the interassembly effects that are neglected by cell calculations.

## Chapter 4

### EVALUATION OF APPROXIMATE EQUIVALENCE PARAMETERS FROM LOCAL HETEROGENEOUS PROBLEMS

#### 4.1 INTRODUCTION

In Chapter 3, a method for computing approximate equivalence parameters from heterogeneous cell calculations was described. The solutions to several BWR benchmark problems that are obtained with these approximate equivalence parameters were demonstrated to be significantly more accurate than the solutions which are obtained using conventional flux-weighting techniques. The accuracy of such equivalence parameters is limited by the fact that the cell calculations can not account for many of the interassembly effects. The accuracy of BWR solutions obtained through use of equivalence parameters derived from heterogeneous cell calculations (CDF or MCDF) may be sufficient for many applications. However, if a higher degree of accuracy is desired, more sophisticated methods for determining equivalence parameters are required.

In this present chapter, several methods for obtaining more accurate (although approximate) equivalence parameters are presented. These methods account for most of the interassembly effects that are implicitly neglected by simple cell calculations. The accuracy of homogenized solutions which are obtained through use of these more sophisticated methods is established by examining three BWR benchmark problems.

#### 4.2 EVALUATION OF EXACT EQUIVALENCE PARAMETERS FROM LOCAL HETEROGENEOUS PROBLEMS

The inaccuracies of approximate equivalence parameters that are computed from simple cell calculations arise from the fact that zero net current boundary conditions are imposed for the cell calculations. Because of this, all the effects of neighboring assemblies on the equivalence parameters of other assemblies are neglected. However, if the actual boundary conditions that exist on the surfaces of an assembly were known, a fixed-source cell calculation could be performed to obtain equivalence parameters. For example, consider the case of multigroup diffusion theory cell calculations. If the actual net currents that exist on the surfaces of an assembly were known (as well as the global reactor eigenvalue), a fixed-source problem could be solved to obtain the flux distributions and equivalence parameters for that assembly. The effects of neighboring assemblies on the equivalence parameters of that particular assembly would be included via the net currents that are used as boundary conditions. By performing such fixed-source calculations for each assembly, one could obtain equivalence parameters for every assembly. Such parameters would be exact in the sense that global homogenized solutions obtained by using them would reproduce all the node-integrated properties of a full heterogeneous diffusion theory calculation. Unfortunately, determining the net currents on the surfaces of all assemblies is just as difficult as solving the full heterogeneous problem. Nevertheless, the observation that such fixed-current calculations could produce the desired equivalence parameters provides a starting point from which reasonable approximations can be deduced.

The traditional approaches to homogenization assume that homogenized parameters are computed without knowledge of the global heterogeneous (or homogenized) solutions. Subsequently, the homogenized parameters are used to compute global homogenized solutions which are then considered to be the best estimates of the global heterogeneous solutions. If one desires to include the interassembly effects on the homogenized parameters, this traditional approach can be abandoned. For example, one could solve the global homogenized problem using approximate homogenized parameters (FWC, CDF, MCDF, etc.). From this solution, one could then extract approximate net currents (for each assembly surface) which could then be used to approximate the surface conditions for each of the fixed-source assembly calculations. By performing such fixed-source calculations, one could then obtain approximate equivalence parameters which reflect many of the interassembly effects. These equivalence parameters could then be used to generate a new global homogenized solution. Presumably, this latter homogenized solution would be more accurate than its predecessor because the equivalence parameters that were used to generate it reflect many of the interassembly effects. Naturally, this process of using homogenized solutions to update equivalence parameters could be repeated if one so chooses.

The details of how such a procedure could be implemented remain to be specified. One such detail is the method by which the boundary conditions for the fixed-source calculations are approximated from the homogenized solution. The spatial shape of any quantity (fluxes, net currents, partial currents, etc.) on the surface of a homogenized

assembly can not be expected to represent accurately the actual shape which exists on the surface of a heterogeneous assembly. Nevertheless, it is quite likely that the average value of such a quantity can be inferred from the homogenized solution. Hence, the fixed-source problem can be solved assuming that the spatial shape of the heterogeneous surface quantity is flat and that the magnitude of the quantity is the same as the homogenized surface quantity. A fixed-source calculation which makes such an assumption does reflect many of the interassembly effects such as gross flux tilts and spectral effects that are caused by neighboring assemblies. Unfortunately, such a fixed-source calculation neglects all of the effects that are due to the spatial shapes of the surface conditions. The simplest method for eliminating this shortcoming is to include more assemblies in the fixed-source calculation, and thus, move the approximate surface conditions farther away from the assembly of interest. For example, an assembly and its four nearest neighbors (in 2-D) could be used for the fixed-source calculation. With the source of errors (the approximate boundary conditions) moved to the outer surfaces of adjoining assemblies, no explicit limitations on the shapes of the surface quantities need be made for the center assembly. Consequently, the equivalence parameters for the center assembly are less sensitive to the boundary conditions of the fixed-source problem than they are in the case of a single-assembly calculation. Naturally, one could choose to include even more assemblies in the fixed-source calculation, and the corresponding equivalence parameters would be even more accurate.

Regardless of the number of assemblies that are included in the fixed-source calculation, a separate calculation must be performed for each assembly in the reactor to obtain all of the necessary equivalence parameters. If more than one assembly is included in the fixed-source calculation, additional information as to the shapes of the surface quantities for the center assembly is obtained. When the fixed-source calculation for the adjoining assembly is performed, this information can then be used to approximate more accurately the actual heterogeneous boundary conditions. This overall procedure for solving the global homogenized problem is summarized in the following seven steps:

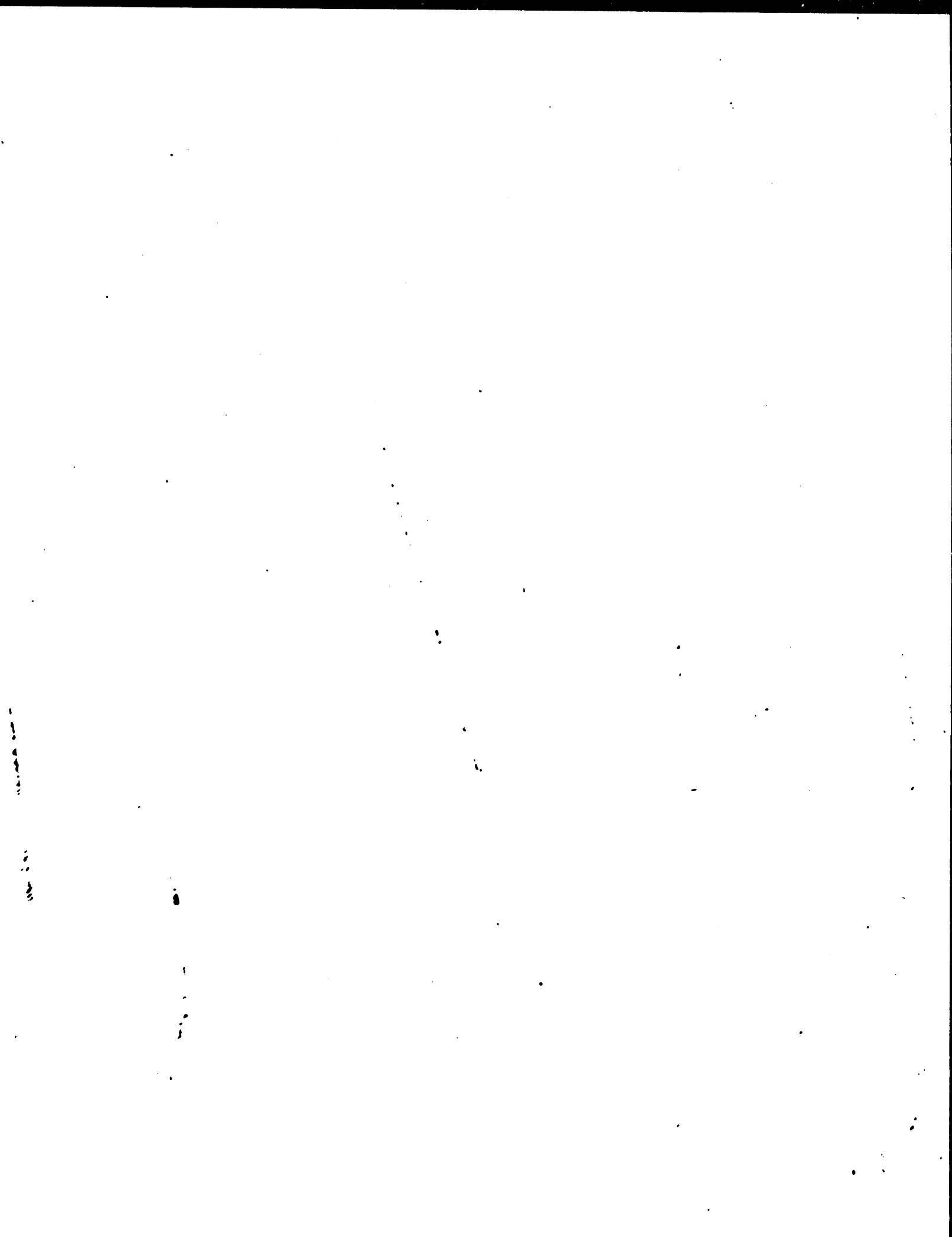
1. Approximate homogenized parameters are computed (FWC, CDF, or MCDF, etc.).
2. The global homogenized problem is solved.
3. The approximate magnitudes of the assembly surface quantities (fluxes, net currents, partial currents, etc.) are inferred from the homogenized solution.
4. A fixed-source calculation is performed for each assembly (including as many neighboring assemblies as one desires) with the magnitudes of the boundary conditions taken from Step 3 and the shapes of the boundary quantities taken from previous fixed-source calculations (or assumed flat if the required surface shape is yet to be computed).
5. Equivalence parameters are computed from the fixed-source solution.
6. The global homogenized problem is re-solved with the most

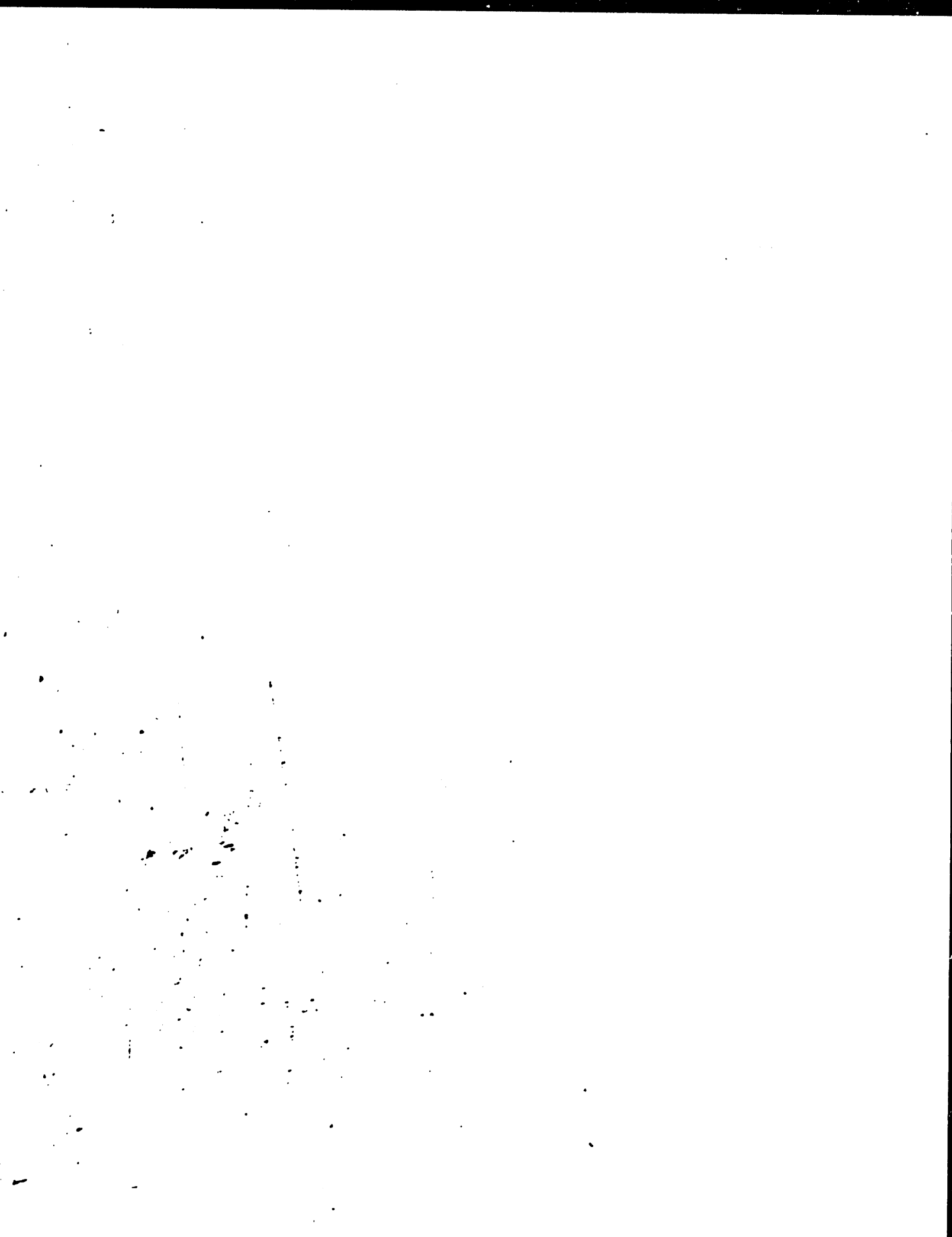
recent values of the equivalence parameters.

7. If the global solution is not converged, the process continues at Step 3.

This homogenization procedure, although complicated, has some unique features. If multiple assemblies are included in the fixed-source calculation, the converged homogenized solution which is obtained by this procedure will be identical (in the node-averaged sense) to the solution that would be obtained if the full heterogeneous problem had been solved (using the same method as is used in solving the fixed-source problem). In this sense, such a homogenization procedure can be viewed as an alternate method of solving the full heterogeneous problem or as a means of accelerating the heterogeneous solution method.

In principle, one need only choose the desired method for solving the fixed-source problem and this procedure will produce a homogenized solution which preserves all of the node-integrated quantities that would be obtained if the full heterogeneous problem were solved. In practice, the aforementioned homogenization method has many aspects which require additional consideration. In addition, many prudent assumptions can be made to simplify this procedure without significantly degrading the accuracy of the final homogenized solution.





#### 4.3 TECHNIQUES FOR SOLVING THE LOCAL FIXED-SOURCE PROBLEMS

No restrictions need to be imposed with respect to the methods employed to solve the local fixed-source problems. However, it is quite clear that if such methods are not computationally efficient, this complicated homogenization scheme may require as much (or more) computation effort as solving directly the full heterogeneous problem. Should this prove to be the case, the homogenization scheme would have no practical value.

In terms of computational efficiency, response matrix methods<sup>2</sup> appear to be very well-suited for solving the fixed-source problems. Heterogeneous response matrices can be precomputed for each type of assembly in a reactor (as a function of fuel type, exposure, coolant density, fuel temperature, etc.). In a response matrix problem (with the double- $P_0$  angular approximation), the unknowns are the interface partial currents which can be related to the interfacial fluxes and net currents.<sup>2</sup> Response matrix methods have been developed which permit many different approximations for the spatial shapes of the partial currents (flat, multiple flats, linear, modulated eigenvalue shapes, etc.).<sup>15</sup> The principle reason that the response matrix methods appear so attractive for solving the fixed-source problems is that the only unknowns (partial currents) can be related directly to the quantities (surface fluxes and net currents) which are required to define the equivalence parameters. Reaction-rate and average-flux response matrices are also easily computed, and the additional quantities that are required to calculate equivalence parameters are readily available.

Despite the fact that response matrix methods appear to be the best choice of methods for solving the local fixed-source problems, an alternate method was utilized to solve the fixed-source problems in this thesis. The reasons for avoiding response matrix methods at this stage were twofold. First, the use of response matrix methods requires that choices be made with respect to the representation of the spatial shapes of the partial currents. Such choices should be based on the accuracy which is desired in the global homogenized solution. Hence, determining what shapes are required for a certain level of accuracy requires a considerable amount of preliminary exploration. Secondly, many of the possible simplifications of the overall homogenization scheme are easily investigated by using alternate (although more expensive) methods for solving the fixed-source problems. (The incorporation of response matrix methods into this homogenization scheme is presently being investigated by A. F. Henry and A. Y. C. Cheng.<sup>16</sup>)

The technique that is used to solve all of the heterogeneous fixed-source problems in this thesis is the same method that was used for the heterogeneous cell calculations in Chapter 3, the Analytic Nodal Method (QUANDRY with the flat transverse leakage approximation). It is quite clear that this method for solving the fixed-source problems is very inefficient. Nevertheless, many of the features of the proposed homogenization scheme which need to be investigated are independent of the methods used to solve the fixed-source problems. As a consequence, it is anticipated that much of the insight that is gained from examining the homogenization scheme with heterogeneous diffusion

theory fixed-source calculations will also be valid when more efficient methods are used to solve the fixed-source problems.

The boundary conditions which are required for the fixed-source (diffusion theory) problems are the net current distributions on the outermost assembly surfaces. Since the shapes of the true heterogeneous net currents and the homogenized net currents are very different, the boundary conditions for the fixed-source problems are approximated as spatially flat and equal in magnitude to the surface-averaged currents from the most recently computed homogenized solution. One possible consequence of using the flat shape and the approximate magnitude (from the latest homogenized global solution) for the net current boundary condition in the fixed-source problem is that the problem may be ill-posed. For example, consider the case of a single homogeneous assembly which is a net producer of neutrons. If one attempts to impose inward-directed net currents on all surfaces of this assembly, clearly the "fixed-source" problem cannot converge to an everywhere positive solution. The simplest approach for alleviating this difficulty is to introduce an eigenvalue ( $k_{eff}$ ) which can be adjusted (increased) until the local fixed-source problem becomes well-posed. The occurrences of such ill-posed fixed-source problems are indeed rare. This problem is a direct manifestation of the net current boundary condition, and such problems cannot occur if response matrix methods, for which partial currents become the boundary conditions, are used.

The QUANDRY code has been modified such that it is capable of solving the global homogenized problem and the local heterogeneous

fixed-source problems in the tandem process that has been outlined. By virtue of the flat net current approximation, the overall homogenization scheme will not converge to the solution that would be obtained if the full heterogeneous diffusion calculation were performed. However, this approximation will introduce only very small inaccuracies into the homogenization process. The magnitudes of these inaccuracies are discussed in forthcoming sections of this chapter.

#### 4.4 RESULTS OBTAINED BY USING APPROXIMATE DISCONTINUITY FACTORS OBTAINED FROM LOCAL HETEROGENEOUS FIXED-SOURCE CALCULATIONS

The proposed homogenization scheme is somewhat complicated, and its usefulness depends upon the efficiency with which it can be adapted to realistic homogenization problems. In order to establish the efficiency of the method, many pertinent questions must be answered. In this section, numerical results are presented in an attempt to answer the following questions:

1. How many assemblies must be included in each fixed-source problem to achieve a given level of accuracy?
2. How many times must the global and local fixed-source problems be repeated in order to achieve a converged homogenized solution?
3. To what solution does the overall homogenization process converge?
4. What implications are there with respect to the use of response matrix techniques for solving the local fixed-source problems?

5. Can the homogenization method be utilized without introducing significant computational burdens?

#### 4.4.1 Results Obtained Using Single-Assembly Fixed-Source Calculations

The case for which the most iterations (i.e., a fixed-source calculation for each assembly and a new global homogenized calculation) are required to converge the global solution is that for which the equivalence parameters are the most sensitive to the net current boundary conditions (which are approximated). Clearly, when more assemblies are included in the fixed-source calculations the equivalence parameters become less sensitive to the approximate boundary conditions. As a consequence, the homogenization process will be the slowest to converge for the case in which a single-assembly geometry is used in the fixed-source calculation. In order to establish the corresponding convergence rate of the overall homogenization process, three BWR benchmark problems were solved using QUANDRY with single-assembly fixed-source geometries. Since the fixed-source problems are sensitive to the values of the net currents that are used as boundary conditions, it is reasonable to start the iterative process with the most accurate homogenized parameters that are available. For this reason, the CDF are used to generate the initial (zeroth iterate) global solutions and corresponding nodal surface currents. For reasons of consistency, the spatial meshes for the heterogeneous fixed-source calculations are taken to be the same as the meshes used to generate the reference solutions.

The results obtained at each iteration of the Henry-Worley BWR problem are summarized in Table 4-1, and the corresponding assembly power densities are presented in Fig. A2-12 of Appendix 2. From these results, it is clear that the converged solution obtained by using the single-assembly fixed-source calculation is much more accurate than the solution obtained with CDF. It is also clear that the homogenization-global solution process converges very rapidly. For most purposes, one would conclude that the iterative process is converged after 2 iterations. It is also significant that the converged global solution is essentially the same as the solution which is obtained when the reference values of the net currents (spatially flat) are used for the fixed-source boundary conditions and the resulting equivalence parameters are used to generate a global solution. This observation implies that one can obtain the converged global solution by performing a

TABLE 4-1

Summary of Results for the Henry-Worley BWR Homogenization Problem Using Single-Assembly Fixed-Source Calculations

	<u>Iteration Number</u>			Solution Which Uses Reference Surface Currents
	<u>0 (CDF)</u>	<u>1</u>	<u>2</u>	
Error in eigenvalue	-0.49%	-0.13%	-0.24%	-0.27%
Maximum error in assembly power	+4.10%	+1.73%	-0.58%	-0.57%
Average error in assembly powers	1.34%	0.34%	0.39%	0.35%

single iteration with the reference values of the surface-averaged net currents used as boundary conditions for the fixed-source problems, instead of starting from the solution obtained with CDF and iterating until the global solution is converged. This shortcut is of course useful only in determining the accuracy of the homogenization method in problems for which the reference solutions are known. In practice, the reference solution is not known, and one must iterate to obtain the converged solution.

Summaries of results obtained for the CISE and HAFAS BWR problems are presented in Tables 4-2 and 4-3. The corresponding assembly power densities are displayed in Figs. A2-13 and A2-14 of Appendix 2. From these results, it appears that the homogenization process is essentially converged after one iteration. This rapid converge is probably a result of the explicit modeling of the interassembly water gaps (that are not present in the Henry-Worley problem) which tend to decouple adjacent assemblies. This rapid convergence of the homogenization scheme is a very important practical consideration, as much computational effort is saved when a single iteration is sufficient. The results for the CISE problem do not display the dramatic improvement in accuracy (compared to the solution obtained with CDF) that is achieved in the Henry-Worley problem. The maximum error in assembly power is reduced from 3.06% to 2.64%. However, for the more realistic HAFAS BWR problem, the maximum error in assembly power is reduced from 5.29% to 2.10%. The significant reduction in the average errors of the assembly powers also indicates that the solution obtained with single assembly fixed-source calculations is

TABLE 4-2

Summary of Results for the CISE BWR Homogenization Problem  
Using Single-Assembly Fixed-Source Calculations

	<u>Iteration Number</u>		<u>Solution Which</u> <u>Uses Reference</u> <u>Surface Currents</u>
	<u>0 (CDF)</u>	<u>1</u>	
Error in eigenvalue	-0.03%	+0.16%	+0.18%
Maximum error in assembly power	-3.06%	-2.76%	-2.64%
Average error in assembly powers	0.90%	0.97%	0.95%

TABLE 4-3

Summary of Results for the HAFAS BWR Homogenization Problem  
Using Single-Assembly Fixed-Source Calculations

	<u>Iteration Number</u>		<u>Solution Which</u> <u>Uses Reference</u> <u>Surface Currents</u>
	<u>0 (CDF)</u>	<u>1</u>	
Error in eigenvalue	-0.06%	+0.12%	+0.13%
Maximum error in assembly power	-5.29%	+2.21%	+2.10%
Average error in assembly powers	1.33%	0.86%	0.83%

considerably more accurate than the solution obtained with CDF. The results obtained by using single-assembly fixed-source calculations for the CISE and HAFAS BWR problems indicate that the reactor eigenvalues are predicted with less accuracy than is obtained from calculations which use CDF. However, the values of the equivalence parameters obtained from the single-assembly fixed-source calculations are more accurate than the CDF. Hence, it appears that some fortuitous cancellation of errors occurs in the solutions which use CDF.

All of the results obtained using single-assembly fixed-source calculations suggest that two of the previously-posed questions have been answered. Namely, the overall homogenization process converges in one or two iterations. Also, the converged global solution is essentially the same as that which is obtained when the reference values of the surface-averaged net currents are used as boundary conditions for the fixed-source problems and the resulting equivalence parameters are used to generate a global homogenized solution.

#### 4.4.2 Results Obtained Using Five-Assembly Fixed-Source Calculations

The accuracy of the homogenized BWR solutions obtained by using single-assembly fixed-source calculations are such that one would expect a maximum homogenization error in assembly power of less than 2.5%. Such accuracy is sufficient for much of the reactor analysis that is routinely performed. If, however, one desires that homogenization errors be reduced further, larger numbers of assemblies can be included in the fixed-source calculations such that the errors

which arise from the approximate boundary conditions are reduced. The obvious first choice for such calculations (in 2-D) is to include the four assemblies that surround the assembly for which the equivalence parameters are to be computed.

The results from the single-assembly fixed-source calculations suggest that it is reasonable to expect the overall homogenization process to be essentially converged after one iteration. For this reason, the five-assembly fixed-source problems for the CISE and HAFAS BWR problems were solved using the reference values of the surface-averaged net currents to save the expense of generating a converged solution by iteration. The global solutions obtained with these five-assembly fixed-source calculations are compared to the solutions which used CDF and single-assembly calculations in Tables 4-4 and 4-5, for the CISE and HAFAS problems, respectively. From these results, it is evident that the homogenized solutions generated with five-assembly fixed-source calculations are considerably more accurate than the solutions which used single-assembly fixed-source calculations. Since the maximum error in assembly powers for these two solutions is 1.07%, there seems to be very little incentive to add additional assemblies to the fixed-source problems. Spatial homogenization errors of this magnitude are of comparable magnitude to the errors that are introduced by other sources (multigroup approximation, transport effects, manufacturing tolerances, etc.). For these reasons, the use of more than five assemblies in the fixed-source calculations appears unwarranted.

TABLE 4-4  
Comparison of Results for the CISE BWR Problem

	<u>Method for Generating Equivalence Parameters</u>		
	<u>CDF</u>	<u>Single-Assembly Fixed-Source Calculation</u>	<u>5-Assembly Fixed-Source Calculation</u>
Error in eigenvalue	-0.03%	+0.18%	-0.06%
Maximum error in assembly power	-3.06%	-2.64%	+0.77%
Average error in assembly powers	0.90%	0.95%	0.29%

TABLE 4-5  
Comparison of Results for the HAFAS BWR Problem

	<u>Method for Generating Equivalence Parameters</u>		
	<u>CDF</u>	<u>Single-Assembly Fixed-Source Calculation</u>	<u>5-Assembly Fixed-Source Calculation</u>
Error in eigenvalue	-0.06%	+0.13%	-0.04%
Maximum error in assembly power	-5.29%	+2.10%	+1.07%
Average error in assembly powers	1.33%	0.83%	0.52%

## 4.5 POSSIBLE MODIFICATIONS OF THE SOLUTION METHOD FOR THE GLOBAL HOMOGENIZED PROBLEM

One of the interesting features of equivalence parameters that was discussed in Chapter 2 is that rigorous equivalence parameters can be defined (from a known reference solution) for any global solution method such that the homogenized solution will match all of the node-integrated properties of the reference solution. When reference solutions are not known, it is still possible to simplify global solution methods by defining appropriate equivalence parameters. If adequate equivalence parameters can be determined by approximate methods, the resulting homogenization scheme may be attractive since the amount of computational effort required to solve the global homogenized problem may be reduced significantly.

### 4.5.1 Simplified Flux-Current Coupling Relationships in Global Solution Methods

In order to investigate such possibilities, equivalence parameters were generated for the HAFAS BWR problem from the converged single-assembly fixed-source calculations. Equivalence parameters and the corresponding global homogenized solutions were computed for each of the three spatial approximations that are incorporated in QUANDRY (quadratic, flat and CMFD). The global solutions obtained with the quadratic and flat spatial approximations agree to within 0.1%. If the CMFD approximation is used, the maximum errors in the homogenized solution increase from 2.1% to 2.9%. The CMFD approximation (a finite-difference approximation with one mesh point per

assembly) is a very crude spatial approximation, but the equivalence parameters compensate for most of its inaccuracy and the homogenized solution is quite accurate. These results indicate that virtually any global solution method could be used, and the converged homogenized solution will be practically independent of the chosen method. The number of iterations that are required for the homogenization-global solution process to converge may, however, depend on the global solution method. Certainly, if the global solution method is very inaccurate, the initial approximations for the assembly surface currents (which are used as boundary conditions for the fixed-source calculations) will be significantly in error, and many iterates may be required to converge the homogenization process. The effects of the global solution methods on the convergence rate have not been investigated, but all evidence suggests that modest simplifications in global solution methods (such as relaxing the quadratic transverse leakage approximation to the flat approximation) will have very little effect on the convergence rate.

#### 4.5.2 Simplified Neutron Energy Group Representations

It is also possible that the global homogenized problem can be solved with fewer neutron energy groups than the fixed-source calculations without a loss in accuracy. Such a simplification would be most attractive when it is desired to obtain the global solution to a many-group problem. Clearly, the group-to-group ratios of the surface currents (that are required for the fixed-source boundary conditions) would not be available from the first global solution. However,

as the fixed-source problems are solved, this information is generated (provided at least five assemblies are used in the fixed-source calculations) and can be updated at each pass through the homogenization process. This process will converge to the desired result, but more iterations may be required to obtain convergence.

In order to demonstrate the feasibility of such an approach, the global homogenized solution to the CISE BWR problem was generated with one-group equivalence parameters defined from the converged five-assembly, two-group fixed-source calculations. The resultant global solution is essentially identical to that which is obtained when the two-group homogenized problem is solved. This indicates that the same multigroup solution can be obtained when a collapsed group formulation of the global problem is used. The actual advantages of using a one-group global calculation instead of the two-group approximation are probably minimal. However, such a scheme may be attractive in collapsing four-group thermal reactor calculations to two-group calculations. The effects of collapsing groups on the convergence rate of the overall homogenization scheme have not been investigated.

#### 4.5.3 The Use of Multi-Assembly Nodes in the Global Solution

Some of the quantities of interest in any global reactor calculation are the powers in each of the fuel assemblies. This being the case, one might think that the global solution method must represent each individual assembly as a distinct node. For most reactors, such a representation would require many hundreds of nodes in each two-dimensional reactor plane, and hence, the global calculation would

require considerable computation effort. However, if equivalence parameters are determined from local fixed-source problems, there exist no fundamental reasons why each assembly must be treated as a distinct node. For example, clusters of four assemblies could be treated as distinct nodes in the global calculation. This would reduce the computational burden on the global homogenized solution method; moreover, the information which characterizes each assembly (such as assembly power fractions) can be determined from the fixed-source calculations. If such an approach is adopted, the global homogenized solution will produce net current information for nodes whose surfaces correspond to two assembly surfaces. Consequently, the boundary current information that can be taken from the homogenized solution is restricted to average values over two assemblies, and the values of the current splits between assemblies must be obtained from subsequent fixed-source calculations. Despite the reduction in computational effort required for the global homogenized solutions, such a homogenization procedure would probably require more iterations to converge than the case in which each assembly is treated as a distinct node in the glcbal calculation.

The first iterate in the homogenization process with four-assembly nodes was computed for the HAFAS BWR problem. In this problem, surface currents were taken from a homogenized solution (which used CDF), and the corresponding four-assembly (single node) heterogeneous fixed-source calculations were performed with flat surface current boundary conditions. Equivalence parameters were then defined from the fixed-source calculations and the corresponding homogenized

problem was solved. The resulting solution displayed errors in assembly powers as large as seven percent. These results are much less accurate than those obtained on the first iteration with single-assembly nodes (the maximum error in assembly power is approximately 2.2%). Clearly, more iterations would be required to improve the accuracy of the fixed-source surface currents and the homogenized solution. The existing version of QUANDRY is restricted to flat net current shapes on the nodal surfaces of the fixed-source problems. Hence, the actual convergence rate of the homogenization process with four-assembly nodes was not investigated.

The attractiveness of the possible modifications discussed in this section depends to a large extent on the relative computation efficiencies of the global solution method and the fixed-source calculational method. Since the computationally-inefficient QUANDRY method for solving the fixed-source problems was used for the present study, only the feasibility of the proposed homogenization scheme was tested, and no firm conclusions can be drawn with respect to the overall attractiveness of the potential modifications. If, however, efficient methods for solving the fixed-source problems are developed, an investigation of possible modifications of the global model is certainly warranted. The use of equivalence parameters makes it quite clear that the homogenization method and the global solution method are by no means independent of one another.

#### 4.6 SUMMARY

In this chapter, a method for computing approximate equivalence parameters from local heterogeneous fixed-source calculations was introduced. This method is capable of accounting for the interassembly effects that are neglected by the cell calculations used to obtain CDF and MCDF. It requires, however, that the quantities to be used as boundary conditions in the fixed-source problems be approximated from global homogenized solutions. Therefore, a nonlinear iterative process for obtaining equivalence parameters was introduced in which the net current boundary conditions for the fixed-source problems are updated from the most recent global homogenized solutions (which use the most recently-computed equivalence parameters).

The accuracy of this homogenization scheme was investigated with single- and five-assembly fixed-source calculations. The maximum errors (in assembly powers) for homogenized BWR solutions obtained using single-assembly fixed-source calculations were approximately 2.5%. The corresponding errors in the solutions obtained using five-assembly fixed-source calculations were approximately 1.0%. In both cases it was found that the homogenized solutions were essentially converged after only one iteration. That is, converged equivalence parameters were obtained from local fixed-source calculations with net current boundary conditions taken from global homogenized solutions which used CDF. Thus, in a practical sense, the nonlinear iterative process was avoided.

In Chapter 5, the applicability of these results to the more practical case in which fixed-source problems are solved by response matrix methods is discussed.

## Chapter 5

### SUMMARY AND CONCLUSIONS

#### 5.1 OVERVIEW OF THE INVESTIGATION

The objective of this research effort was to develop accurate and efficient spatial homogenization methods for coarse mesh analysis of light water reactors. Initially, a method for determining spatially flat homogenized parameters which could reproduce all of the node-integrated properties of a known reference solution was sought. It was shown that the conventional diffusion equation lacks sufficient degrees of freedom to allow this condition to be met. As a consequence, conventional flux-weighting techniques for cross section homogenization were abandoned.

In Chapter 2, Koebke's "equivalence theory" homogenization method<sup>14</sup> was introduced and formally derived. The unique feature of this method is the introduction of two additional degrees of freedom (per direction and group) to the conventional diffusion equation. Koebke defined group diffusion coefficients and "heterogeneity factors" for each homogenized node (and each direction). The heterogeneity factor is defined to be the ratio of the known reference surface flux to the homogenized nodal surface flux. In this fashion, Koebke permitted the homogenized fluxes to be discontinuous at nodal interfaces and treated the magnitude of the discontinuity as a homogenization parameter. Koebke's method was shown to be capable of reproducing rigorously all of the node-integrated properties of any known reference solution.

Koebke's homogenization scheme was then extended to obtain a "generalized equivalence theory" homogenization method. In this formulation, diffusion coefficients are treated as directionally independent, and "discontinuity factors" (the ratios of reference surface fluxes to homogenized nodal surface fluxes) are defined for each surface of the homogenized nodes. This formulation avoids several of the difficulties of Koebke's method, but it is still capable of reproducing rigorously all the node-integrated properties of any known reference solution. This homogenization scheme suffers from the same drawback as Koebke's scheme, in that the rigorous equivalence parameters cannot be found without a priori knowledge of the reference (heterogeneous) solution.

Koebke's published work gives no indications as to how the equivalence parameters can be found (or approximated) without knowledge of the reference solution. Consequently, the primary objective of this thesis became the development of approximate methods for computing equivalence parameters. In Chapter 3, a method for computing approximate equivalence parameters from heterogeneous cell calculations was introduced. Through use of these parameters, homogenized BWR power distributions were predicted with maximum errors in assembly powers of approximately 3%. When compared to conventional flux-weighting homogenization methods, these approximate equivalence parameters (MCDF) were found to predict assembly powers with three to five times greater accuracy than the flux-weighting methods. In addition to their accuracy, these approximate equivalence parameters have several desirable characteristics. First, they can be derived at

no additional cost from the same cell calculations that are used to compute conventional flux-weighted parameters. Secondly, no restrictions need be imposed with respect to the methods used to perform the heterogeneous cell calculations. As a consequence, the use of cell discontinuity factors (CDF) fits very nicely into the framework of conventional homogenization schemes, regardless of the methods (multi-group diffusion theory, integral transport theory, Monte Carlo, etc.) used to perform the cell calculations.

In Chapter 4, more sophisticated (and more accurate) methods for computing approximate equivalence parameters were introduced. These methods make use of nonlinear iterations between global homogenized reactor calculations and local fixed-source calculations to compute equivalence parameters. It was shown that homogenized BWR power distributions can be predicted with maximum errors in assembly powers of approximately 1.0%. It was also found that the nonlinear iterative process converges very rapidly; practical convergence was usually obtained with only one iteration.

Many different schemes for approximating equivalence parameters have been investigated in this thesis. The appropriate choice of homogenization schemes to be used for a certain class of reactor analyses depends upon the accuracy that is required of the homogenized solutions. As a consequence, no one homogenization scheme can be singled out as the appropriate choice for all classes of analyses. A comparison of solutions to the highly heterogeneous HAFAS BWR homogenization problem obtained by various homogenization schemes is presented in Table 5-1, to indicate the relative accuracy that can be expected of the various homogenization schemes in BWR analysis.

TABLE 5-1

Comparison of Solutions to the HAFAS BWR Homogenization Problem  
Obtained by Various Homogenization Schemes

Method Used to Evaluate Homogenized Parameters

	<u>FWC</u>	<u>CDF</u>	<u>MCDF</u>	<u>Single Assembly Fixed-Source Calculations</u>	<u>Five-Assembly Fixed-Source Calculations</u>
Error in eigenvalue <sup>a</sup>	-0. 44%	-0. 06%	-0. 02%	+0. 16%	-0. 04%
Maximum error in assembly power	+16. 95%	-5. 29%	+4. 00%	+2. 10%	+1. 07%
Average error in assembly powers	6. 14%	1. 33%	1. 05%	0. 83%	0. 52%

<sup>a</sup> Reference: 1.0442

## 5.2 POSSIBILITIES OF USING RESPONSE MATRIX METHODS FOR SOLVING THE LOCAL FIXED-SOURCE PROBLEMS

The techniques used in Chapter 4 of this thesis to solve the local heterogeneous fixed-source problems were very useful in demonstrating the accuracy of the proposed homogenization schemes. However, the QUANDRY solution method was developed for coarse mesh reactor analysis, and consequently, this method is a very inefficient means of solving fine mesh heterogeneous problems. As a result, it was not possible to evaluate the efficiency with which the proposed homogenization scheme can be adapted to actual reactor analysis. This fact is strikingly clear when one considers that the homogenization process for the HAFAS problem requires from 30% to 150% (depending upon the fixed-source geometry) of the CPU time that is required to solve the full heterogeneous diffusion theory problem. Clearly, much more efficient methods for solving the local fixed-source problems are required to make the homogenization schemes of Chapter 4 economically attractive.

The most attractive methods for solving the local fixed-source problems appear to be response matrix methods. If accurate heterogeneous response matrices are precomputed for each type of assembly in a reactor (as a function of exposure, coolant density, fuel temperature, etc.), it may be possible to solve the local fixed-source problems in an accurate, yet efficient manner. Since the only unknowns in the response matrix methods are interface partial currents, only a small number of unknowns are required to model the local fixed-source problems, and the calculational effort required to solve the local problems can be minimized.

In this thesis, the fixed-source problems were solved by imposing spatially flat net currents on all of the outermost assembly surfaces. If response matrix methods are used to solve the fixed-source problems, incoming partial currents are required as the boundary conditions. It seems doubtful that this difference will have any significant effect on the accuracy of the fixed-source solutions. Many options are available as to the spatial shapes which are used to represent the partial currents in response matrix problems.<sup>15</sup> The evidence from the single-assembly fixed-source calculations in this thesis suggests that if partial currents are assumed spatially flat, homogenized power distributions should be predicted with a maximum error of approximately 2%. This accuracy will be unaffected by the geometry which is used in the fixed-source calculations, as both the single- and five-assembly fixed-source calculations converge to the solution that is obtained when the reference values of the surface currents are used.

The five-assembly calculations that were performed in this thesis show a significant increase in accuracy over the single-assembly calculations. This is primarily due to the fact that there are no explicit restrictions on the shapes of the surface currents for the center assembly. However, if response matrix methods are used, the spatial shapes of the surface currents for the center assembly are restricted by the choices that are made for the shapes of the partial currents. Consequently, depending on the generality that is chosen for the partial current shapes, the accuracy of the solutions will probably be somewhere in the range between the accuracy of the single-assembly and the five-assembly results ( $\sim 2.\%$  -  $1.\%$ ) obtained in this thesis.

If response matrix methods for solving the fixed-source problems are implemented, all of the possible simplifications to the global solution method (that were discussed in Section 4.5 of Chapter 4 and demonstrated to be theoretically feasible) can be investigated to ascertain their effects on the computational efficiency of the overall homogenization scheme.

### 5.3 RECOMMENDATIONS FOR FUTURE RESEARCH

During the course of this investigation, many items of potential interest have been left unresolved. Many of these items warrant additional investigation, and this section contains a description of the potential research areas.

#### 5.3.1 Refinements in Cell Calculations Used to Obtain Approximate Equivalence Parameters

The accuracy of the homogenized BWR solutions obtained by using CDF is quite good (3.% - 5.% maximum errors). However, additional refinements of the methods used for the cell calculations could lead to even more accurate solutions. For instance, albedo boundary conditions could be used in the cell calculations for the peripheral fuel assemblies (instead of zero net current boundary conditions) to treat more correctly the reflector effects. Similarly, in the calculation of MCDF, a two-cell treatment could be utilized for the peripheral fuel assemblies.

All of the cell calculations used in this thesis were two-group diffusion theory calculations, but no such restrictions need be imposed,

The use of more sophisticated techniques for performing cell calculations (such as multigroup integral transport methods) have become common in recent years. Since CDF can be generated by any of these methods, the accuracy of such approaches should be investigated.

### 5.3.2 PWR Applications

Spatial homogenization difficulties are generally more severe in BWRs than in PWRs. For this reason, all of the analysis in this thesis was restricted to the case of BWRs. However, the methods developed in this thesis are equally applicable to the analysis of PWRs. The equivalence theory homogenization schemes will probably be most useful in transient PWR calculations in which control rod movements and non-equilibrium thermal-hydraulic effects are important.

It is also likely that equivalence parameters may be quite useful in representing the core baffle and reflector, as the baffle is a very localized absorber which might be modeled accurately by discontinuity factors. Such PWR applications should be pursued.

### 5.3.3 3-D Effects

All of the analysis in this thesis was restricted to two-dimension radial planes. Although the spatial heterogeneity in the radial planes is usually more severe than the axial heterogeneity, there do exist certain exceptions. The most important of the axial heterogeneities is caused by the presence of control blades. These heterogeneities seem as equally amenable to equivalence theory treatment as the radial effects. In addition, the control rod "cusp" difficulties<sup>5</sup> which arise

in transient problems could also be treated with equivalence theory parameters.

#### 5.3.4 Response Matrix Considerations

If response matrix methods are to be used to solve the local fixed-source problems, many items will require additional investigation. The optimum representation of the partial current shapes must be determined. In addition, the optimum fixed-source geometry must be determined (although five or fewer assemblies should suffice), since the optimum choice depends on the partial current representation. In addition, the incorporation of the simplifications to the global solution method becomes possible when response matrix methods are used. Hence, the economic advantages of including some of these modifications can be examined. The difficulties of representing response matrix elements as functions of exposure, moderator density, fuel temperature, etc. must also be addressed in order to determine the actual computational efficiency of the proposed homogenization scheme.

## REFERENCES

1. G.I. Bell and S. Glasstone, Nuclear Reactor Theory, Van Nostrand-Reinhold, New York, N.Y. (1970).
2. A.F. Henry, Nuclear Reactor Analysis, M.I.T. Press, Cambridge, Mass. (1975).
3. A.F. Henry, B.A. Worley, and A.A. Morshed, "Spatial Homogenization of Diffusion Theory Parameters," Paper presented at the IAEA Technical Committee Meeting on Homogenization Methods in Reactor Physics, Lugano, Switzerland (Nov. 1978).
4. K.S. Smith, "An Analytic Nodal Method for Solving the Two-Group, Multidimensional, Static and Transient Neutron Diffusion Equation," Department of Nuclear Engineering Thesis, M.I.T., Cambridge, Mass. (March 1979).
5. H. Finnemann, F. Bennewitz, and M.R. Wagner, "Interface Current Techniques for Multidimensional Reactor Calculations," Atomkernenergie (ATKE) Bd. 30 (1977).
6. R.D. Lawrence, "A Nodal Green's Function Method for Multi-dimensional Neutron Diffusion Calculations," Ph.D. thesis, Department of Nuclear Engineering, University of Illinois at Urbana-Champaign (1979).
7. G.P. Bottoni, R. Guandalini, G. Vimercati, and P. Peroni, "Neutronic Aspects of the LWR Core Simulator CETRA," ANS/ENS (May 1979).
8. S. Borresen, "A Simplified, Coarse-Mesh, Three-Dimensional Diffusion Scheme for Calculating Gross Power Distributions in a BWR," NSE 44 (1971).
9. B.A. Worley and A.F. Henry, "Spatial Homogenization of Diffusion Theory Parameters," MITNE-210, Department of Nuclear Engineering, M.I.T. (1977).
10. A.F. Henry, personal communication (1980).
11. G. Pierini, "A Consistent Homogenization Procedure to Obtain Few-Group Cell Parameters," Atomkernenergie (ATKE) Bd. 34 (1970).
12. R.A. Bonalumi, "A Rigorous Calculation of Homogenized Diffusion Theory Parameters," Trans. Am. Nucl. Soc., 30 (1978).

13. R.A. Bonalumi, F. La Briola, and G.C. Pierini, "Homogenized-Cell Diffusion Parameters from Transport Codes," *Trans. Am. Nucl. Soc.*, 26 (1977).
14. K. Koebke, "A New Approach to Homogenization and Group Condensation," Paper presented at the IAEA Technical Committee Meeting on Homogenization Methods in Reactor Physics, Lugano, Switzerland (Nov. 1978).
15. T.C. Sbarounis, "Treatment of the Spatial Shape of the Currents in the Response Matrix Method," Ph.D. thesis, Department of Nuclear Engineering, M.I.T. (November 1977).
16. A.F. Henry and A.Y.C. Cheng, personal communication (1980).

Appendix 1  
DESCRIPTION OF BWR TEST PROBLEMS

A1.1 The Henry-Worley BWR Benchmark Problem

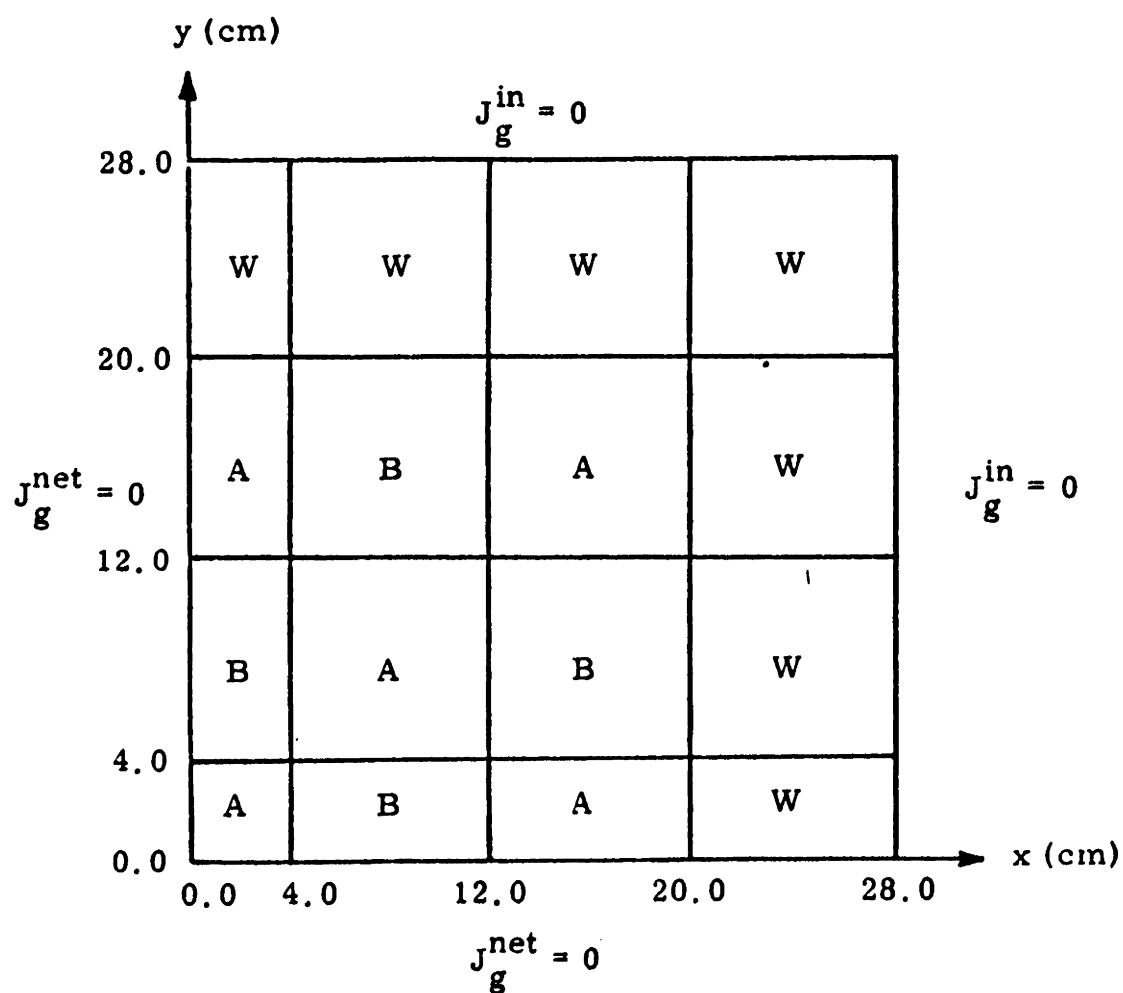
A1.2 The CISE BWR Homogenization Problem

A1.3 The HAFAS BWR Homogenization Problem

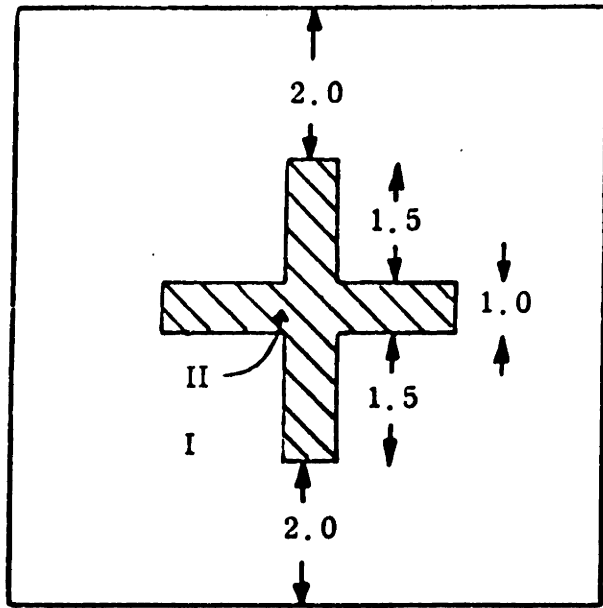
## A1.1 THE HENRY-WORLEY BWR BENCHMARK PROBLEM

### Geometry:

Quadrant of the 2-D Reactor



Fuel Assembly Description:



Composition to Zone Assignment by Assembly Type:

Zone	Assembly Type		
	A	B	W
I	1	1	2
II	3	2	2

Material Properties:

Composition	Group, g	D <sub>g</sub> (cm)	Σ <sub>a<sub>g</sub></sub> (cm <sup>-1</sup> )	ν Σ <sub>f<sub>g</sub></sub> (cm <sup>-1</sup> )	Σ <sub>gg'</sub> (cm <sup>-1</sup> )
1 (Fuel)	1 2	1.4360 0.3868	0.01051 0.1018	0.007293 0.15310	0.01596 0.0
2 (Water)	1 2	1.5450 0.3126	0.000444 0.008736	0.0 0.0	0.02838 0.0
3 (Control blade)	1 2	1.0920 0.3507	0.03185 0.4021	0.0 0.0	0.0 0.0

$$x_1 = 1.0$$

$$x_2 = 0.0$$

$$\nu = 2.5$$

Flux-Weighted Constants for the Henry-Worley BWR Problem

Assembly Type	Group, g	$\hat{D}_g$ (cm)	$\hat{\Sigma}_{a_g}$ (cm <sup>-1</sup> )	$\nu \hat{\Sigma}_{f_g}$ (cm <sup>-1</sup> )	$\hat{\Sigma}_{gg'}$ (cm <sup>-1</sup> )
A	1	1.3880	0.00971	0.006499	0.01422
	2	0.3842	0.1218	0.14290	0.0
B	1	1.4470	0.0942	0.006505	0.01730
	2	0.3748	0.08929	0.13250	0.0
W	1	1.5450	0.000444	0.0	0.02838
	2	0.3126	0.008736		0.0

$$x_1 = 1.0$$

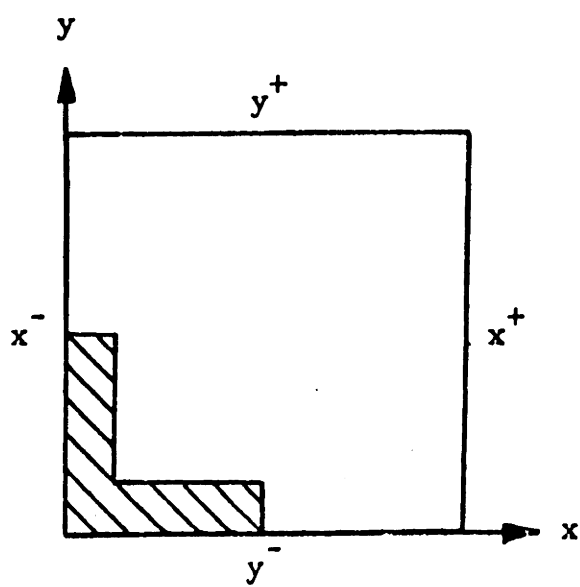
$$x_2 = 0.0$$

$$\nu = 2.5$$

Cell Discontinuity Factors for the Henry-Worley Problem

Assembly Type	Group, g	$\frac{f_x^-}{g}$	$\frac{f_x^+}{g}$	$\frac{f_y^-}{g}$	$\frac{f_y^+}{g}$
A	1	0.9976	1.0020	0.9976	1.0020
	2	0.7996	1.1390	0.7996	1.1390
B	1	0.9939	1.0040	0.9939	1.0040
	2	1.1180	0.9222	1.1180	0.9222
W	1	1.0	1.0	1.0	1.0
	2	1.0	1.0	1.0	1.0

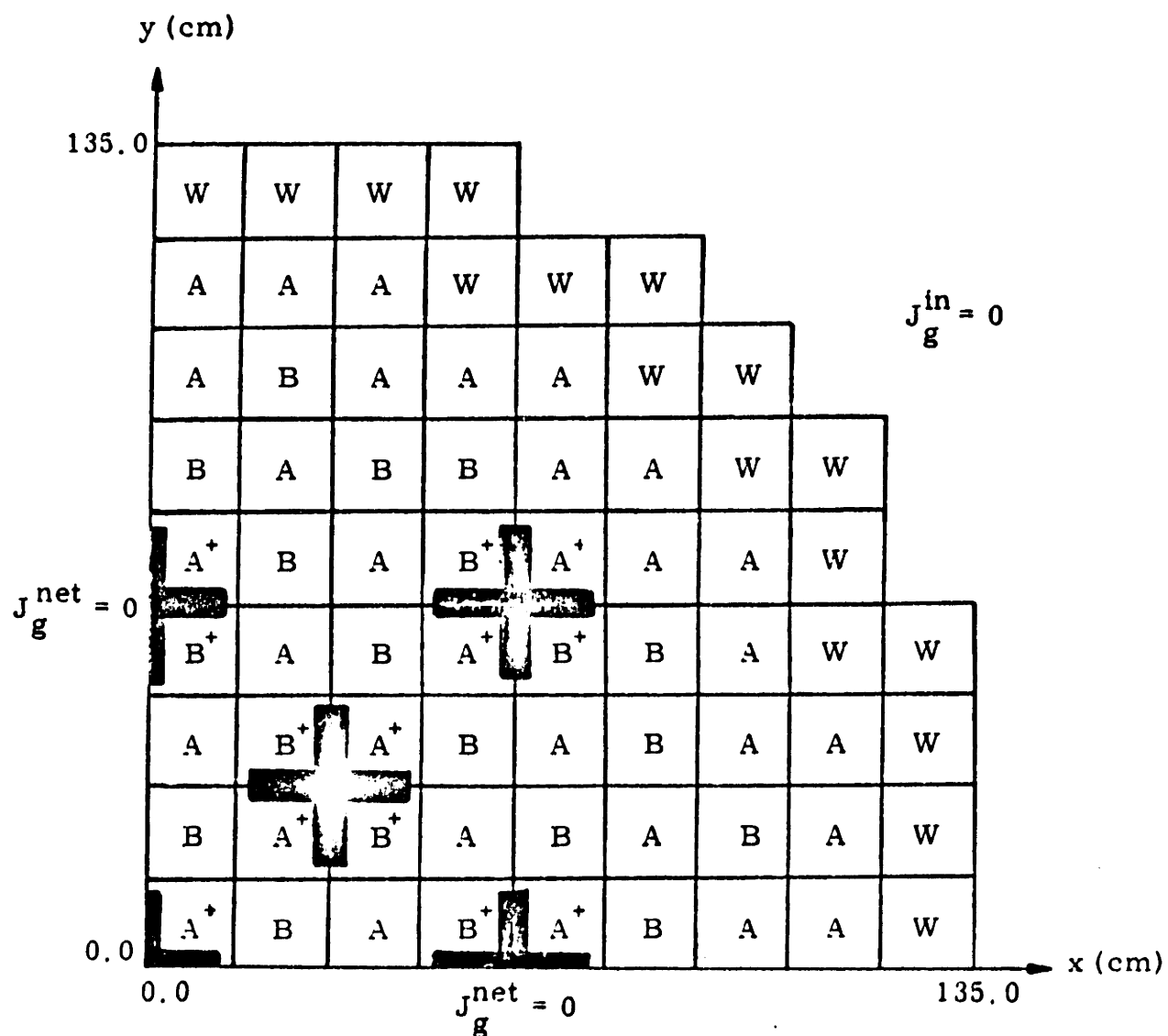
Cell Surface Orientations



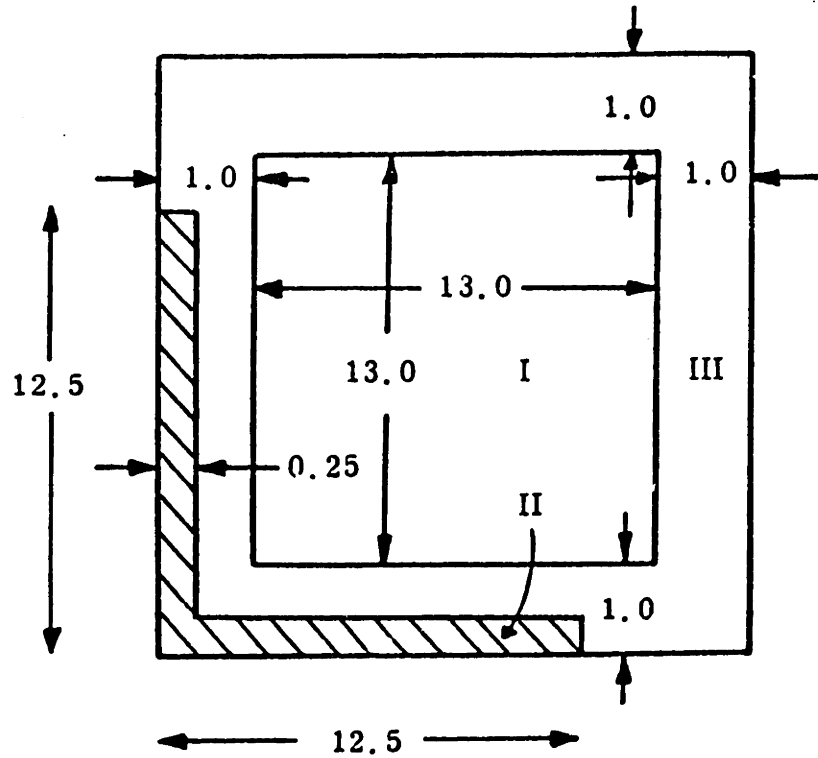
## A1.2 THE CISE BWR HOMOGENIZATION PROBLEM

### Geometry:

Quadrant of the 2-D Reactor



Fuel Assembly Description by Zone:



Composition to Zone Assignments by Assembly Type:

Zone	Assembly Type				
	A	$A^+$	B	$B^+$	W
I	3	3	4	4	2
II	2	1	2	1	2
III	2	2	2	2	2

Material Properties:

<u>Composition</u>	<u>Group, g</u>	$D_g$ (cm)	$\Sigma_{ag}$ (cm $^{-1}$ )	$\nu \Sigma_{fg}$ (cm $^{-1}$ )	$\Sigma_{gg'}$ (cm $^{-1}$ )
1 (Control blade)	1 2	3.00 0.15	0.08 1.00	0.0 0.0	0.0 0.0
2 (Water)	1 2	2.00 0.30	0.0 0.01	0.0 0.0	0.04 0.0
3 (Fresh fuel)	1 2	1.80 0.55	0.008 0.085	0.006 0.110	0.012 0.0
4 (Depleted fuel)	1 2	1.80 0.55	0.008 0.085	0.005 0.100	0.012 0.0

---


$$x_1 = 1.0$$

$$x_2 = 0.0$$

$$\nu = 2.5$$

Flux-Weighted Constants for the CISE BWR Problem

Assembly Type	Group, g	$\hat{D}_g$ (cm)	$\hat{\Sigma}_{ag}$ (cm $^{-1}$ )	$\nu \hat{\Sigma}_{fg}$ (cm $^{-1}$ )	$\hat{\Sigma}_{gg'}$ (cm $^{-1}$ )
A	1	1.8440	0.00607	0.004556	0.01874
(Fresh fuel)	2	0.4284	0.05946	0.07254	0.0
B	1	1.8440	0.00608	0.003796	0.01874
(Depleted fuel)	2	0.4284	0.05946	0.06595	0.0
A <sup>+</sup>	1	1.8580	0.00804	0.004565	0.01772
(Fresh fuel, controlled)	2	0.4283	0.07416	0.07558	0.0
B <sup>+</sup>	1	1.8580	0.00804	0.003804	0.01772
(Depleted fuel, controlled)	2	0.4283	0.07415	0.06870	0.0
W	1	2.0000	0.0	0.0	0.04
(Water)	2	0.3000	0.01	0.0	0.0

$$x_1 = 1.0$$

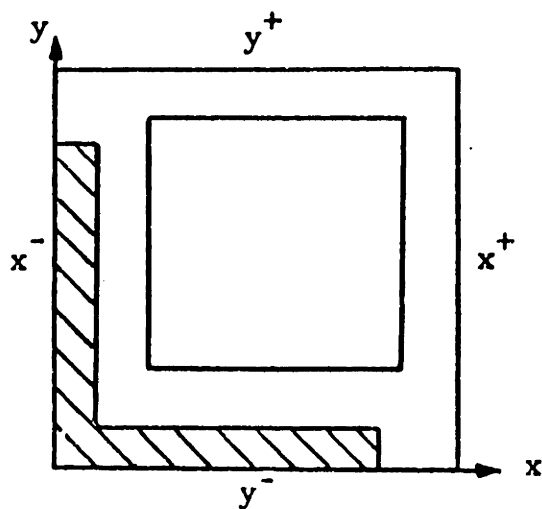
$$x_2 = 0.0$$

$$\nu = 2.5$$

Cell Discontinuity Factors for the CISE BWR Problem

Assembly Type	Group, g	$\frac{f^x}{g}^-$	$\frac{f^x}{g}^+$	$\frac{f^y}{g}^-$	$\frac{f^y}{g}^+$
A	1	0.9623	0.9623	0.9623	0.9623
	2	1.4510	1.4510	1.4510	1.4510
B	1	0.9625	0.9625	0.9625	0.9625
	2	1.4510	1.4510	1.4510	1.4510
$A^+$	1	0.8955	1.0150	0.8955	1.0150
	2	0.6492	1.8880	0.6492	1.8880
$B^+$	1	0.8949	1.0160	0.8949	1.0160
	2	0.6488	1.8890	0.6488	1.8890
W	1	1.0	1.0	1.0	1.0
	2	1.0	1.0	1.0	1.0

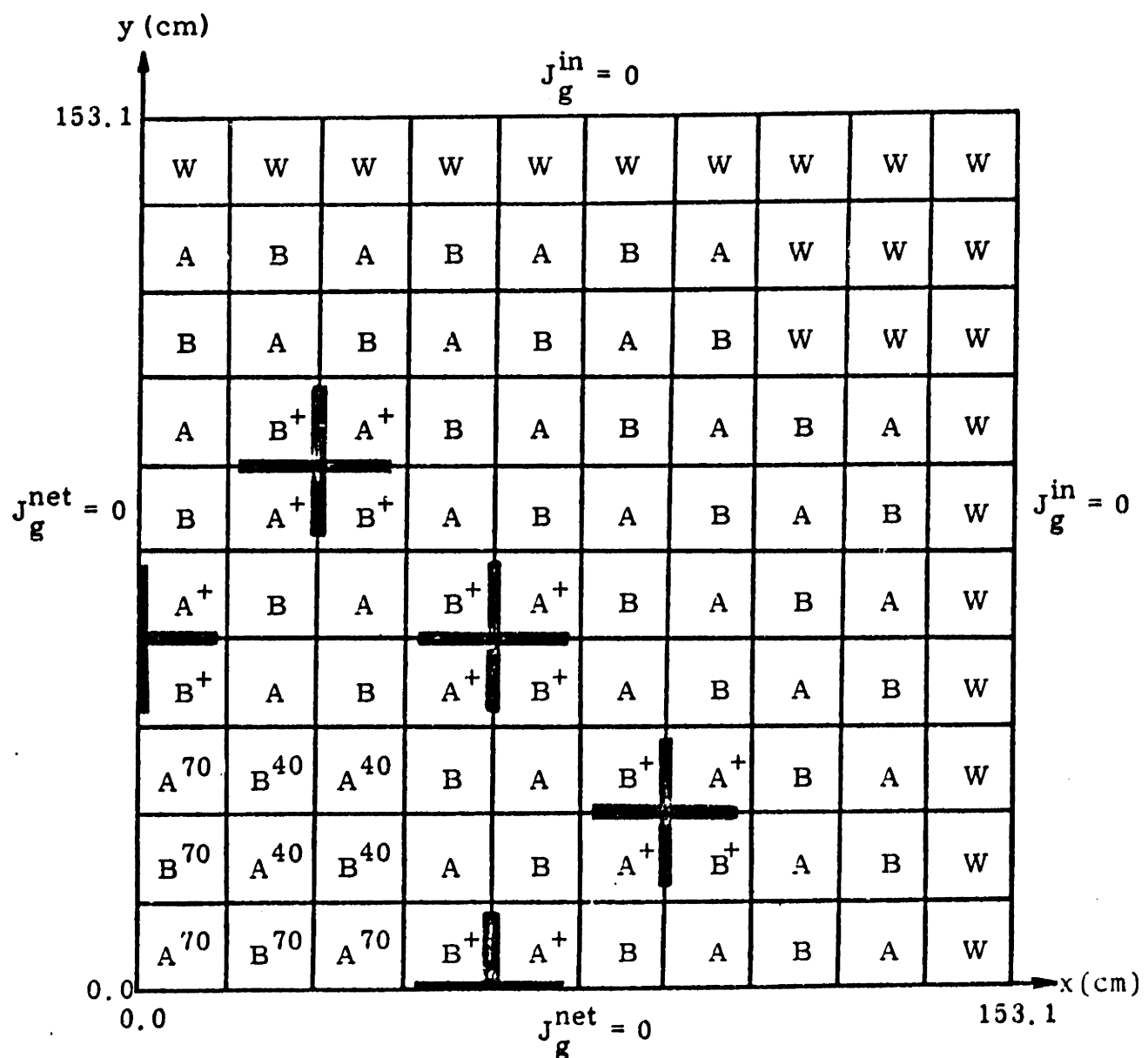
Cell Surface Orientation



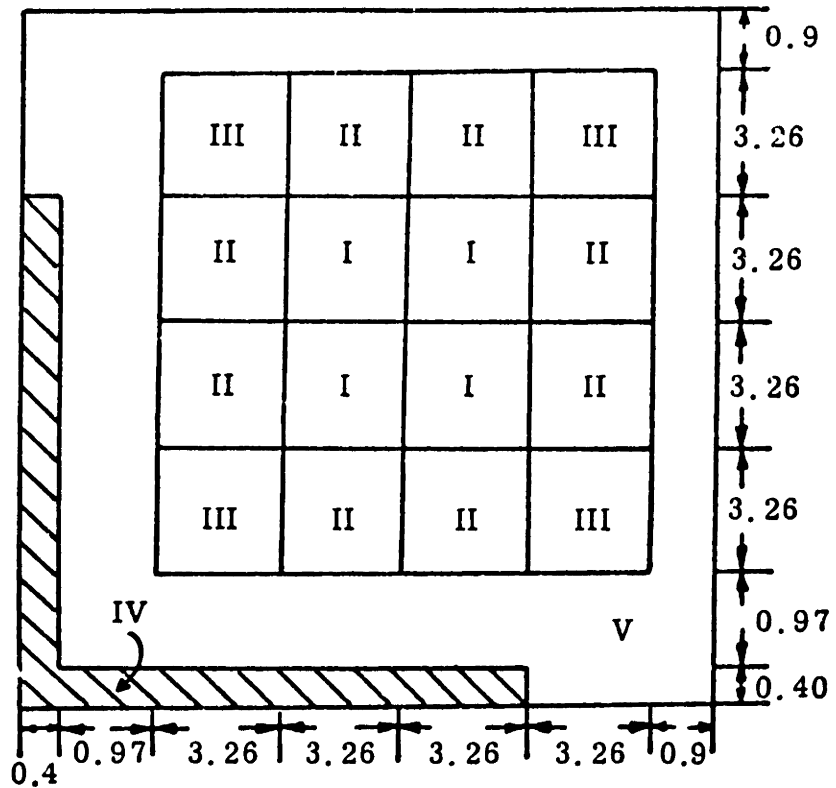
### A1.3 THE HAFAS BWR HOMOGENIZATION PROBLEM

#### Geometry:

Quadrant of the 2-D Reactor



Fuel Assembly Description by Zone:



Composition to Zone Assignments by Assembly Type:

Zone	Assembly Type								
	A	A <sup>40</sup>	A <sup>70</sup>	A <sup>+</sup>	B	B <sup>40</sup>	B <sup>70</sup>	B <sup>+</sup>	W
I	1	5	9	1	2	6	10	2	15
II	2	6	10	2	3	7	11	3	15
III	3	7	11	3	4	8	12	4	15
IV	13	13	13	14	13	13	13	14	15
V	13	13	13	13	13	13	13	13	15

Material Properties:

Composition	Group, g	D <sub>g</sub> (cm)	$\Sigma_{a_g}$ (cm <sup>-1</sup> )	$\nu \Sigma_{f_g}$ (cm <sup>-1</sup> )	$\Sigma_{21}$ (cm <sup>-1</sup> )
1 (Fuel a, void = 0%)	1	1.400	0.009	0.0065	0.016
2 (Fuel b, void = 0%)	1	1.400	0.009	0.0057	0.017
3 (Fuel c, void = 0%)	1	1.400	0.009	0.0051	0.018
4 (Fuel d, void = 0%)	1	1.400	0.009	0.0051	0.018
5 (Fuel a, void = 40%)	1	1.680	0.008	0.0063	0.010
6 (Fuel b, void = 40%)	1	1.680	0.0085	0.0055	0.0105
7 (Fuel c, void = 40%)	1	1.680	0.009	0.0049	0.0110
8 (Fuel d, void = 40%)	1	1.680	0.009	0.0049	0.0010

(continued)

Material Properties (continued)

Composition	Group, g	D <sub>g</sub> (cm)	Σ <sub>a<sub>g</sub></sub> (cm <sup>-1</sup> )	Σ <sub>f<sub>g</sub></sub> (cm <sup>-1</sup> )	Σ <sub>21</sub> (cm <sup>-1</sup> )
9 (Fuel a, void = 70%)	1 2	2.000 0.800	0.0078 0.073	0.0061 0.1140	0.0052
10 (Fuel b, void = 70%)	1 2	2.000 0.800	0.0082 0.0630	0.0053 0.0920	0.0053
11 (Fuel c, void = 70%)	1 2	2.000 0.800	0.0086 0.0530	0.0047 0.0720	0.0054
12 (Fuel d, void = 70%)	1 2	2.000 0.800	0.086 0.043	0.0047 0.0620	0.0054
13 (Fuel can and water)	1 2	1.530 0.295	0.0005 0.0090	0.000 0.000	0.031
14 (Control blade)	1 2	1.110 0.185	0.08375 0.950	0.000 0.000	0.00375
15 (Water)	1 2	2.00 0.300	0.000 0.010	0.000 0.000	0.04

---


$$x_1 = 1.0$$

$$x_2 = 0.0$$

$$\nu = 2.5$$

Flux-Weighted Constants for the HAFAS BWR Problem

Assembly Type	Group, g	$\hat{D}_g$ (cm)	$\hat{\Sigma}_{ag}$ ( $\text{cm}^{-1}$ )	$\nu\hat{\Sigma}_{fg}$ ( $\text{cm}^{-1}$ )	$\hat{\Sigma}_{gg'}$ ( $\text{cm}^{-1}$ )
A	1	1.4320	0.00678	0.004255	0.02065
(Fresh fuel, 0% void)	2	0.3414	0.04713	0.06249	0.0
$A^{40}$	1	1.6380	0.00639	0.004099	0.01588
(Fresh fuel, 40% void)	2	0.4097	0.04486	0.05972	0.0
$A^{70}$	1	1.8500	0.00616	0.003946	0.01208
(Fresh fuel, 70% void)	2	0.4890	0.04221	0.05661	0.0
$A^+$	1	1.4170	0.00927	0.004304	0.01974
(Fresh fuel, controlled)	2	0.3441	0.06099	0.06894	0.0
B	1	1.4320	0.0678	0.003879	0.02121
(Depleted fuel, 0% void)	2	0.3424	0.04144	0.05255	0.0
$B^{40}$	1	1.6380	0.0667	0.003725	0.01617
(Depleted fuel, 40% void)	2	0.4128	0.0392	0.05052	0.0

(continued)

Flux-Weighted Constants for the HAFAS BWR Problem (continued)

Assembly Type	Group, g	$\hat{D}_g$ (cm)	$\hat{\Sigma}_{ag}$ (cm $^{-1}$ )	$\nu\hat{\Sigma}_{fg}$ (cm $^{-1}$ )	$\hat{\Sigma}_{gg'}$ (cm $^{-1}$ )
$B^{70}$ (Depleted fuel, 70% void)	1	1.8500	0.0638	0.003573	0.01214
	2	0.4955	0.03655	0.04677	0.0
$B^+$ (Depleted fuel, controlled)	1	1.4160	0.00926	0.003924	0.02031
	2	0.3451	0.05405	0.05773	
W (Water)	1	2.0	0.0	0.0	0.04
	2	0.3	0.01	0.0	0.0

$$x_1 = 1.0$$

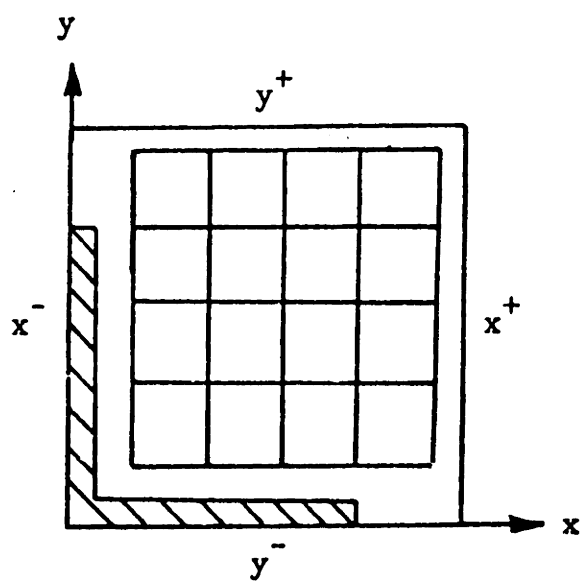
$$x_2 = 0.0$$

$$\nu = 2.5$$

Cell Discontinuity Factors for the HAFAS BWR Problem

Assembly Type	Group, g	$\frac{r_x^-}{g}$	$\frac{f_x^+}{g}$	$\frac{f_y^-}{g}$	$\frac{f_y^+}{g}$
A	1	0.9311	0.9677	0.9311	0.9677
	2	1.4740	1.2470	1.4740	1.2470
$A^{40}$	1	0.9368	0.9709	0.9368	0.9709
	2	1.5330	1.2550	1.5330	1.2550
$A^{70}$	1	0.9406	0.9739	0.9406	0.9739
	2	1.5830	1.2560	1.5830	1.2560
$A^+$	1	0.8169	1.0570	0.8169	1.0570
	2	0.6264	1.7320	0.6264	1.7320
B	1	0.9313	0.9694	0.9313	0.9694
	2	1.4070	1.2130	1.4070	1.2130
$B^{40}$	1	0.9372	0.9724	0.9372	0.9724
	2	1.4610	1.2200	1.4610	1.2200
$B^{70}$	1	0.9407	0.9750	0.9407	0.9750
	2	1.5060	1.2210	1.5060	1.2210
$B^+$	1	0.8151	1.0610	0.8151	1.0610
	2	0.5902	1.6830	0.5902	1.6830
W	1	1.0	1.0	1.0	1.0
	2	1.0	1.0	1.0	1.0

## Cell Surface Orientations



Appendix 2  
NORMALIZED ASSEMBLY POWER DENSITIES

- A2.1 Henry-Worley Problem with FWC
- A2.2 Henry-Worley Problem with Reference Equivalence Parameters (Two-Group)
- A2.3 Henry-Worley Problem with Reference Equivalence Parameters (One-Group)
- A2.4 CISE Problem with FWC
- A2.5 Henry-Worley Problem with CDF (Entire Assemblies)
- A2.6 Henry-Worley Problem with CDF (Quarter Assemblies)
- A2.7 CISE Problem with CDF
- A2.8 HAFAS Problem with CDF
- A2.9 Henry-Worley Problem with MCDF
- A2.10 CISE Problem with MCDF
- A2.11 HAFAS Problem with MCDF
- A2.12 Henry-Worley Problem with Single-Assembly Fixed-Source Calculations
- A2.13 CISE Problem with Single-Assembly Fixed-Source Calculations
- A2.14 HAFAS Problem with Single-Assembly Fixed-Source Calculations
- A2.15 CISE Problem with Five-Assembly Fixed-Source Calculations
- A2.16 HAFAS Problem with Five-Assembly Fixed-Source Calculations

FIGURE A2-1 NORMALIZED ASSEMBLY POWER DENSITIES AND ERRORS FOR THE HENRY-WORLEY BWR PROBLEM  
FLUX-WEIGHTED SOLUTIONS

0.6997      Y = 3  
2.19 X  
2.56 X

HETEROGENEOUS REFERENCE SOLUTION -- 0.9949  
QUANDRY WITH FWC. 8 CM MESH ----- 5.88 X  
QUANDRY WITH FWC. 4 CM MESH ----- 6.09 X  
1.0079      Y = 2  
-3.97 X  
-4.23 X

1.2033      1.3077      0.9312      Y = 1  
6.64 X      -3.93 X      4.04 X  
6.21 X      -3.94 X      4.24 X  
X =      1      2      3

FIGURE A2-2. NORMALIZED ASSEMBLY POWER DENSITIES AND ERRORS FOR THE HENRY-WORLEY BWR PROBLEM  
WITH TWO-GROUP GENERALIZED EQUIVALENCE PARAMETERS

	0.6590	Y = 5		
HETEROGENEOUS REFERENCE SOLUTION -----	0.7075	0.7161		
QUANDRY ERRORS WITH QUADRATIC, 2-GROUP EQUIVALENCE -----	0.00 X	0.00 X		
QUANDRY ERRORS WITH FLAT, 2-GROUP EQUIVALENCE -----	0.00 X	0.00 X		
QUANDRY ERRORS WITH CMFD, 2-GROUP EQUIVALENCE -----	0.00 X	0.00 X		
	0.8772	0.9348		
	0.00 X	0.00 X		
	0.00 X	0.00 X		
	-0.00 X	0.00 X		
	0.9921	1.0308		
	-0.00 X	-0.00 X		
	-0.00 X	-0.00 X		
	-0.00 X	-0.00 X		
	1.1181	1.0812		
	-0.00 X	0.00 X		
	-0.00 X	0.00 X		
	-0.00 X	0.00 X		
	1.3705	1.2450		
	-0.01 X	-0.00 X		
	-0.01 X	-0.00 X		
	-0.00 X	-0.00 X		
X = 1	2	3	4	5

**FIGURE A2-3. NORMALIZED ASSEMBLY POWER DENSITIES AND ERRORS FOR THE HENRY-WORLEY BWR PROBLEM  
WITH ONE-GROUP GENERALIZED EQUIVALENCE PARAMETERS**

	Y = 5	Y = 4	Y = 3	Y = 2	Y = 1
0.6590	0.7161	0.9348	1.0308	1.1181	1.2033
0.00 X	0.00 X	0.00 X	-0.01 X	-0.00 X	-0.00 X
0.00 X	0.00 X	0.00 X	-0.01 X	-0.00 X	-0.00 X
0.00 X	0.00 X	0.00 X	-0.01 X	-0.00 X	-0.00 X
					X = 1      2      3      4      5
HETEROGENEOUS REFERENCE SOLUTION	-----	-----	-----	-----	-----
QUANDRY ERRORS WITH QUADRATIC, 1-GROUP EQUIVALENCE	---	0.00 X	0.00 X	0.00 X	0.00 X
QUANDRY ERRORS WITH FLAT, 1-GROUP EQUIVALENCE	----	0.00 X	0.00 X	0.00 X	0.00 X
QUANDRY ERRORS WITH CMFD, 1-GROUP EQUIVALENCE	-----	0.00 X	0.00 X	0.00 X	0.00 X

**FIGURE A2-4.** NORMALIZED ASSEMBLY POWER DENSITIES AND ERRORS FOR THE CISE BWR PROBLEM  
COMPARISON OF FLUX-WEIGHTED(CELL) AND EXACT FLUX-WEIGHTED SOLUTIONS

	Y = 6			
	0.6493	0.0	0.0	0.0
8.37 %	8.30 %	0.0 %	0.0 %	0.0 %
8.30 %	8.30 %	0.0 %	0.0 %	0.0 %
3.87 %	3.87 %	0.0 %	0.0 %	0.0 %
 HETEROGENEOUS REFERENCE SOLUTION -----				
QUANDRY ERRORS WITH FWC, 15 CM MESH --	0.6846	0.7850	0.6270	0.0
QUANDRY ERRORS WITH FWC, 7.5 CM MESH -	9.15 %	1.39 %	10.21 %	0.0 %
QUANDRY ERRORS WITH EXACT FWC -----	9.19 %	1.09 %	9.86 %	0.0 %
QUANDRY ERRORS WITH EXACT FWC -----	7.56 %	-0.46 %	5.66 %	0.0 %
 Y = 5				
0.8820	0.7304	0.8841	0.8655	0.0
1.46 %	4.52 %	-0.66 %	5.95 %	0.0 %
1.48 %	4.64 %	-0.76 %	5.77 %	0.0 %
3.77 %	5.51 %	-1.33 %	3.07 %	0.0 %
 Y = 4				
0.9108	1.0824	1.2814	1.1197	1.0642
0.22 %	-6.64 %	-3.47 %	-0.76 %	2.38 %
0.27 %	-6.62 %	-3.50 %	-0.63 %	2.37 %
2.80 %	-4.87 %	-2.72 %	-1.18 %	0.87 %
 Y = 3				
0.8887	0.8101	1.2566	1.2195	1.4165
-1.11 %	-0.59 %	-6.86 %	-3.89 %	-1.05 %
-1.08 %	-0.41 %	-6.90 %	-3.86 %	-1.02 %
1.79 %	2.12 %	-5.12 %	-3.00 %	-1.26 %
 Y = 2				
0.8814	1.0362	1.2094	0.8404	1.0294
-1.46 %	-9.52 %	-8.76 %	1.43 %	3.13 %
-1.35 %	-9.52 %	-8.84 %	1.53 %	3.24 %
1.54 %	-6.91 %	-6.48 %	3.38 %	4.98 %
 Y = 1				
0.9722	0.9722	1.3359	1.3359	0.9722
6.34 %	6.34 %	1.31 %	1.31 %	6.34 %
6.43 %	6.43 %	1.33 %	1.33 %	6.43 %
3.43 %	3.43 %	0.25 %	0.25 %	3.43 %
 X = 1      2      3      4      5      6      7      8				

FIGURE A2-5. NORMALIZED ASSEMBLY POWER DENSITIES AND ERRORS FOR THE HENRY-WORLEY BWR PROBLEM  
 COMPARISON OF FLUX-WEIGHTED AND CELL EQUIVALENCE SOLUTIONS (ENTIRE ASSEMBLIES)

	X = 1	X = 2	X = 3
HETEROGENEOUS REFERENCE SOLUTION	1.2033	1.3077	0.9512
QUANDRY ERRORS WITH FWC	6.64 %	-3.93 %	4.04 %
QUANDRY ERRORS WITH CDF	3.30 %	0.60 %	-1.75 %
	0.6997	Y = 3	
	2.19 %		
	-3.44 %		
	0.9949	Y = 2	
	5.68 %	-3.97 %	
	0.25 %	0.87 %	
	1.0079	Y = 1	

**FIGURE A2-6.** NORMALIZED ASSEMBLY POWER DENSITIES AND ERRORS FOR THE HENRY-WORLEY BWR PROBLEM  
COMPARISON OF FLUX-WEIGHTED AND CELL EQUIVALENCE SOLUTIONS (QUARTER ASSEMBLIES)

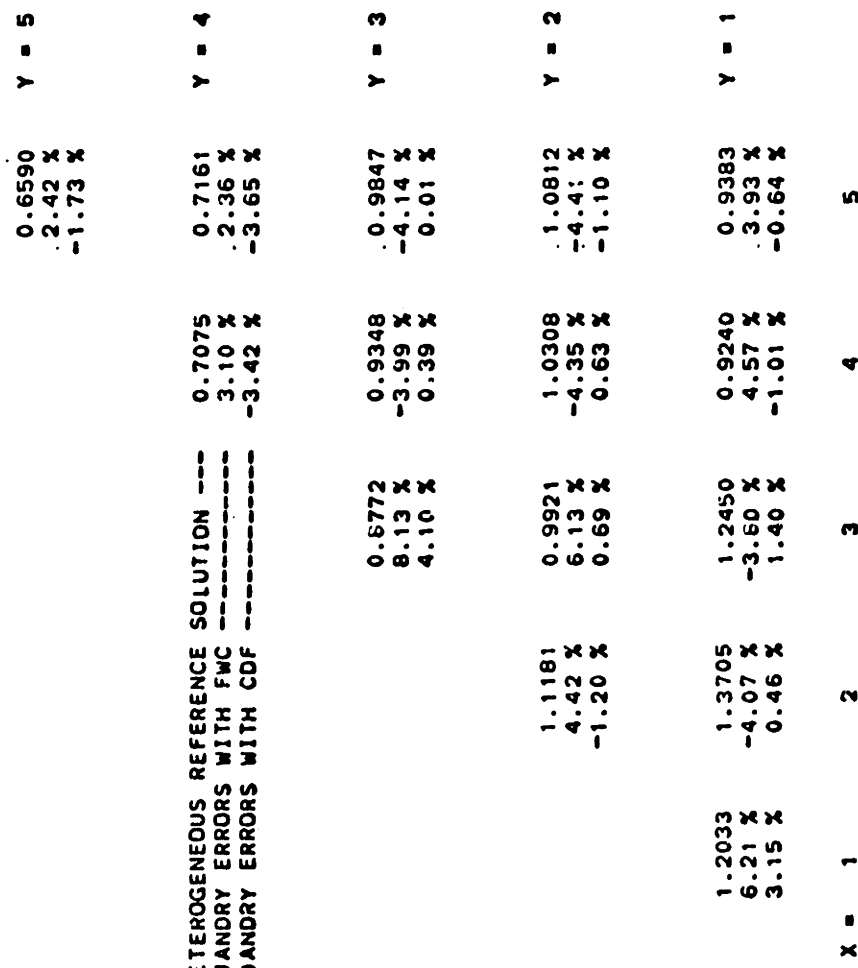


**FIGURE A2-7.** NORMALIZED ASSEMBLY POWER DENSITIES AND ERRORS FOR THE CISE BWR PROBLEM COMPARISON OF FLUX-WEIGHTED AND CELL EQUIVALENCE SOLUTIONS

					$\gamma = 1$	$\gamma = 2$	$\gamma = 3$	$\gamma = 4$	$\gamma = 5$	$\gamma = 6$
HETEROGENEOUS REFERENCE	SOLUTION	---	0.6846	0.7850	0.6270	0.0	0.0	0.0	0.0	0.0
QUANDRY ERRORS WITH FWC	---	9.19 %	1.09 %	9.86 %	0.0	0.0	0.0	0.0	0.0	0.0
QUANDRY ERRORS WITH CDF	---	-0.15 %	-0.03 %	-0.60 %	0.0	0.0	0.0	0.0	0.0	0.0
0.8820	0.7304	0.8841	0.8655	0.0	0.0	0.0	0.0	0.0	0.0	0.0
1.48 %	4.64 %	-0.76 %	5.77 %	0.0	0.0	0.0	0.0	0.0	0.0	0.0
-3.06 %	-2.41 %	0.12 %	-0.28 %	0.0	0.0	0.0	0.0	0.0	0.0	0.0
0.9108	1.0824	1.2814	1.1197	1.0642	0.7515	0.0	0.0	0.0	0.0	0.0
0.27 %	-6.62 %	-3.50 %	-0.63 %	2.37 %	9.82 %	0.0	0.0	0.0	0.0	0.0
-1.69 %	1.11 %	1.00 %	-0.07 %	-0.23 %	-0.71 %	0.0	0.0	0.0	0.0	0.0
0.8887	0.8101	1.2566	1.2195	1.4165	1.1008	0.8753	0.0	0.0	0.0	0.0
-1.08 %	-0.41 %	-6.90 %	-3.86 %	-1.02 %	1.46 %	6.61 %	0.0	0.0	0.0	0.0
-0.87 %	-1.31 %	1.72 %	0.90 %	0.06 %	-0.27 %	-0.54 %	0.0	0.0	0.0	0.0
0.8814	1.0362	1.2094	0.8404	1.0294	1.2581	1.3359	0.9722	0.0	0.0	0.0
-1.35 %	-9.52 %	-8.84 %	1.53 %	3.24 %	-1.82 %	1.33 %	6.43 %	0.0	0.0	0.0
-0.51 %	2.10 %	2.26 %	-0.66 %	-2.21 %	0.44 %	-0.00 %	-0.49 %	0.0	0.0	0.0

**FIGURE A2-8.** NORMALIZED ASSEMBLY POWER DENSITIES AND ERRORS FOR THE HAFAS BRW PROBLEM COMPARISON OF FLUX-WEIGHTED AND CELL EQUIVALENCE SOLUTIONS

HETEROGENEOUS REFERENCE SOLUTION ---			Y = 7		
QUANDRY ERRORS WITH FWC	0.9642	1.1996	0.6886	0.3936	Y = 7
QUANDRY ERRORS WITH CDF	10.63 %	5.51 %	10.75 %	16.95 %	
	1.31 %	1.38 %	1.54 %	1.86 %	
1.4634	1.4634	1.1996	0.9887	0.5091	Y = 6
4.52 %	4.52 %	5.51 %	8.30 %	10.57 %	
0.55 %	0.55 %	1.38 %	0.62 %	1.43 %	
1.1174	1.1174	1.2596	1.3550	0.9697	Y = 5
2.51 %	2.51 %	-0.59 %	4.96 %	4.99 %	
-5.29 %	-5.29 %	1.38 %	0.97 %	0.93 %	
1.6583	1.6583	1.2401	1.0813	0.9988	Y = 4
-6.05 %	-6.05 %	-3.81 %	-0.48 %	3.98 %	
-0.79 %	-0.79 %	0.75 %	1.60 %	0.14 %	
1.7191	1.7191	1.3736	0.7878	0.7339	Y = 3
-4.69 %	-4.69 %	-8.38 %	2.40 %	1.63 %	
-0.29 %	-0.29 %	0.64 %	-4.65 %	-1.93 %	
1.4962	1.4962	1.7175	1.2374	0.6215	Y = 2
-4.57 %	-4.57 %	-7.67 %	-10.02 %	3.66 %	
-0.41 %	-0.41 %	0.08 %	1.47 %	-4.17 %	
1.2997	1.2997	1.0752	0.9239	0.9993	Y = 1
-5.84 %	-5.84 %	-7.97 %	0.75 %	-8.95 %	
0.00 %	0.00 %	-1.35 %	-4.44 %	5.83 %	

**FIGURE A2-9.** NORMALIZED ASSEMBLY POWER DENSITIES AND ERRORS FOR THE HENRY-WORLEY BWR PROBLEM  
COMPARISON OF FLUX-WEIGHTED, CELL, AND MODIFIED-CELL EQUIVALENCE SOLUTIONS

	Y = 5	Y = 4	Y = 3	Y = 2	Y = 1
0.6590					
2.42 %					
-1.73 %					
-0.79 %					
HETEROGENEOUS REFERENCE SOLUTION	- - - - -	0.7075	0.7161		
QUANDRY ERRORS WITH FWC	- - - - -	3.10 %	2.36 %		
QUANDRY ERRORS WITH CDF	- - - - -	-3.42 %	-3.65 %		
QUANDRY ERRORS WITH MCDF	- - - - -	-2.33 %	-2.77 %		
0.8772		0.9348	0.9847		
8.13 %		-3.99 %	-4.14 %		
4.10 %		0.39 %	0.01 %		
2.90 %		0.73 %	-0.24 %		
1.1181		0.9921	1.0308	1.0812	
4.42 %		6.13 %	-4.35 %	-4.41 %	
-1.20 %		0.69 %	0.63 %	-1.10 %	
-0.56 %		1.02 %	0.36 %	-0.46 %	
1.2033		1.3705	1.2450	0.9240	0.9383
6.21 %		-4.07 %	-3.10 %	4.57 %	3.93 %
3.15 %		0.46 %	1.40 %	-1.01 %	-0.64 %
1.16 %		0.57 %	0.63 %	-0.71 %	-1.17 %
X = 1	2	3	4	5	

**FIGURE A2-10.** NORMALIZED ASSEMBLY POWER DENSITIES AND ERRORS FOR THE CISE BWR PROBLEM  
COMPARISON OF FLUX-WEIGHTED. CELL. AND MODIFIED-CELL EQUIVALENCE SOLUTIONS

					$y = 6$							
HETEROGENEOUS REFERENCE SOLUTION --	0.6846	0.7850	0.6270	0.0								
QUANDRY ERRORS WITH FWC	9.19 %	1.09 %	9.86 %	0.0								
QUANDRY ERRORS WITH CDF	-0.15 %	-0.03 %	-0.60 %	0.0								
QUANDRY ERRORS WITH MCDF	2.33 %	-0.62 %	-1.48 %	0.0								
0.8820	0.7304	0.8841	0.8655	0.0								
1.48 %	4.54 %	-0.76 %	5.77 %	0.0								
-3.06 %	-2.41 %	0.12 %	-0.28 %	0.0								
-0.56 %	0.04 %	-0.71 %	-1.31 %	0.0								
0.9108	1.0824	1.2814	1.1197	1.0642	0.7515	$y = 3$						
0.27 %	-6.62 %	-3.50 %	-0.63 %	2.37 %	9.82 %							
-1.69 %	1.11 %	1.00 %	-0.07 %	-0.23 %	-0.71 %							
1.20 %	0.91 %	0.33 %	-0.99 %	-1.36 %	-1.97 %							
0.8887	0.8101	1.2566	1.2195	1.4165	1.1008	0.8753	$y = 2$					
-1.08 %	-0.41 %	-6.90 %	-3.86 %	-1.02 %	1.46 %	6.61 %						
-0.87 %	-1.31 %	1.72 %	0.90 %	0.06 %	-0.27 %	-0.54 %						
2.42 %	1.83 %	1.41 %	0.35 %	-0.85 %	-1.43 %	-1.85 %						
0.8814	1.0362	1.2094	0.8494	1.0294	1.2581	1.3359	0.9722	$y = 1$				
-1.35 %	-9.52 %	-8.84 %	1.53 %	3.24 %	-1.82 %	1.33 %	6.43 %					
-0.51 %	2.10 %	2.26 %	-0.66 %	-2.21 %	0.44 %	-0.00 %	-0.49 %					
2.58 %	2.61 %	2.39 %	2.36 %	-0.06 %	-0.45 %	-1.17 %	-1.81 %					
X = 1	2	3	4	5	6	7	8					

FIGURE A2-11. NORMALIZED ASSEMBLY POWER DENSITIES AND ERRORS FOR THE HAFAS BWR PROBLEM  
COMPARISON OF FLUX-WEIGHTED, CELL, AND MODIFIED-CELL EQUIVALENCE SOLUTIONS

	$x = 1$	$x = 2$	$x = 3$	$x = 4$	$x = 5$	$x = 6$	$x = 7$	$x = 8$	$x = 9$
<b>HETEROGENEOUS REFERENCE SOLUTION</b>									
QUANDRY ERRORS WITH FWC	-0.9642	0.9642	1.2596	1.3550	0.9697	0.6886	0.3936	0.1000	$y = 7$
QUANDRY ERRORS WITH CDF	10.63 %	-0.59 %	4.96 %	4.99 %	4.99 %	10.75 %	16.95 %	16.95 %	
QUANDRY ERRORS WITH MCDF	-2.52 %	1.38 %	0.97 %	0.93 %	0.93 %	1.54 %	1.86 %	1.86 %	
	1.50 %	0.53 %	-0.15 %	-0.36 %	-0.36 %	0.62 %	1.43 %	1.43 %	
	-0.60 %	-0.03 %	-0.92 %	-0.92 %	-0.92 %	-0.10 %	-0.19 %	-0.19 %	
<b>Y = 6</b>									
QUANDRY ERRORS WITH FWC	1.4634	1.1996	0.9887	0.5091	0.5091	0.6886	0.3936	0.1000	$y = 7$
QUANDRY ERRORS WITH CDF	4.52 %	5.51 %	8.30 %	10.57 %	10.57 %	10.75 %	16.95 %	16.95 %	
QUANDRY ERRORS WITH MCDF	0.55 %	1.38 %	0.62 %	1.43 %	1.43 %	1.54 %	1.86 %	1.86 %	
	-0.60 %	-0.03 %	-0.92 %	-0.92 %	-0.92 %	-0.10 %	-0.19 %	-0.19 %	
	-0.60 %	-0.03 %	-0.92 %	-0.92 %	-0.92 %	-0.10 %	-0.19 %	-0.19 %	
<b>Y = 5</b>									
QUANDRY ERRORS WITH FWC	1.1174	0.8669	1.2401	1.0813	0.9988	0.6886	0.3936	0.1000	$y = 7$
QUANDRY ERRORS WITH CDF	2.51 %	5.15 %	-3.81 %	-0.48 %	3.98 %	10.75 %	16.95 %	16.95 %	
QUANDRY ERRORS WITH MCDF	-5.29 %	-2.13 %	0.75 %	1.60 %	0.14 %	1.54 %	1.86 %	1.86 %	
	-1.55 %	1.46 %	0.30 %	0.86 %	0.86 %	0.62 %	1.43 %	1.43 %	
	-1.55 %	1.46 %	0.30 %	0.86 %	0.86 %	0.62 %	1.43 %	1.43 %	
<b>Y = 4</b>									
QUANDRY ERRORS WITH FWC	1.6583	1.5325	1.3736	0.7878	0.7339	0.7761	0.5737	0.1000	$y = 7$
QUANDRY ERRORS WITH CDF	-6.05 %	-8.91 %	-8.35 %	2.40 %	11.63 %	-0.83 %	6.98 %	6.98 %	
QUANDRY ERRORS WITH MCDF	-0.79 %	0.48 %	0.64 %	-4.65 %	-1.93 %	0.75 %	1.03 %	1.03 %	
	-1.93 %	-0.40 %	0.19 %	-0.98 %	2.57 %	0.50 %	0.48 %	0.48 %	
	-1.93 %	-0.40 %	0.19 %	-0.98 %	2.57 %	0.50 %	0.48 %	0.48 %	
<b>Y = 3</b>									
QUANDRY ERRORS WITH FWC	1.7191	1.5115	1.7175	1.2374	0.8282	0.6215	0.8096	0.4973	$y = 7$
QUANDRY ERRORS WITH CDF	-4.69 %	-7.18 %	-7.67 %	-10.02 %	-3.66 %	9.01 %	-0.79 %	3.92 %	
QUANDRY ERRORS WITH MCDF	-0.29 %	-0.10 %	0.08 %	1.47 %	-4.17 %	-0.51 %	0.54 %	1.55 %	
	-1.82 %	-1.42 %	-0.80 %	1.14 %	0.55 %	4.00 %	0.68 %	1.30 %	
	-1.82 %	-1.42 %	-0.80 %	1.14 %	0.55 %	4.00 %	0.68 %	1.30 %	
<b>Y = 2</b>									
QUANDRY ERRORS WITH FWC	1.4962	1.2997	1.3517	1.0752	0.9239	0.9993	1.0152	0.7833	$y = 7$
QUANDRY ERRORS WITH CDF	-4.57 %	-5.84 %	-7.97 %	0.75 %	5.83 %	-8.95 %	-3.95 %	-1.85 %	
QUANDRY ERRORS WITH MCDF	-0.41 %	0.00 %	-1.35 %	-4.44 %	-0.85 %	1.18 %	1.10 %	0.49 %	
	-2.10 %	-1.61 %	-2.64 %	-1.34 %	3.90 %	1.81 %	1.53 %	0.56 %	
	-2.10 %	-1.61 %	-2.64 %	-1.34 %	3.90 %	1.81 %	1.53 %	0.56 %	

**FIGURE A2-12.** NORMALIZED ASSEMBLY POWER DENSITIES AND ERRORS FOR THE HENRY-WORLEY BWR PROBLEM  
COMPARISON OF SOLUTIONS OBTAINED WITH SINGLE-ASSEMBLY FIXED-SOURCE CALCULATIONS

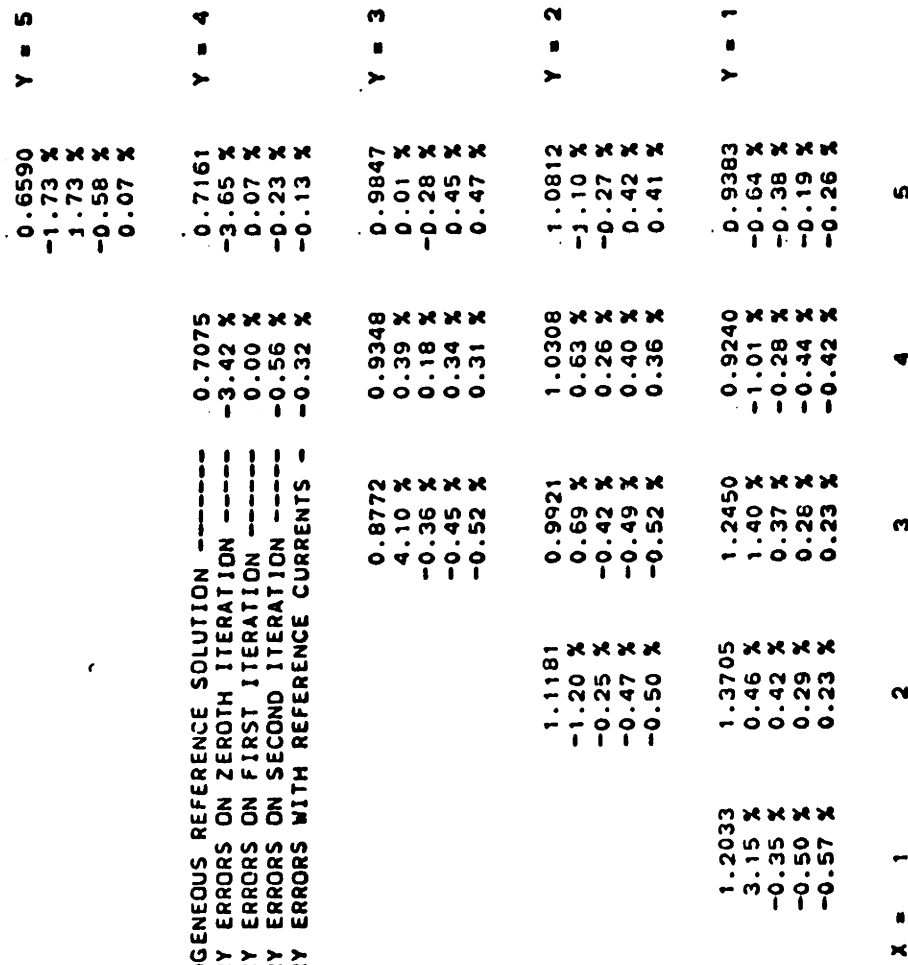


**FIGURE A2-13.** NORMALIZED ASSEMBLY POWER DENSITIES AND ERRORS FOR THE CISE BWR PROBLEM  
COMPARISON OF SOLUTIONS OBTAINED WITH SINGLE-ASSEMBLY FIXED-SOURCE CALCULATIONS

HETEROGENEOUS REFERENCE SOLUTION -----	0.6846	0.7850	0.6270	0.0	Y = 6			
QUANDRY ERRORS ON ZEROTH ITERATION -----	-0.15 X	-0.03 X	-0.60 X	0.0	X			
QUANDRY ERRORS ON FIRST ITERATION -----	-1.49 X	0.41 X	-1.51 X	0.0	X			
QUANDRY ERRORS WITH REFERENCE CURRENTS -	-0.70 X	0.47 X	-1.15 X	0.0	X			
0.8820	0.7304	0.8841	0.8655	0.0	Y = 4			
-3.06 X	-2.41 X	0.12 X	-0.28 X	0.0	X			
-0.25 X	-1.06 X	-0.19 X	-0.73 X	0.0	X			
0.06 X	-0.95 X	-0.10 X	-0.66 X	0.0	X			
0.9108	1.0824	1.2814	1.1197	1.0642	0.7515	Y = 3		
-1.69 X	1.11 X	1.00 X	-0.07 X	-0.23 X	-0.71 X			
-0.46 X	1.41 X	0.94 X	-1.05 X	-0.89 X	-1.51 X			
-0.27 X	1.46 X	1.02 X	-1.00 X	-0.94 X	-1.72 X			
0.8887	0.8101	1.2566	1.2195	1.4165	1.1008	0.8753	Y = 2	
-0.87 X	-1.31 X	1.72 X	0.90 X	0.06 X	-0.27 X	-0.54 X		
0.46 X	-0.22 X	1.70 X	0.69 X	-0.69 X	-1.22 X	-0.64 X		
0.41 X	-0.43 X	1.68 X	0.73 X	-0.65 X	-1.27 X	-0.96 X		
0.8814	1.0362	1.2094	0.8404	1.0294	1.2581	1.3359	0.9722	Y = 1
-0.51 X	2.10 X	2.26 X	-0.66 X	-2.21 X	0.44 X	-0.00 X	-0.49 X	
0.49 X	2.67 X	2.75 X	-0.02 X	-0.92 X	-0.36 X	-0.23 X	-0.44 X	
0.36 X	2.53 X	2.64 X	-0.21 X	-0.72 X	-0.35 X	-0.26 X	-0.70 X	
X = 1	2	3	4	5	6	7	8	

**FIGURE A2-14.** NORMALIZED ASSEMBLY POWER DENSITIES AND ERRORS FOR THE HAFAS BWR PROBLEM  
COMPARISON OF SOLUTIONS WITH SINGLE-ASSEMBLY FIXED-SOURCE CALCULATIONS

HETEROGENEOUS REFERENCE SOLUTION				Y = 7			
QUANDRY ERRORS ON ZEROTH ITERATION				Y = 6			
QUANDRY ERRORS ON FIRST ITERATION				Y = 5			
QUANDRY ERRORS WITH REFERENCE CURRENTS				Y = 4			
1.0885	0.6886	0.3936		1.31 %	1.54 %	1.86 %	
-0.19 %	-0.92 %	-1.37 %		-0.42 %	-1.17 %	-1.80 %	
1.4634	1.1996	0.9887	0.5091	0.55 %	1.38 %	0.62 %	1.43 %
-0.10 %	0.21 %	0.26 %	-0.30 %	-0.27 %	0.04 %	0.04 %	-0.63 %
0.9642	1.2596	1.3550	0.9697	-2.52 %	1.38 %	0.97 %	0.93 %
-1.07 %	1.11 %	1.00 %	0.39 %	-0.24 %	0.97 %	0.82 %	-0.34 %
-1.08 %	0.97 %	0.82 %	0.16 %	-0.32 %	0.24 %	1.23 %	-0.71 %
1.1174	0.8669	1.2401	1.0813	0.8669	1.2401	1.0813	0.9988
-5.29 %	-2.13 %	0.75 %	1.60 %	-1.66 %	-0.24 %	1.23 %	0.14 %
-1.66 %	-0.24 %	1.23 %	1.07 %	-1.07 %	-0.32 %	1.15 %	-0.19 %
1.6583	1.5325	1.3736	0.7878	0.7878	1.3736	0.7339	0.7761
-0.79 %	0.48 %	0.64 %	-4.65 %	-1.10 %	0.82 %	1.33 %	1.93 %
-1.10 %	0.82 %	1.33 %	-0.83 %	-0.76 %	1.09 %	1.48 %	-1.18 %
-0.76 %	1.09 %	1.48 %	-0.78 %	-0.78 %	-0.78 %	-0.78 %	-1.31 %
1.7191	1.5115	1.7175	1.2374	0.8262	1.2374	0.8262	0.6215
-0.29 %	-0.10 %	0.08 %	1.47 %	-1.47 %	-0.10 %	0.08 %	-0.51 %
-1.47 %	-1.26 %	0.52 %	1.38 %	-1.10 %	-0.91 %	1.56 %	-0.94 %
-0.91 %	-0.76 %	-0.76 %	-0.87 %	-0.87 %	-0.87 %	-0.87 %	-0.91 %
1.4962	1.2997	1.3517	1.0752	0.9239	1.3517	1.0752	0.9993
-0.41 %	0.00 %	-1.35 %	-4.44 %	-0.59 %	-1.26 %	-1.53 %	1.18 %
-1.16 %	-1.24 %	-0.86 %	-1.26 %	-1.53 %	-0.76 %	-1.13 %	-0.70 %
-0.72 %	-0.86 %	-0.76 %	-0.52 %	-0.52 %	-0.52 %	-0.52 %	-0.80 %

**FIGURE A2-15.** NORMALIZED ASSEMBLY POWER DENSITIES AND ERRORS FOR THE CISE BWR PROBLEM  
COMPARISON OF SOLUTIONS OBTAINED BY VARIOUS EQUIVALENCE SCHEMES

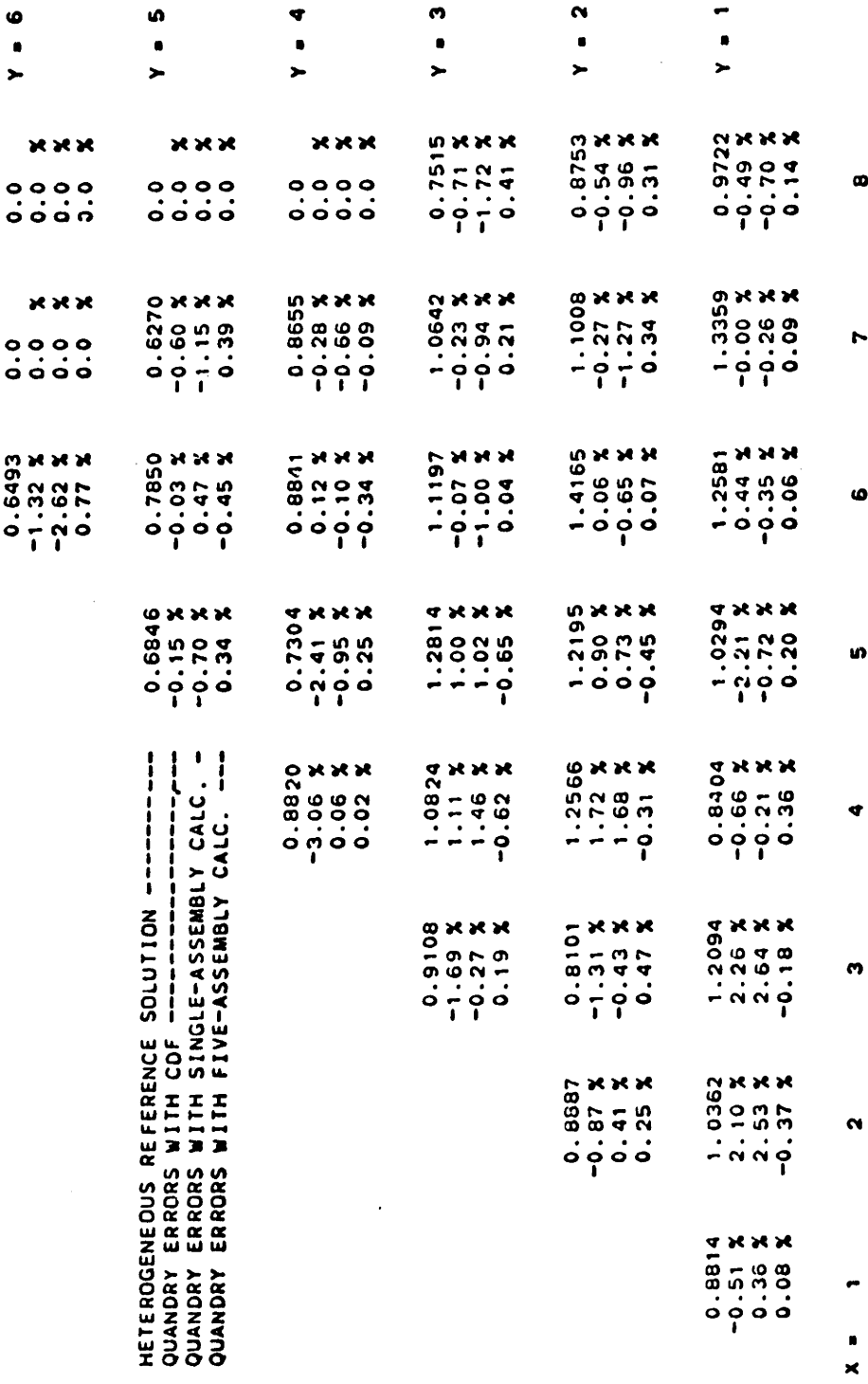


FIGURE A2-16. NORMALIZED ASSEMBLY POWER DENSITIES AND ERRORS FOR THE HAFAS BWR PROBLEM  
COMPARISON OF SOLUTIONS OBTAINED BY VARIOUS EQUIVALENCE SCHEMES

	$x = 1$	$x = 2$	$x = 3$	$x = 4$	$x = 5$	$x = 6$	$x = 7$	$x = 8$	$x = 9$
1.0885	0.6886	0.3936	$y = 7$						
1.31 %	1.54 %	1.86 %							
-0.42 %	-1.17 %	-1.80 %							
-0.72 %	-0.34 %	-0.24 %							
1.4634	1.1996	0.9887	$y = 6$						
0.55 %	1.38 %	0.62 %							
-0.27 %	0.04 %	0.04 %							
-0.70 %	-0.85 %	-0.84 %							
0.9642	1.2596	1.3550	0.9697	0.6332	$y = 5$				
-2.52 %	1.38 %	0.97 %	0.93 %	1.14 %					
-1.08 %	0.97 %	0.82 %	0.16 %	-0.71 %					
-0.23 %	-0.87 %	-0.95 %	-0.72 %	-0.42 %					
1.1174	0.6669	1.2401	1.0813	0.9988	0.5632	$y = 4$			
-5.29 %	-2.13 %	0.75 %	1.60 %	0.14 %	1.49 %				
-1.07 %	-0.32 %	1.15 %	0.92 %	-0.44 %	-0.50 %				
0.70 %	0.13 %	-0.91 %	-0.54 %	-0.32 %	-0.35 %				
1.6583	1.5325	1.3736	0.7878	0.7339	0.7761	0.5737	$y = 3$		
-0.79 %	0.48 %	0.64 %	-4.65 %	-1.93 %	0.75 %	1.03 %			
-0.76 %	1.09 %	1.48 %	-0.78 %	-1.31 %	0.30 %	0.20 %			
0.57 %	-0.03 %	-0.60 %	0.21 %	0.77 %	-0.20 %	-0.39 %			
1.7191	1.5115	1.7175	1.2374	0.8282	0.6215	0.8096	0.4973	$y = 2$	
-0.29 %	-0.10 %	0.08 %	1.47 %	-4.17 %	-0.51 %	0.54 %	1.55 %		
-1.10 %	-0.91 %	0.80 %	1.56 %	-0.87 %	-0.91 %	0.11 %	0.03 %		
0.94 %	0.75 %	0.00 %	-0.21 %	0.77 %	1.07 %	0.11 %	-0.08 %		
1.4962	1.2997	1.3517	1.0752	0.9239	0.9993	1.0152	0.7833	0.5503	$y = 1$
-0.41 %	0.00 %	-1.35 %	-4.44 %	-0.49 %	1.18 %	1.10 %	0.49 %	0.92 %	
-0.72 %	-0.86 %	-0.76 %	-1.13 %	-0.52 %	2.10 %	1.55 %	-0.80 %	-1.34 %	
0.88 %	0.88 %	0.74 %	0.63 %	0.59 %	0.10 %	0.15 %	0.62 %	0.59 %	